Effects of reactive oxygen species scavengers on adipogenesis

By

Ladislaus Tapiwa Adam

14456550

Submitted in fulfilment of the requirements for the degree

Masters of Science (Medical Immunology)

In the Faculty of Health Sciences

Department of Immunology

University of Pretoria

South Africa

2018

Supervisor:

Dr. Melvin Anyasi Ambele

Co-supervisors:

Prof. Michael Sean Pepper

Dr. Chrisna Durandt

Declaration of originality

University of Pretoria

Full names of student: **Ladislaus Tapiwa Adam**

Student number: **14456550**

Declaration

1. I understand what plagiarism is and am aware of the University's policy in this regard.
2. I declare that this dissertation is my own original work. Where other people's work has been used (either from a printed source, Internet or any other source), this has been properly acknowledged and referenced in accordance with departmental requirements.
3. I have not used work previously produced by another student or any other person to hand in as my own.
4. I have not allowed, and will not allow, anyone to copy my work with the intention of passing it off as his or her own work.

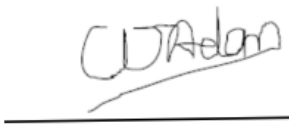

Ladislaus Adam

Abstract

Reactive oxygen species (ROS) have been implicated in regulating adipogenesis. Lack of a thorough understanding of the interplay between ROS and adipogenesis has hampered efforts to develop effective therapeutic solutions for obesity and its comorbidities. Thus, this study was initiated to investigate the effects of ROS and the ROS scavengers Trolox and apocynin on adipogenic differentiation of adipose-derived stromal/stem cells (ASCs). ASCs are generally viewed as the cells of origin of adipocytes, therefore ASCs derived from human fat tissue samples were chosen as a model to study adipogenesis *in vitro*. ASCs were induced to differentiate in the presence and absence of ROS scavengers. ASCs were also induced to differentiate during exposure to exogenous hydrogen peroxide (H_2O_2) in the presence and absence of ROS scavengers. Quantification of adipogenic differentiation and intracellular ROS levels were done using flow cytometry while extracellular ROS release was determined using a spectrofluorimeter.

The results of this study showed that extracellular ROS (H_2O_2) treatment of ASCs accelerated adipogenesis with faster differentiation kinetics in cells that differentiated in the continuous presence of H_2O_2. However, the study showed that there was no extracellular ROS release during adipogenesis. Treatment of differentiating ASCs with Trolox had no effect on adipogenesis in the presence and absence of extracellular H_2O_2. There was also no corresponding change in total intracellular and mitochondrial ROS levels with Trolox addition to differentiating human ASCs. Addition of apocynin to differentiating ASCs also had no change in total intracellular and mitochondrial ROS levels. However, apocynin addition suppressed adipogenesis in ASCs that were pre-treated with H_2O_2 for 24 hours prior differentiation during the early phases of differentiation. This adipogenic inhibition effect was not associated with changes in total intracellular and mitochondrial ROS levels. These findings suggest that extracellular ROS pre-treatment possibly refines or influences the action of apocynin as an anti-adipogenic agent in differentiating ASCs. Thus, apocynin could be protective in conditions of oxidative stress where cells are exposed to ROS.

This study showed that Trolox has no effect on adipogenesis as well as on intracellular ROS levels in differentiating human ASCs. Apocynin was also shown to have no effect on intracellular ROS levels. However, the study demonstrated that apocynin could potentially be a useful anti- adipogenesis agent that can possibly find applications in the prevention or treatment strategies for obesity. The mechanisms involved during apocynin enhancement of adipogenic differentiation is however not clear and need further investigation.

Key words

Adipose-derived stromal/stem cells (ASCs), Hydrogen peroxide (H_2O_2), Reactive oxygen species (ROS), Reactive oxygen species scavengers, Trolox, apocynin, Adipogenesis, Antioxidants, Flow cytometry, Mitochondria

Thesis outputs

Peer reviewed publications

Danielle de Villiers, Marnie Potgieter, Melvin A. Ambele, **Ladislaus Adam**, Chrisna Durandt, and Michael S. Pepper. The Role of Reactive Oxygen Species in Adipogenic Differentiation. In: Advances in Experimental Medicine and Biology. Springer, Boston, MA; 2017. p. 1–20.

Conference presentations

Posters

Ladislaus Adam, Melvin A. Ambele, Chrisna Durandt, and Michael S. Pepper. Effects of reactive oxygen species scavengers on adipogenesis. Faculty Day: Research Café, Faculty of Health Sciences, University of Pretoria, South Africa, 2018.

Acknowledgements

This research project would not have been possible without the aid and support of my supervisor and co-supervisors. I would like to firstly thank my supervisor Dr. Melvin Ambele, for the support, dedication and guidance offered throughout this study. A special thank you goes to my co-supervisor Dr. Chrisna Durandt for all the help especially in setting up and executing cell culture and flow cytometry experimental work. To my other co-supervisor, Professor Michael Pepper I am profoundly grateful for the opportunity to embark on this study. Your active participation, financial assistance and intellectual input in this work has not gone unnoticed and I do greatly appreciate.

I also would like to thank the Centre for Neuroendocrinology of the Faculty of Health Sciences at the University of Pretoria for allowing me to use their spectrofluorimeter for my extracellular reactive oxygen species work. I also would like to express my gratitude to Professor Annette Theron and Professor Ronald Anderson from the Department of Immunology at the University of Pretoria for their advice and help with extracellular reactive oxygen species measurements. I am most grateful to Professor Duncan Cromarty from the Department of Pharmacology at the University of Pretoria for the generous donation of hydrogen peroxide which I used for my entire project.

Successful completion of this masters research would not have been possible without the support from my family. I express my profound gratitude to my wife Julia Adam who has been my pillar of strength and support especially in times of need. Not forgetting Debra Adam my mother and my grandmother Benhilda Bukhu for their unwavering support both financially and emotionally. I also thank my children Elaine, Mufaro and Adrian for bearing with me during the time of my studies. A special thank you and gratitude goes to my best friend forever Tafadzwa Dzimbanhete, I would not have asked for a better friend. Finally, I thank the South African Medical Research Council (Extramural Unit and Flagship programs) for funding this research project.

Table of Contents

List of figures

List of tables

List of equations

List of abbreviation and symbols

AIDS	Acquired Immunodeficiency Syndrome
ASCs	Adipose-derived stromal/stem cells
ATP	Adenosine triphosphate
BAT	Brown adipose tissue
BMAL1	Brain and Muscle ARNT-like Protein 1
BMI	Body mass index
BMP4	Bone morphogenetic protein 4
C/EBP	CCAAT/enhancer-binding protein
CD	Cluster of differentiation
CHOP 10	C/EBP homologous protein 10
CO_2	Carbon dioxide
$CO_3^{\bullet-}$	Carbonate
CoQ10	Coenzyme Q10
CREB	cAMP response element binding protein
DAPI	4`,6-diamidino-2-phenylindole
DCFH-DA	Dichlorodihydrofluorescein diacetate
DMEM	Dulbecco's Modified Eagle's medium
DMSO	Dimethyl sulfoxide
DNA	Deoxyribonucleic acid
DUOX	Dual oxidase
EBF1	Early B cell factor-1
EGR2	Early growth response-2
EPAS1	Endothelial PAS domain Protein 1
FABP 4	Fatty-acid-binding protein 4
FAD	Flavin adenine dinucleotide
$FADH_2$	Flavin adenine dinucleotide
FOXO1	Forkhead Box O1

FS	Forward scatter
GATA2	GATA binding protein 2
GLUT 4	Glucose transporter 4
GPX	Glutathione peroxidase
GSH	Glutathione
h	Human
H_2O_2	Hydrogen peroxide
HIV	Human Immunodeficiency Virus
$HO_2^{\bullet}$	Hydroperoxyl
HOBr	Hypobromous acid
HOCl	Hypochlorous acid
$HOOCO_2^-$	Peroxomonocarbonate
IBMX	3-isobutyl-1-methylxanthine
IFATS	International Federation for Adipose Therapeutics and Science
ISCT	International Society of Cellular Therapy
KLF4	Kruppel-Like Factor 4
MCE	Mitotic clonal expansion
mES	Mouse embryonic stem
MFI	Mean fluorescence intensity
ml	Microgram/millilitre
MnTBAP	Manganese (III) tetrakis (4benzoic acid) porphyrin
mRNA	Messenger Ribonucleic acid
MSCs	Mesenchymal stem cells
MTT	3-(4,5-dimethylthiazol-2-yl)-2,5-diphenyltetrazolium bromide
SRB	Sulforhodamine B
NAC	N-acetylcysteine
NADPH	Nicotinamide adenine dinucleotide phosphate
NO	Nitric oxide
NOX	NADPH oxidases
O_2	Oxygen

$O_2^{\bullet-}$	Superoxide
O_3	Ozone
OCl^-	Hypochlorite
Oct3/4	Octamer-binding transcription factor 4
OH•	Hydroxyl radical
$ONOO^-$	Peroxynitrite
ONOOH	Peroxynitrous acid
OS	Oxidative stress
PBS	Phosphate buffered saline
PDTC	Pyrrolidine dithiocarbamate
PPARγ	Peroxisome proliferator-activated receptor-γ
Pref-1	Preadipocyte factor 1
$RO^{\bullet}$	Alkoxyl
$RO_2^{\bullet}$	Peroxyl
ROOH	Organic peroxides
ROS	Reactive oxygen species
SADHS	South Africa Demographic and Health Survey
SCD1	Stearoyl-CoA desaturase-1
SD	Standard deviation
SOD	Superoxide dismutase
Sox2	Sex determining region Y-box 2
SREBP1c	Sterol regulatory element binding transcription factor 1
SS	Side scatter
SVF	Stromal vascular fraction
TAZ	Transcriptional-coactivator with PDZ-binding motif
TCA	Trichloroacetic acid
VDC	Vybrant® DyeCycle™
WAT	White adipose tissue
WHO	World Health Organization
ZFP423	Zinc finger proteins 423

α	Alpha
β	Beta
δ	Delta
µ	Micro
%	Percentage
˚C	Degrees Celsius
<	Less than
>	Greater than
µg	Microgram
µl	Microliter
µm	Micrometer
µM	Micromolar
7-AAD	7-aminoactinomycin D

Chapter 1: Literature Review

1.1 Background

Obesity is a condition characterized by excess accumulation of adipose tissue either by an increase in adipocyte number from precursor cells (hyperplasia) or the size of adipocytes (hypertrophy)[1,2]. Obesity is a major global health concern affecting both adults and children. Although the pandemic is most widespread in developed countries, there has been an increase in the incidence and prevalence of obesity in developing nations especially in urban settings[3,4]. The World Health Organization (WHO) has reported the prevalence of obesity to have nearly tripled between 1975 and 2016[4]. In 2016, the WHO also reported that among adults aged 18 years and over, 39% were overweight and 13% were obese globally[4]. The South Africa Demographic and Health Survey (SADHS) report in 2016 states that 68% of women and 31% of men in South Africa were either overweight or obese[5].

There are different methods that can be used to assess obesity, each of the methods measuring different aspects of obesity. The suitability and scientific acceptibility of each method depending on each particular situation[6]. Body weight and body dimension measurements provide a cheap and rapid way to estimate body fatness and fat distribution[6,7]. The Body mass index (BMI) is one such measurement and has been traditionally used to identify individuals most likely to be obese, or overweight especially in large studies or clinical settings[6]. According to the WHO, using this scale, individuals can be classified as underweight (<18.5), normal weight (18.5-24.9), overweight (25-29.9), obese (30-39.9), and morbidily obese (>40)[6,8]. Obesity is associated with a wide range of disease conditions which include cardiovascular disease, hypertension, stroke, atherosclerosis, cancers among others[9–11]. In South Africa, non-communicable diseases including those associated with obesity are a major cause of mortality. This has seen South Africa and other developing countries succumb to a double burden of disease, since we are still struggling with communicable diseases like HIV/AIDS and tuberculosis. Consequently, this has brought an additional burden on the already strained health care

system of South Africa[5,12]. As such it is of great importance to scale up the current efforts to reduce obesity in South Africa.

Obesity is a chronic disease that is associated with increased reactive oxygen species (ROS) production leading to oxidative stress (OS)[13]. It is however still unclear whether ROS are a cause or a result of obesity[14,15]. White adipose tissue was previously thought to be a mere fat storage tissue, but it was later discovered that it also serves as an endocrine organ that secretes proinflammatory cytokines. Since adipose tissue is a source of proinflammatory cytokines, obesity is thus considered a state of chronic low grade inflammation[13,16]. Proinflammatory cytokines are potent stimulators of ROS production thus, generate OS[13,16]. Various studies have demonstrated that at physiological concentrations, ROS (regardless of source) can mediate adipocyte differentiation (fat cell formation)[17]. However, the mechanisms by which ROS regulate adipogenesis remain to be fully understood[1,15,18]. Under normal physiological conditions, ROS production is countered by antioxidant defence mechanisms (ROS scavengers). Antioxidants are substances that prevent or reduce oxidation of other molecules such as free radicals and ROS[19–21]. Several antioxidants have been described to ameliorate adipocyte differentiation; however, the effects of these antioxidants on adipogenesis remain largely unknown[22–24]. A better understanding of the association between ROS, ROS scavengers and adipocyte differentiation will provide new knowledge on how to combat obesity and its related complications.

1.2 An introduction to adipose tissue

Adipose tissue is a complex loose connective tissue that serves as the major storage site of energy in the form of triglycerides[25]. It consists of many different cell types which include mature adipocytes (constituting approximately one-third of adipose tissue), pre-adipocytes (in different stages of development), fibroblasts, adipose tissue associated monocytes/macrophages, lymphocytes, endothelial cells, adipose-derived stromal/stem cells (ASCs), hematopoietic stem/progenitor cells, erythrocytes and other cells[26–29].

Structurally, cells in adipose tissue are held together by a framework of collagen fibres. The tissue is highly vascularized and innervated[30,31]. As mentioned earlier, adipose tissue is metabolically highly active and has endocrine functions[32]. There are two main types of adipose tissue: white and brown adipose tissue. White adipose tissue (WAT) is the most abundant type and functions mainly as an energy storage organ, whereas brown adipose tissue (BAT) regulates body temperature through heat generation[25]. There is however another class of adipocytes called beige or brite adipocytes, which is found within WAT depots. In the basal state these cells phenotypically resemble white adipocytes, but upon stimulation by cold temperatures they transform into brown-like adipocytes. As a result they are often described to possess characteristics of both white and brown adipocytes. Like brown adipocytes, beige adipocytes also mainly seem to play a role in thermogenesis[32,33]. This study is based on WAT and the term adipose tissue further on refers to WAT unless otherwise stated.

Adipose tissue is widely distributed throughout the human body and is generally classified into subcutaneous and visceral/intra-abdominal adipose tissue. In humans, subcutaneous adipose tissue is found beneath the skin, within the abdominal cavity and interspersed among skeletal muscles. The major body locations of subcutaneous adipose tissue are the abdomen (abdomenal adipose tissue), thighs (femoral adipose tissue), buttocks (gluteal adipose tissue) and hips. Visceral adipose tissue is widely spread around internal organs, and can further be classified into mesenteric, retroperitoneal, and omental adipose tissue[32,33] (Figure 1.1).

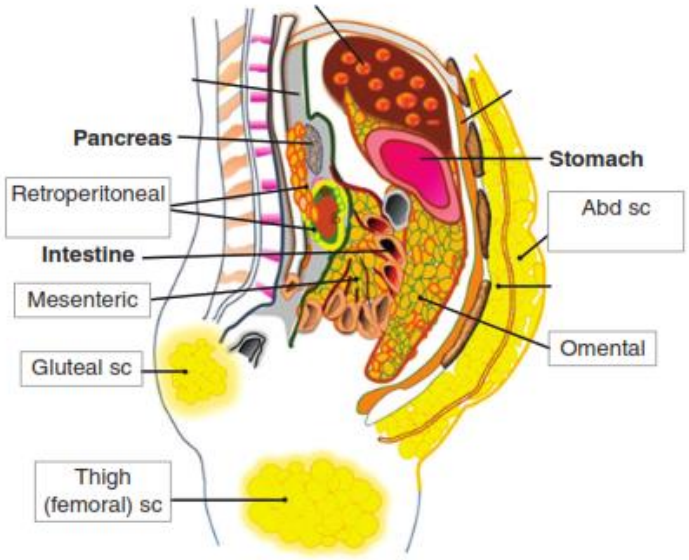

Figure 1.1 Location of major adipose tissue depots in humans
Subcutaneous (sc) adipose tissue sources includes abdominal, femoral and gluteal. Visceral adipose tissue depots are found around internal organs and comprise of mesenteric, retroperitoneal, as well as omental. *Adapted from Lee M-J. Hormonal Regulation of Adipogenesis. Compr Physiol. 2017;7:1151–95*.

Adipose tissue in these different depots exhibits differences in cellular composition, vasculature, innervation as well as metabolic and endocrine functions[34,35]. For example, subcutaneous adipose tissue has a low secretion profile of proinflammatory adipokines as compared to visceral adipose tissue with a secretion profile related to that observed during inflammation and type 2 diabetes[34]. Furthermore, visceral adipose tissue hormones are secreted into the hepatic portal system giving them direct access to the liver. Thus, visceral adipose tissue has a greater regulatory effect on hepatic metabolism[36]. This is in contrast to subcutaneous adipose tissue, which secretes hormones into the systemic circulation[36]. However, the exact mechanisms for these differences remain largely unknown. This heterogeneity in adipose tissue depots strongly suggests that adipose tissue depots may represent similar but unique endocrine organs[35,36].

1.3 Origins of the adipocyte cell

Details pertaining to the origin and development of the adipocyte are largely unknown and still debated[37,38]. Metabolic heterogeneity has been observed in adipose tissue from different body depots. This suggests that there maybe differences in the progenitors from which they arise from[39,40]. To fully understand the developmental processes associated with adipose tissue formation and pathogenesis, a clear and deeper understanding of the cellular origins of adipocytes is necessary[41].

Currently, it is widely accepted that adipocytes are derived from adipocyte precursor cells (preadipocytes). These precursor cells are considered to originate from mesenchymal stem cells (MSCs), which in turn are believed to arise from the mesodermal germ cell layer. Some studies have reported that adipocyte progenitors are adipose resident, existing within the adipose tissue vasculature[37,38,42,43]. Although it is generally assumed that adipocytes originate from adipose resident MSCs, there is evidence they may also originate from other tissue types, such as the bone marrow and neuroectoderm[44,45].

Majka and colleagues (2010), through lineage and cytogenetic analysis, argue that a subpopulation of adipocytes arises from bone marrow progenitor cells via the myeloid lineage[46]. Based on their findings, they hypothesized that bone marrow hematopoietic stem cells give rise to myeloid progenitor cells, which then migrate to adipose tissue though the circulatory system where they transdifferentiate into mesenchymal adipocyte progenitors[46]. This hypothesis was supported in studies by Crossno and colleagues (2006). In their experiments, rosiglitazone treatment and high fat diet feeding in mice promoted transmigration of bone marrow-derived progenitor cells to adipose tissue where they differentiated into multilocular adipocytes[47].

On the other hand, MSCs can also arise from the neuroectoderm germ cell layer. To investigate whether adipocyte progenitors could be of neuroectodermal origin, mouse embryonic stem (mES) cells were genetically engineered to produce ES cell-derived neuroepithelial progenitors. These progenitors could be differentiated *in vitro* to adipocytes, demonstrating that adipose progenitors could be of neuroectoderm origin[48].

To confirm this observation, isolated neural crest cells from developing quail embryos could also be induced *in vitro* to adipocytes[48]. In a separate study, Sowa and colleagues (2013) isolated a subpopulation of neural crest-derived ASCs in subcutaneous adipose tissues of adult myelin protein zero (P_0) -Cre and Wnt1-Cre/Floxed reporter mice. These cells also differentiated to adipocytes upon induction *in vitro*[49]**.** Although there has been research describing a neuroectoderm origin of adipocytes, the exact relationship between adipocyte progenitors and the neuroectoderm remains to be fully defined.

1.4 From stem cell to adipocyte: adipocyte differentiation

The formation of adipocytes is controlled by an intricate network of communication between cells and the extracellular environment or between cells themselves. This is facilitated by various hormones and growth factors modulating cell growth and differentiation[50]. Adipocytes arise from a population of multipotent stem cells, whose origins are believed to be from mesodermal germ cell layer[51]. The conversion of stem cells to mature adipocytes entails a complex process known as adipogenesis or adipocyte differentiation/maturation[27,52,53].

Adipogenesis is a multistep process that involves a complex array of transcription factors, cofactors, corepressors, extranuclear modulators, cell cycle proteins and small molecules which mediate the up- and down-regulation of a well-defined cascade of genes leading to the development of mature adipocytes[44,54–57]. The development of mature adipocytes involves coordination of more than 2000 genes some of which are not completely known or understood[56,57].

1.4.1 *In vitro* cell culture models of adipogenesis

What we currently know about adipocyte differentiation is largely based on studies using cellular models. The ability of primary multipotent stem cells to differentiate into adipocytes upon stimulation together with immortalized preadipocyte cell lines already programmed to the adipocyte lineage, are examples of such model systems[50,51]. Preadipocyte cell lines commonly employed include the murine 3T3-L1, 3T3 F442A and Ob17 cell lines[51,56]. Adipose lineage committed cell lines are useful models in that they

are homogenous cell populations and can maintain a more stable differentiated state[51]. This therefore allows for uniform responses to different treatments which are reported to be similar to adipocytes *in vivo*[50,51].

Both primary and immortalized multipotent and pluripotent stem cell lines provide excellent model systems to study early events in adipogenesis such as the commitment of stem cells to the adipogenic lineage as opposed to the already committed preadipocyte cell lines which are more useful for terminal differentiation studies[29,50]. Examples include pluripotent embryonic stem cells (ES) from both mice and humans as well as ASCs harvested from either human or murine fat tissue. The C3H10T1/2 cell line derived from 14 to 17 day old C3H mouse embryos is a commonly used mouse pluripotent stem cell line[29,51,58]. However, primary pluripotent embryonic stem cell (ES) use is limited due to ethical and political considerations[29,51]. Induced pluripotent stem cells derived from reprograming somatic cells with the transcription factors (Oct3/4, Sox2, KLF4, c-Myc), offer an alternative to ES and are not restricted by ethical and political problems of ES. However, they are not a homogenous cell population and are reported to have lower adipogenic potential compared to other cell lines[29,51].

1.4.2 Multistep process of adipocyte differentiation

Conversion of the stem cell to form mature adipocytes occurs through different developmental phases. Key events leading to this development are discussed below.

1.4.2.1 Commitment phase

The initial step during adipogenesis is the commitment of stem cells to the adipocyte lineage. In this phase, stem cells lose their multilineage differentiation potential and become committed only to the adipogenic lineage[51]. At this point the cells become known as preadipocytes (Figure 1.2). They are however still morphologically indistinguishable from mesenchymal stem cells[59]. Signals initiating the commitment phase are believed to be secreted within the adipose tissue stroma. A number of factors have been identified *in vitro* that play a role in committing stem cells to the adipogenic lineage[29]. These factors however appear to be cell type specific. Treatment of multipotent C3H10T1/2 cells with

bone morphogenetic protein 4 (BMP4) committed stem cells to the preadipocyte stage, as the cells were observed to undergo adipogenic differentiation upon induction. In contrast to C3H10T1/2, NIH 3T3 fibroblasts and human ASCs were committed to the preadipocyte stage by the transcription factor ZFP423[29,51,59,60].

Interestingly, McBeath and colleagues (2004), using human mesenchymal stem cells (hMSCs), described that cell shape and density maybe involved in cell lineage commitment. High density plated hMSCs had a higher probability of differentiating into adipocytes whereas low density plating encouraged osteogenic differentiation. Spread restricted hMSCs resulted in a contracted morphology, and these cells could only be differentiated into adipocytes. On the other hand, cells allowed to spread and flatten only differentiated to osteoblasts[61]. However the exact molecular mechanisms involved in the commitment phase remain largely unknown[29,51].

1.4.2.2 Growth arrest phase

Before preadipocytes enter the terminal phase of differentiation, they must exit the cell cycle and enter a growth arrest stage. Growth arrest but not cell contact is a prerequisite for terminal differentiation to occur. Evidence to support this comes from studies in which low density seeded murine preadipocytes could still be differentiated even though they lacked cell contact[50]. In addition, other investigators reported that confluent 3T3-F442A cells could still differentiate to adipocytes even when transferred to suspension culture (where the cells were not in contact), which again supports the observation that cell contact is not absolutely necessary for differentiation to occur[62].

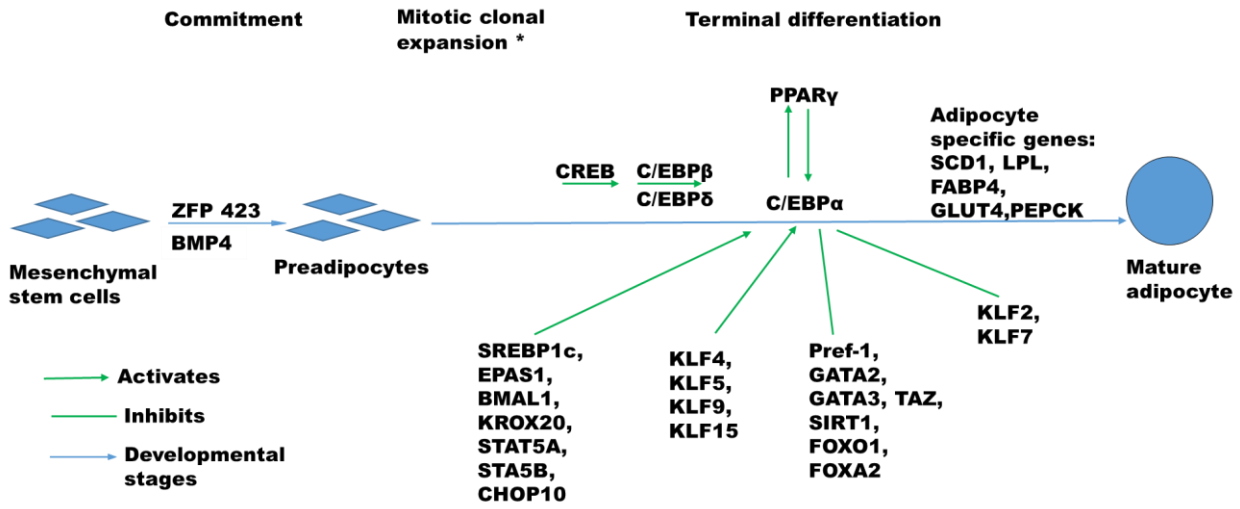

Figure 1.2 Transcriptional regulation of adipogenic differentiation.
Mesenchymal stem cells (MSCs) can be committed to the adipogenic lineage and converted to preadipocytes, which further differentiate into mature adipocytes. During the conversion of MSCs to adipocytes, growth arrest occurs at the preadipocyte stage. The subsequent activation of adipocyte genes by the transcription factors CCAAT/enhancer-binding protein (C/EBPα) and peroxisome proliferator-activated receptor-γ (PPARγ) drives adipogenesis. Changes in morphology include the acquisition of a more spherical shape and the accumulation of lipid droplets. ***:** The requirement for mitotic clonal expansion during adipogenesis is still controversial particulary in human MSCs, however it has been suggested to be prerequisite in murine cell lines.

1.4.2.3 Mitotic clonal expansion phase

Following growth arrest, preadipocytes require adipogenic and mitogenic signals to activate subsequent differentiation steps. *In vitro,* a combination of hormones in the form of a cocktail termed MDI is commonly used to induce differentiation. This cocktail consists of M: 3-isobutyl-1-methylxanthine (IBMX), D: dexamethasone and I: insulin. Sometimes MDI is supplemented with indomethacin or rosiglitazone[53,63,64]. Several studies suggest that, upon receiving signals for induction, some cell lines notably 3T3-F442A, 3T3-L1 and Ob17 synchronously re-enter the cell cycle and undergo mitotic clonal expansion (MCE) [50,56,65]. In MCE, preadipocytes undergo several rounds of cell division, after which they exit cell cycle and commence terminal differentiation[50,56,65]. Other studies however

suggest that human derived preadipocytes differentiate without post confluency mitosis after receiving signals to differentiate[15,50,66] (Figure.1.2).

In the MDI induction cocktail, IBMX, a phosphodiesterase inhibitor enhances adipogenesis by promoting the expression of C/EBPβ through cAMP response element binding protein (CREB)[29]. Dexamethasone a glucocorticoid stimulates adipogenesis through direct induction of genes responsible for C/EBPβ and C/EBPδ expression[53,67]. Insulin promotes glucose uptake into cells which is then stored as triacyglycerols[53]. Insulin also plays a role in activating proliferation and differentiation of preadipocytes. When used in high concentrations it mimics insulin-like growth factor-1, and activates the mitogen-activated protein kinase pathway[67]. On the other hand, indomethacin (cyclooxygenase inhibitor) and rosiglitazone (PPARγ agonist) both induce adipogenesis by stimulating PPARγ expression and transcriptional activity, respectively[63].

1.4.2.4 Terminal differentiation phase

Terminal differentiation involves the activation of a plethora of transcription factors that orchestrate positive and negative regulation of numerous genes involved in adipocyte development[29,50,68]. The initial stages of transcriptional regulation are marked by the rapid induction of CCAAT/enhancer binding protein-β (C/EBPβ) and C/EBPδ following hormonal induction[51]. Firstly, C/EBPβ is hyperphosphorylated and activated by glycogen synthase kinase-3 β and mitogen-activated protein kinase (MAPK)[56]. There is evidence however that the transcription factor, CREB is also involved in the initial activation of C/EBPβ (Figure1.2). In studies by Zhang and colleagues (2004) and Reusch and colleagues (2000), expression of CREB strongly activated C/EBPβ and adipogenesis, suggesting CREB is necessary for the activation of C/EBPβ[51,69,70]. Upon activation of C/EBPβ, both C/EBPβ and C/EBPδ induce the expression of peroxisome proliferator-activated receptor- γ (PPARγ) and C/EBPα[51,53,56,71].

PPARs are members of the nuclear hormone receptor superfamily of transcription factors that comprise of three different subtypes namely PPARα, PPARβ and PPARγ[53]. These subtypes play a role in lipid and glucose metabolism in different tissue types[72]. PPARγ is

expresssed in two major isoforms which are PPARγ1 and PPARγ2[72]. PPARγ1 is ubiquitously expressed in different cell types whereas PPARγ2 is mainly expressed in adipose tissues and plays a key role in adipogenesis[53,72]. The transcription factors PPARγ and C/EBPα are at the centre of the adipogenic transcriptional cascade. These are the key transcription factors regulating adipogenesis. Their expression induces many downstream genes that are involved in creating and maintaining the adipocyte phenotype[56,68]. In addition to PPARγ and C/EBPα, there are many other transcription factors that act upstream or downstream of these two key factors. Some of the factors are pro-adipogenic whilst others are anti-adipogenic. The whole process of adipogenesis is a result of an equilibrium between these various intertwining factors[56,68] (Figure 1.2). Although C/EBPα is a critical factor in adipogenesis that induces many adipocyte specific genes, no transcription factor has yet been identified to promote adipogenesis in the absence of PPARγ[53,56]. Mouse fibroblasts expressing C/EBPα but lacking PPARγ expression could not differentiate to mature adipocytes. However, C/EBPα deficient cells expressing PPARγ could be induced to the adipogenic lineage but with less lipid accumulation[73,74]. These observations clearly indicate that PPARγ is the master regulator of adipogenesis. In addition, cross regulation between PPARγ and C/EBPα is important for maintaining the differentiated state[74].

There are many proadipogenic and antiadipogenic factors that play vital roles along the differentiation process. Kruppel-Like Factor Family (KLF) of C2H2 zinc finger proteins are factors known to regulate cell differentiation, proliferation and apoptosis[56]. KLFs that promote adipogenesis include KLF4 which is induced during early differentiation and increases the expression of C/EBPβ[75]. KLF5 is proadipogenic acting together with C/EBPβ and C/EBPδ in activating PPARγ[76]. In addition, KLF9, KLF15 and the sterol regulatory element binding transcription factor 1 (SREBP1c) a lipogenic gene regulator, have been implicated in enhancing adipogenesis. Similar to KLF5, the mechanism of action of KLF9 is through the activation of PPARγ, although it activates PPARγ through C/EBPα[76–79]. Additional positive regulators in the adipogenic transcriptional network encompass the signal transducer and activator of transcription 5A (STAT5A), STAT5B, endothelial PAS domain protein 1 (EPAS1), Brain and Muscle ARNT-like Protein 1

(BMAL1), early growth response-2 (EGR2) alternatively known as KROX20, early B cell factor-1 (EBF1) among other factors. The list of transcription factors is long and ever expanding with new factors being discovered and incorporated into the list regularly[29,56,57,68].

Studies have also shown that not all KLFs are proadipogenic as KLF2 and KLF7 repress adipogenesis. KLF2 represses through the inhibition of PPARγ, C/EBPα and SREBP1c[56,57,80]. Whereas KLF7 blocks adipogenesis by decreasing PPARγ and C/EBPα expression[81]. The transcription factors GATA2 and GATA3 inhibit adipogenesis using mechanisms involving either direct suppression of PPARγ or protein complex formation with C/EBPα and C/EBPβ[82]. Preadipocyte factor 1 (Pref-1) is a transmembrane protein synthesized and expressed by preadipocytes. Pref-1 is further processed to soluble forms which are implicated in inhibiting adipogenesis. Inhibition by Pref-1 is through maintenance of the preadipocyte state and thereby blocking adipocyte differentiation[83,84]. Other examples of antiadipogenic factors include the transcriptional-coactivator with PDZ-binding motif (TAZ), the histone deacetylase Sirtuin 1 (SIRT1), Forkhead Box O1 (FOXO1), Forkhead Box A2 (FOXA2), C/EBP homologous protein 10 (CHOP10) among others[29,56].

Several other factors ranging from bioactive molecules, cellular processes, cytokines to pharmacological compounds have been shown to influence adipogenesis either positively or negatively[53,56]. Negative regulators include oxysterols, phytochemicals e.g. genistein, epigallochatechin, resveratrol, quercetin[53,85,86]. Epigenetic factors and microRNAs have also been shown to have an influence on adipogenesis as well. However, much research still needs to be done in this area to gain a deeper understanding on their role in adipogenesis[56,71]. Above all, the terminal phase of differentiation is marked by preadipocytes losing their fibroblastic shape and acquiring a spherical morphology characteristic of mature adipocytes. There is also a marked increase in cell activity and increased mRNA and enzymatic protein expression levels that play a role in triacyglycerol metabolism e.g. ATP citrate lyase, malic enzyme, acetyl-CoA carboxylase, stearoyl-CoA desaturase (SCD1), glycerol-3- phosphate acyltransferase, glycerol-3-

phosphate dehydrogenase, fatty acid synthase, and glyceraldehyde-3-phosphate dehydrogenase[50]. In addition, glucose transporters e.g. GLUT4 and insulin receptor numbers also increase during differentiation[50]. Adipocytes at this stage begin synthesizing adipose tissue specific proteins notably fatty-acid-binding protein (FABP4), FAT/CD36 and perilipin[50,87]. Secreted products are also synthesized at this stage which include, monobutyrin, adipsin, Acrp30/AdipoQ; PAI-1 and angiotensinogen[50,56].

One of the major challenges in gaining complete insight into the process of adipogenesis is that most of the available information on adipogenesis is through *in vitro* studies mainly involving murine cell lines. Translating findings from mice studies to humans comes with several limitations[88]. Also, *in vitro* findings do not necessarily reflect the picture *in vivo*[89]. The use of primary cells of human origin and appropriate experimental animal models to develop a deeper understanding of adipogenesis is therefore vital in order to develop, identify and improve treatment strategies for obesity and its related complications.

1.5 Introduction to reactive oxygen species

Reactive oxygen species (ROS) are a group of short lived, highly reactive oxygen containing ions, free radicals and molecules[90]. In all living aerobic organisms oxygen is a central molecule for cellular respiration[91]. However, the production of ROS is an unavoidable consequence of cellular respiration[90]. The ROS group of molecules comprises free radicals and non-radical species[91]. Free radicals of biological significance include, singlet oxygen (O_2), superoxide ($O_2^{\bullet-}$), hydroxyl radical ($OH^{\bullet}$), hydroperoxyl ($HO_2^{\bullet}$), carbonate ($CO_3^{\bullet-}$), peroxyl ($RO_2^{\bullet}$) and alkoxyl ($RO^{\bullet}$). Non-radical examples include hydrogen peroxide (H_2O_2), hypobromous acid (HOBr), hypochlorous acid (HOCl), ozone (O_3), organic peroxides (ROOH), peroxynitrite ($ONOO^-$), peroxynitrous acid (ONOOH), peroxomonocarbonate ($HOOCO_2^-$), nitric oxide (NO), and hypochlorite (OCl^-)[92,93].

ROS react spontaneously with a wide range of chemical structures within their vicinity. These structures include lipids, sugars, nucleic acids and proteins[94]. Due to their highly reactive nature, ROS were initially considered harmful in biological systems since high concentrations of ROS have been implicated in oxidative damage of fatty acids, DNA,

proteins and other cellular structures[94]. It is now generally accepted that ROS at physiological levels have a role in regulating cellular function, such as proliferation, cell signalling, differentiation and phagocytic pathogen killing[94–96].

ROS are generated either endogenously or exogenously from different sources[91]. Exogenous ROS production can be from environmental sources such as UV light, ionizing radiation and pollutants. Radiation can generate ROS through radiolysis of water molecules or UV-light mediated irradiation of H_2O_2 creating hydroxyl and superoxide radicals. Pollutants such as chemicals can react to form various ROS species for example peroxides, ozone or superoxides which can exert damaging effects to cells[91]. Other extracellular ROS sources include tobacco smoke whose aerosol contains free radicals and ROS[97]. Some drugs notably the anti-tumour drugs cisplatin and adriamycin have been reported to produce ROS at high concentrations resulting in cell damage[91]. Endogenous ROS are produced through multiple biochemical and physiological mechanisms which are tissue and cell type dependent[91,94]. Endogenous cellular ROS producers include the NADPH oxidases (NOX) family of transmembrane enzymes, mitochondria, xanthine oxidase, cytochrome P450, nitric oxide synthase, lipoxygenase, heme oxygenase, cyclooxygenase, myeloperoxidase and monoamineoxidases. Other cellular locations of ROS production are the endoplasmic reticulum and in peroxisomes[91,94].

1.5.1 NADPH oxidases

The NOX family of enzymes consist of seven isoforms namely NOX1 to 5, dual oxidase 1 and 2 (DUOX1 and DUOX2)[98,99]. NOX are generators of superoxide and H_2O_2[98]. NOX1, 2, 3 and 5 generate superoxide as their primary product, whereas NOX4, DUOX1 and DUOX2 generate H_2O_2[94,100]. The reasons behind the different ROS products generated are not clear but it is hypothesized that there are likely to be regions in NOX4, DUOX1, and DUOX2 that serve as enhancers of spontaneous dismutation from superoxide to H_2O_2[94,101].

Structurally, NOX enzymes are comprised of flavin adenine dinucleotide (FAD) and NADPH binding sites, two haem molecules and six transmembrane alpha helices with N and C cytosolic termini. DUOX1 and DUOX2 on the other hand do possess a seventh transmembrane domain and peroxidase pair (Figure 1.3), otherwise there is great homology between the basic structures of NOX and DUOX[99,100] (Figure 1.3). NADPH oxidase enzymes are widely distributed in various tissues and can also be found in different cellular compartments (Table 1.1). The NOX enzymes are transmembrane proteins located on plasma membrane surfaces. Intracellularly, they are located in the endoplasmic membrane, mitochondria, nuclear membrane and traffic vesicles. Intracellular localization has mainly been described for NOX1, NOX4 and NOX5[99–101].

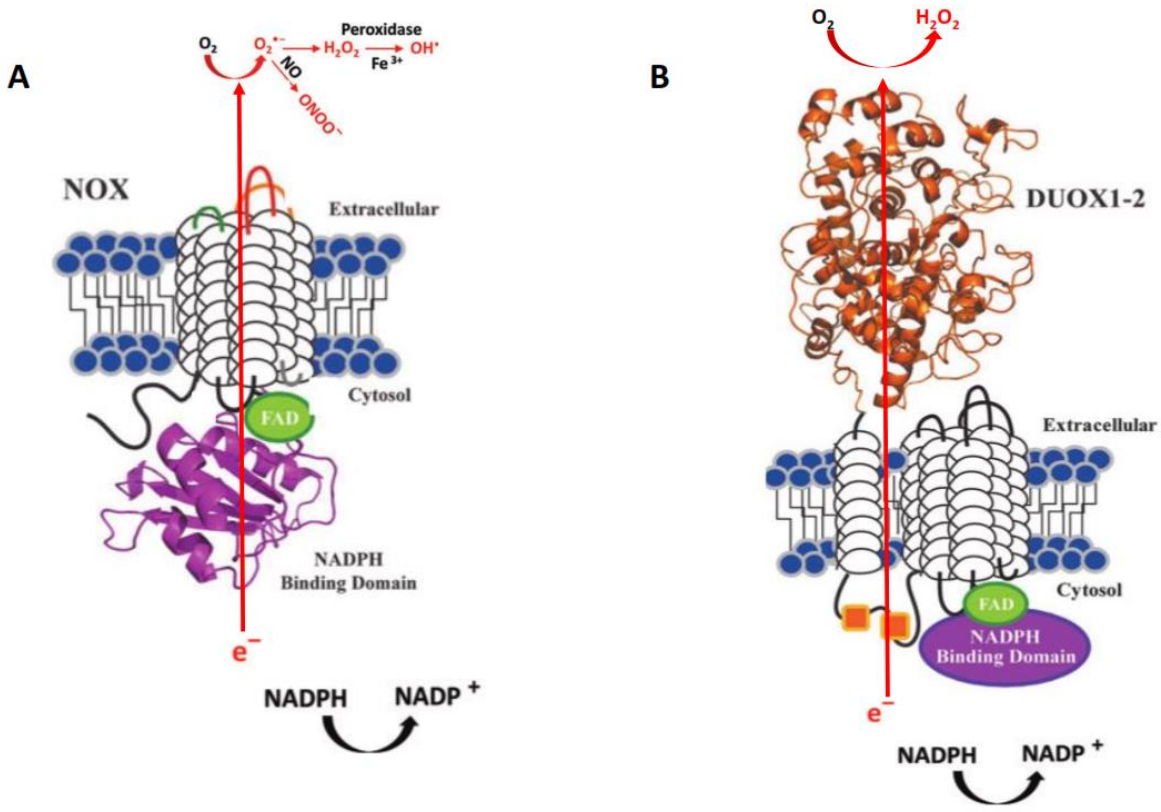

Figure 1.3 Structure of and ROS production of NOX and DUOX enzymes.
NOX and DUOX enzymes consist of six transmembrane alpha helices (white cylindrical loops) with FAD (green) and NADPH binding domains (purple). DUOX isoforms have an extra transmembrane alpha helix, a peroxidase homology located in the extracellular space and two cytosolic calcium binding sites (orange squares). NOX enzymes catalyse the reduction of molecular oxygen to form superoxide using NADPH as the electron donor and oxygen as the electron acceptor. $O_2^{\bullet-}$ can be dismutated by superoxide dismutase to H_2O_2 which in turn can react with nitric oxide to give peroxynitrate. DUOX isoforms can directly generate H_2O_2 from molecular oxygen. *Adapted from Atashi F, Modarressi A, Pepper MS. The role of reactive oxygen species in mesenchymal stem cell adipogenic and osteogenic differentiation: a review. Stem Cells Dev. 2015;24(10):1150–63 and Meitzler JL, Antony S, Wu Y, Juhasz A, Liu H, Jiang G, et al. NADPH Oxidases: A Perspective on Reactive Oxygen Species Production in Tumor Biology. Antioxid Redox Signal. 2014;20(17):2873–89.*

To initiate ROS production, it has been reported that NOX isoforms interact with one or more cytoplasmic and membrane associated proteins. These interaction partners play a role in facilitating electron transfer by bringing FAD and NADPH into close proximity[101]. Generally, NOX1 to 4 all form complexes with the membrane bound $p22^{phox}$ association factor as a binding partner. In addition to $p22^{phox}$, NOX isoforms also bind to other different

cytosolic regulatory components depending on the isoform as shown in Table 1.1. In contrast, NOX5, DUOX1, DUOX2, have no known binding partners necessary to initiate ROS production. NOX4 differs from other NOX isoforms by only requiring $p22^{phox}$ for activation[99–101].

Table 1.1 NOX isoforms binding partners, cellular and tissue distribution

Adapted from Meitzler JL, Antony S, Wu Y, Juhasz A, Liu H, Jiang G, et al. NADPH Oxidases: A Perspective on Reactive Oxygen Species Production in Tumor Biology. Antioxid Redox Signal. 2014;20(17):2873–89. and Maraldi T. Natural compounds as modulators of NADPH oxidases. Oxid Med Cell Longev. 2013;2013:271602.

NOX isoform	Interaction partners	Cellular localization	Major tissue distribution
NOX1	$p22^{phox}$, $NOXA1/p67^{phox}$ $NOXO1/p47^{phox}$, Rac, Hsp90	Plasma membrane caveolae, redoxisomes	Colon epithelium, endothelial cells, uterus, placenta, prostate, osteoclasts
NOX2	$p22^{phox}$, $p47^{phox}$, $p67^{phox}$, $p40^{phox}$, Rac1/2	Plasma membrane, phagosomes, cytoskeleton	Phagocytes, CNS, endothelium, fibroblasts, hepatocytes.
NOX3	$p22^{phox}$, $NOXA1/p67^{phox}$, $NOXO1/p47^{phox,}$ Rac	Plasma membrane	Inner ear, fetal tissues
NOX4	$p22^{phox}$	Plasma membrane, nucleus, endoplasmic reticulum, mitochondria	Ubiquitously expressed but highly in the kidney.
NOX5	No partner essential for activity has been discovered.	Plasma membrane, ER, nuclear membrane	Spleen, testis, lymph node, endothelial cells, spleen, uterus.
DUOX1	DUOXA1, Ca^{2+}	Plasma membrane	Thyroid, respiratory epithelium.
DUOX2	DUOXA2, Ca^{2+}	Plasma membrane	Thyroid, colon, pancreas

Rac - Ras-related C3 botulinum toxin substrate 1

Ca^{2+} - Calcium ion

DUOX - Dual oxidase

Hsp90 - heat shock protein 90

NOX - NADPH oxidase

ROS production by NOX enzymes is through one-electron reduction of oxygen to superoxide[101]. Following activation of NOX enzymes, electron transfer from NADPH to FAD is activated. Thereafter, an electron is passed to a haem group which subsequently transfers the electron to molecular oxygen generating superoxide[94,100,101] (Figure 1.3). Other ROS, such as H_2O_2 and peroxynitrite are also produced as secondary products (Figure 1.3). The superoxide can either be dismutated by the action of the enzyme superoxide dismutase (SOD) producing H_2O_2 or can react directly with nitric oxide to generate peroxynitrite[101]. The H_2O_2 produced can also undergo the Fenton reaction where it is converted in a spontaneous reaction catalysed by Fe^{2+} to the highly reactive hydroxyl radical[94,100].

1.5.2 Mitochondria

Mitochondria are the principal sites of adenosine triphosphate (ATP) generation in cells through mitochondrial oxidative phosphorylation[102,103]. Approximately 0.15 - 2% of cellular oxygen consumption by mitochondrial oxidative phosphorylation results in superoxide ROS production[102,104,105]. Mitochondria are the principal generators of ROS in cellular systems through the mitochondrial electron transport chain[92,94]. The electron transport chain system is composed of four multiprotein complexes namely Complex I (NADH-Coenzyme Q oxidoreductase), Complex II (succinate-Coenzyme Q oxidoreductase), Complex III (coenzyme Q-cytochrome c oxidoreductase) and Complex IV (cytochrome c oxidase)[106]. The system also comprises of coenzyme Q and cytochrome C which are mobile electron carriers[107] (Figure 1.4).

In this system, electrons are transferred from electron donors to electron acceptors with the concomitant transfer of protons (H^+) from the matrix into the intermembrane space. This process generates an electrochemical gradient which provides energy to produce ATP by Complex V (ATP synthase). Complex I accepts electrons from NADH via flavin mononucleotide (FMN) and transfers them to oxidized Coenzyme Q (ubiquinone) reducing it to ubiquinol[107–109]. Complex II catalyses the oxidation of succinate to fumarate resulting in an electron transfer from reduced flavin adenine dinucleotide ($FADH_2$) to ubiquinone reducing it to ubiquinol as well[107,110]. Ubiquinol then transfers electrons to

Complex III which in turn passes the electrons to cytochrome C. From cytochrome C, electrons are passed to Complex IV which then in combination with hydrogen ions uses the electrons to reduce molecular oxygen the to water[103,107] (Figure 1.4).

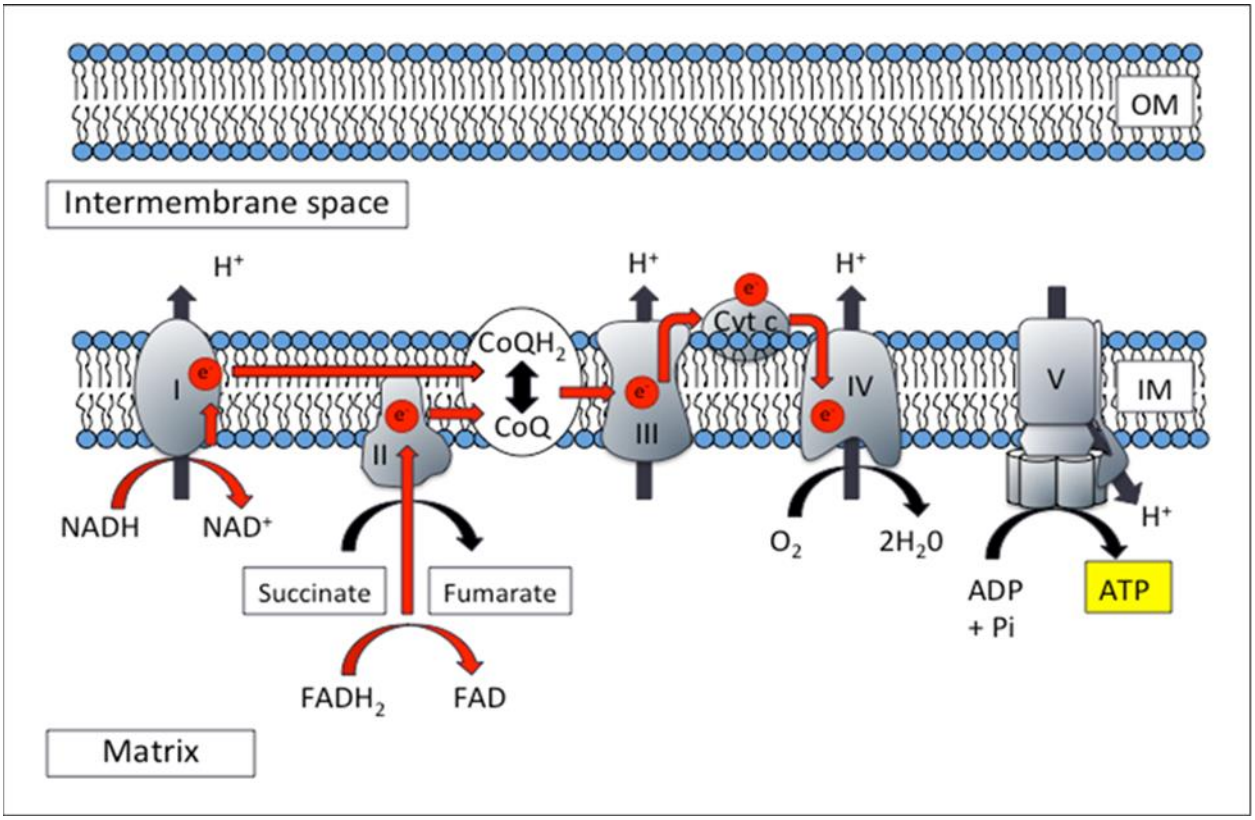

Figure 1.4 Mitochondrial electron transport chain
Electrons flow from Complex I through to Complex IV where they are finally received by molecular oxygen and water is formed. During electron transport, protons are transferred into the intermembrane space generating a proton gradient that provides energy for ATP generation by Complex V. CoQ - Coenzyme Q (ubiquinone); $CoQH_2$ - ubiquinol; Cyto c - cytochrome c; FAD - flavin adenine dinucleotide; $FADH_2$ - reduced flavin adenine dinucleotide; OM - outer membrane; IM - inner membrane. *Reprinted from de Villiers D, Potgieter M, Ambele MA, Adam L, Durandt C, Pepper MS. The role of reactive oxygen species in adipogenic differentiation. in: advances in experimental medicine and biology. Springer, Boston, MA; 2017. p. 125-144. Image reproduced with permission of the rights holder*, *Springer*.

During the electron transfer process, some electrons leak out to molecular oxygen forming superoxide[103,111] (Figure 1.5). Several enzymes have been implicated as sites of ROS production within mitochondria. The major mitochondrial ROS generators are in the electron transport chain notably Complex I and III[112,113]. Complex II has also been described as a possible mitochondrial ROS generator however, its role in this regard remains to be clearly defined[111,112]. Superoxide generated at Complex I is dismutated by the action of the MnSOD to form H_2O_2 which is released into the mitochondrial matrix[103]. Hydrogen peroxide in the presence of Fe^{2+}, and Cu^{+} can be converted into the highly reactive hydroxyl radical through the Fenton reaction[103,114]. Complex III derived superoxide is released into the intermembrane space and in the matrix where it is dismutated by the Cu/ZnSOD to give H_2O_2. Glutathione peroxidase (GPX) present in the matrix is the major enzyme that decomposes mitochondrial H_2O_2 in the matrix to water. Glutathione peroxidase utilises glutathione (GSH) as a substrate and GSH becomes oxidized to GSSG in the reaction[114] (Figure 1.5). Superoxide generated in the mitochondria is not strictly confined to this location. There is some efflux of superoxide into the cytosol where it is converted to H_2O_2 by cytosolic CuZnSOD together with superoxide derived from cytochrome P450 enzymes. In the cytosol H_2O_2 is degraded by catalase into water[115]. Apart from mitochondrial electron transport chain enzymes, other enzymes within the mitochondria are also known to produce ROS, these include $p66^{Shc}$, dihydrolipoamide dehydrogenase, monoamine oxidase A and B, mitochondrial nitric oxide synthase and cytochrome b5 reductase[112]. Interestingly, mitochondria have been reported to contain a NOX4 isoform that is a H_2O_2 generator. However, the role of NOX4 in mitochondria remains to be further clarified[116,117].

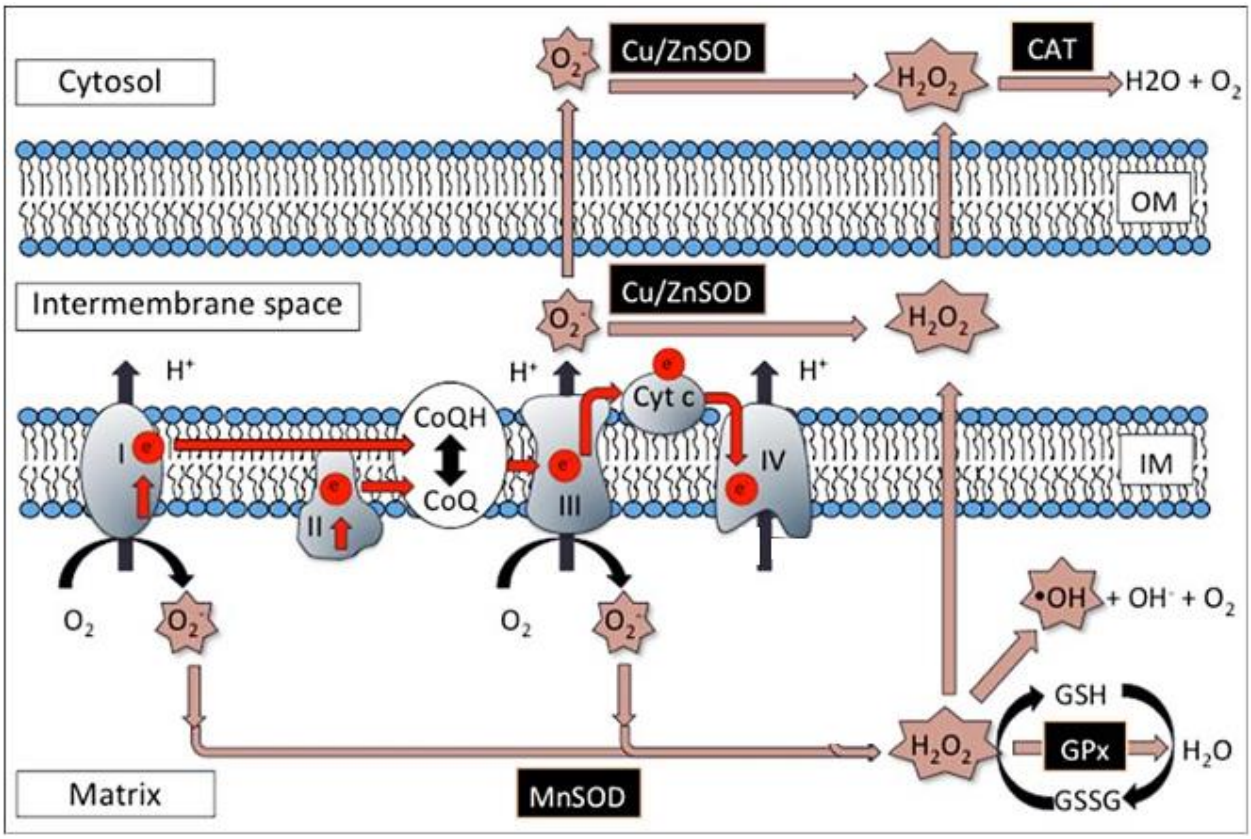

Figure 1.5 Mitochondrial ROS production.
Electron leakage to molecular oxygen occurs during electron transfer and this results in superoxide production either in the matrix or intermembrane space at Complexes I and III. MnSOD in the matrix and CuZnSOD in the intermembrane space or cytosol form H_2O_2 from superoxide. The H_2O_2 is then decomposed by the enzymes catalase or glutathione peroxidase to water and oxygen. Part of the H_2O_2 can also be converted to the hydroxyl radical through the Fenton reaction. MnSOD - manganese superoxide dismutase; Cu/ZnSOD - Copper- and zinc- superoxide dismutase; GPX - Glutathione peroxidase; GSH – glutathione; GSSG - oxidized glutathione. *Reprinted from de Villiers D, Potgieter M, Ambele MA, Adam L, Durandt C, Pepper MS. The role of reactive oxygen species in adipogenic differentiation. in: advances in experimental medicine and biology. Springer, Boston, MA; 2017. p. 125-144. Image reproduced with permission of the rights holder*, *Springer*.

1.6 Antioxidants

Antioxidant systems are developed by cells principally as a defence mechanisms against ROS[21,118]. Antioxidants are substances that when present in small quantities can reduce or prevent the oxidation of other molecules and substances[19–21,119,120]. Antioxidant systems can be derived either endogenously or exogenously. Endogenous antioxidants

are synthesized by various cellular systems in the body which can further be divided into enzymatic and non-enzymatic antioxidants[21,95,121]. Enzymatic antioxidants include superoxide dismutase, catalase, glutathione peroxidases, glutathione reductase etc. while non-enzymatic antioxidants include vitamin E (tocopherols and tocotrienols), vitamin C, flavonoids, carotenoids, N-acetyl cysteine, genistein, resveratrol, Trolox, Coenzyme Q10 (CoQ10) among others[95,121]. Exogenous antioxidants are from external sources like food (e.g. vegetables, fruits), supplements and other dietary sources with examples including vitamins (A, C, E) and phytochemicals (e.g. flavonoids, catechins, apocynin, coumarins etc.)[21]. Antioxidants have different modes of action in their defence against ROS induced damages, which include preventing ROS formation, scavenging of the ROS that is inhibition of chain reaction initiation and/or breaking of breaking chain reactions initiated by ROS and repairing of oxidized molecules (Figure 1.6)[122].

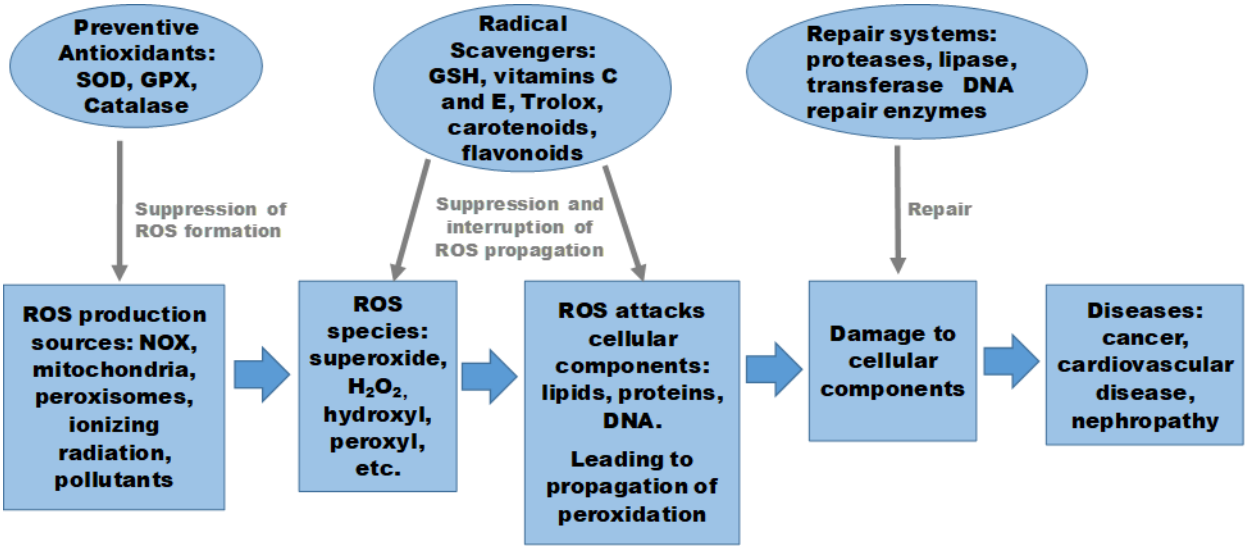

Figure 1.6 Antioxidant defence mechanism against ROS attack
Antioxidants operate at different levels in their defence against ROS damage. Mechanisms range from prevention of ROS formation and propagation, chain breaking by electron donation to free radical forming stable products to repair systems which restore damaged components and molecules. SOD - superoxide dismutase; GPX - Glutathione peroxidase; NOX - NADPH oxidase; ROS - reactive oxygen species; DNA - Deoxyribose nucleic acid.

1.6.1 Preventive antioxidants

Preventive antioxidants block the formation of ROS as their mechanism of action[95]. Examples include SOD that quenches the highly reactive superoxide to H_2O_2 as well as catalase which breaks down H_2O_2 to water and oxygen. Another example is glutathione peroxidase (GPx) that catalyses the reduction of H_2O_2 and lipid hydroperoxide to water using reduced glutathione (GSH) as a substrate[95,118,123].

1.6.2 Radical scavengers

Free radical species can react with other molecules generating secondary radicals that can interact with other molecules to produce more radicals thus resulting in chain reactions[124]. Scavenging of free radicals/ROS is another mode of action by antioxidants against ROS-induced damages. Antioxidants in this class inhibit chain reaction initiation as well as disrupt chain reactions forming resulting in products that are less reactive[21,122,124]. The free radical scavenging mechanism of action is based on scavengers either receiving an electron from a radical or electron donation to a radical forming more stable products[124]. Thus blocking chain reaction formation and/or prevent the propagation of chain reactions[124]. Such radical scavengers include GSH, vitamin C, uric acid, bilirubin, vitamin E, Trolox, carotenoids, flavonoids, apocynin, ubiquinol among others[118,21,124].

Vitamins, particularly vitamins C and E, play a crucial role as ROS scavenging antioxidants. Vitamin C is a water-soluble antioxidant that has been reported to interact indirectly with superoxide, H_2O_2, hydroxyl and peroxyl radicals. The vitamin C scavenging mechanism is based on electron donation to a free radical forming a stable product[124,125]. Vitamin E, notably its biologically active form α-tocopherol is an excellent scavenger of lipid peroxyl radicals both *in vitro* and *in vivo*[126]. Vitamin E scavenges through hydrogen atom or electron transfer to radicals yielding stable non-radical products. The scavenging reaction results in the formation of lipid hydroperoxide and a Vitamin E radical. The vitamin E radical can either react with another radical forming a stable product or may react with ascorbate or ubiquinol regenerating vitamin E. However, *in vivo* vitamin E is not an efficient scavenger of hydroxyl and alkoxyl radicals[125,126].

Trolox (6-hydroxy- 2, 5, 7, 8-tetramethylchromane-2-carboxylic acid) is a cell permeable, water soluble analogue of vitamin E. It is a direct scavenger of peroxyl radicals ($RO_2^{\bullet}$) and H_2O_2[19,127,128]. Trolox is a more efficient ROS scavenger as compared to vitamin E owing to its solubility in both lipid and aqueous phases[19,129]. Like vitamin E, the scavenging action of Trolox is based on rapid one electron or hydrogen atom transfer to peroxyl radicals. This converts peroxyl radical to hydroperoxide (RO_2H) thereby terminating the chain reaction as shown by the equation below[130,131].

Equation 1.1

$$Trolox + RO_2^{\bullet} \longrightarrow Trolox^{\bullet} + RO_2H$$

The donation of a hydrogen atom from Trolox results in the formation of a Trolox phenoxyl radical that is relatively stable and can be repaired by thiols[131]. Trolox has however been reported to be a prooxidant under certain conditions. In a study by Wattamwar and colleagues (2011), the presence of Cu^{2+} changed Trolox from being antioxidant to prooxidant. Suggesting the role of the Cu^{2+}/Cu^{+} redox recycling in the prooxidant mechanism[127,132]. The exact mechanism for Trolox's prooxidant action is not fully defined[133].

Apocynin is a plant derived natural organic compound that can be isolated from the roots of *Picrorhiza kurroa* and *Apocynum cannabinum* (Canadian hemp)[99,134–136]. Apocynin is widely used as an inhibitor of NOX activity both *in vitro* and *in vivo.* The mechanism of action is based on the disruption of NOX assembly through inhibition of $p47^{phox}$ assembly with the membrane thus, inhibiting NOX activation. As a result, apocynin is described as an inhibitor of superoxide production[99,137,138]. Furthermore, apocynin has been reported to also act as a ROS scavenger in some studies. In experiments by Sun and colleagues (2015), treatment of bone marrow stromal cells with 100 µM apocynin was observed to decrease intracellular ROS levels[134]. In agreement with this observation, Heumüller and colleagues (2008) also reported that in vascular endothelial and smooth muscle cells apocynin had a ROS scavenging effect[139]. However, the mechanism of ROS scavenging by apocynin remains largely unknown.

1.6.3 Repair mechanisms

Oxidative stress leads to production of peroxides and free radicals that damage cellular components including proteins, lipids, and DNA[97]. Antioxidative defence mechanisms include repair of oxidative-associated damage to DNA and protein structures and prevention of oxidation of lipids. Antioxidants in this group comprise proteases, lipase, DNA repair enzymes, transferase, methionine sulphoxide reductase among others. The main function of these antioxidants is to restore damaged biomolecules and cell membranes[21,118,122,140]. A disturbance in the balance between production of ROS and antioxidant defences in favour of ROS results in oxidative stress. Oxidative stress contributes to pathological conditions like cancer, atherosclerosis, hypertension, diabetes and asthma[97]. Antioxidants thus play a beneficial role in maintaining a favourable redox balance in cells.

1.7 Role of reactive oxygen species in adipogenesis

ROS play a crucial role in regulating and initiating a number of cellular metabolic processes[141]. Using different cell models, various studies have reported that both endogenous and exogenous ROS enhance the process of adipogenesis[94,142–144]. However, to date the molecular mechanisms governing the role of ROS in adipogenesis is still a subject of debate and requires further research[15,94,144].

In experiments by Higuchi and colleagues (2013), the differentiation of human ASCs into adipocytes was accompanied by an increase in intracellular ROS production. Treatment of these ASCs with the antioxidant N-acetylcysteine (NAC) and EUK-8, a catalase and SOD mimetic throughout the differentiation period inhibited adipogenic differentiation. These observations clearly indicate that ROS are involved in adipogenic regulation[142]. Similar findings were reported in 3T3-L1 cells, where an increase in differentiation was accompanied by an increased in ROS production. This ROS increase was ameliorated in a dose dependent manner by treatment with the antioxidant NAC[145]. Furthermore, in agreement with the above studies, differentiated mouse stromal OP9 preadipocytes showed a positive correlation between lipid droplet accumulation and intracellular superoxide ROS accumulation. This increase was suppressed by fullerenols

(antioxidants)[146]. The above findings suggest that intracellular generated ROS mediate adipogenic differentiation.

Cells can endogenously synthesise ROS from multiple sources, in stem cells and adipocytes the major ROS sources are NOX4, and mitochondrial-derived ROS[106,111]. The influence of ROS generated from each of these sources on adipogenesis is discussed below.

1.7.1 Mitochondrial-derived ROS and adipogenesis

In a study by Tormos and colleagues (2011), mitochondrial Complex III generated ROS promoted adipogenic differentiation of human MSCs. There was an observed increase in lipid accumulation that was accompanied by an increase in mitochondrial ROS production. This increase was attenuated by mitochondrial targeted antioxidants MitoCP and MitoCTPO. Furthermore, adipocyte differentiation previously inhibited by mitochondrial targeted antioxidants was rescued by exogenous addition of H_2O_2. These findings clearly indicate that ROS (regardless of source) are essential for adipogenic differentiation. The possible mechanism of action by mitochondrial ROS was likely through activation of PPARγ2, C/EBPα, FABP4 and adiponectin as the presence of MitoCP and MitoCTPO significantly reduced the level of these proteins[147]. Higuchi and colleagues (2013) confirmed these findings by showing that rotenone (a mitochondrial chain inhibitor) suppressed triglyceride accumulation, thereby indicating that mitochondrial ROS plays a role in mediating adipogenesis[142]. In addition, Kim and colleagues (2013) demonstrated that hypoxia induced mitochondrial ROS production enhanced adipocyte differentiation. This differentiation was inhibited by MitoCP, showing that ROS mediates adipogenesis. The possible mechanism of action in the hypoxia induced adipocyte differentiation was through the PI3K/AKT/mTOR pathway[148].

In contrast however, studies by Carriere and colleagues (2004) revealed a negative correlation between mitochondrial ROS generation and adipogenic differentiation in 3T3 F442A preadipocytes. Mitochondrial complex I and III inhibition by rotenone and antimycin respectively resulted in an increase in ROS production. This increase was

accompanied by a decrease in adipogenesis. Furthermore, treatment of 3T3 F442A preadipocytes with mitochondrial complex I inhibitor propofol (also a free radical scavenger) enhanced adipocyte differentiation. Taken together, these observations demnostrate that in 3T3 F442A preadipocytes, mitochondrial ROS production is associated with inhibition of adipogenesis[149]. The role of mitochondria in regulating adipogenesis is complex and appears to be cell type specific. Above all, the function of mitochondrial ROS in adipogenesis remains largely unknown[17].

1.7.2 NADPH oxidase-derived ROS and adipogenesis

NOX derived ROS are also implicated in modulating adipogenic differentiation. Kanda and colleagues (2011) demonstrated that intracellular generated ROS enhanced adipocyte differentiation in murine CH310T1/2 MSCs. Knockdown of NOX4 by RNA interference and treatment with the antioxidant NAC blocked ROS production and adipocyte differentiation. NOX4 derived ROS mediation of adipogenesis was via regulating the proadipogenic factor CREB which acts upstream of PPARγ and C/EBPα[1]. Similar findings were reported by Schroder and colleagues (2009) who observed that insulin induced adipogenic differentiation in human preadipocytes and mouse 3T3-L1 fibroblasts was dependent on NOX4 generated ROS[150]. These findings were also confirmed by Drehmer and colleagues (2016) where NADPH oxidase-derived ROS production in human ASCs was increased 3 days after adipogenic differentiation. This increase corresponded with an upregulation of key adipogenic genes, FABP4 and PPARγ suggesting that NADPH oxidase-derived ROS maybe involved in differentiation commitment. Apocynin, a NOX inhibitor blocked ROS production, implicating NOX derived ROS as a possible mediator in adipogenesis[151]. Higuchi and colleagues (2013) demonstrated that lentiviral overexpression of NOX4 in human ASCs promote adipogenesis with a concomitant increase in ROS production, further supporting previous studies on the role of NOX4 derived ROS in adipogenesis[142].

Contrary to the positive role of NOX enzymes especially NOX4 in adipogenic differentiation, Kim and colleagues (2013) reported that in human ASCs, NOX4 derived ROS did not induce an increase in adipocyte differentiation. This they confirmed by

inhibiting NOX4 with dibenziodolium chloride and silencing NOX4 through siRNA transfection of human ASCs. Lipid accumulation as well as PPARγ and C/EBPα expression were not suppressed by the inhibition or silencing of NOX4. These findings suggest that NOX4 induced ROS does not mediate adipocyte differentiation[148].

ROS derived from extracellular sources has been implicated in adipogenic regulation both *in vivo* and *in vitro*[142,143,152]. *In vivo*, adipose tissue is the major source of extracellular ROS production[144,153]. This was demonstrated in experiments by Furukawa and colleagues (2004) who showed that adipose tissue of obese KKAy mice have elevated ROS levels when compared to other tissues (liver, skeletal muscle and aorta)[153]. As such, adipose tissue is a source of extracellular ROS production which can have an influence on adipogenesis in an autocrine or endocrine manner[154]. To demonstrate that ROS plays a role in obesity *in vivo,* treatment of mice with the antioxidants apocynin and Tempol has been reported to reduce obesity and obesity-related complications in obese mice models[153,155].

Several *in vitro* studies have also reported on the role of exogenous ROS addition to adipogenesis. Lee and colleagues (2009) treated 3T3-L1 preadipocytes with H_2O_2 followed by hormonal stimulation, this led to enhanced adipocyte differentiation through accelerating mitotic clonal expansion. Differentiation was inhibited by the antioxidants NAC, genistein and resveratrol showing that ROS was involved in the differentiation process[143]. In human ASCs, exogenous addition of 100 μm H_2O_2 for 8 days enhanced adipogenesis as demonstrated by increased Oil Red O staining[142]. Oil red O is a fat soluble dye that is used for the staining of intracellular lipid droplets in adipocytes[156]. Furthermore, extracellular addition of H_2O_2 to 3T3-L1 preadipocytes increased adipogenic differentiation in a dose dependent manner[152].

ROS, regardless of source, mediate adipogenesis in a variety of cellular models. Although the exact mechanism involved in ROS mediation of adipogenesis remains unknown, the upregulation of transcription factors PPARγ and C/EBPβ is most likely involved in the proadipogenic effect of ROS[144]. The regulation of adipogenesis by ROS is also believed

to be through induction of adipogenic differentiation and an increase in intracellular lipid accmulation[142]. Despite decades of study, there is still a gap in our understanding of the exact mechanisms and molecular players involved in adipogenesis, although it is widely accepted that ROS are involved in regulating adipogenesis. ROS appear to exhibit different effects on the adipogenic differentiation process depending on the time of exposure, source, intracellular location, concentration and cellular models used. This study will investigate the effects of ROS scavenging in adipogenic differentiation of primary human ASCs *in vitro*, through the addition of the antioxidants Trolox and apocynin. Outcomes of this study will provide valuable knowledge linking ROS, ROS scavengers and adipogenesis in ASCs. This could potentially be exploited in the identification of novel therapeutic targets for improving treatment strategies for obesity and its comorbidities.

1.8 Aim

To investigate the effect of reactive oxygen species (ROS) and ROS scavengers on adipogenesis.

1.9 Hypothesis

Reactive oxygen species scavengers enhance adipogenesis.

1.10 Objectives

i. To isolate and characterize human adipose derived stroma/stem cells from lipoaspirates and solid fat tissues.

ii. To quantitatively investigate adipogenesis using the stain Nile Red in the presence or absence of Trolox and apocynin.

iii. To measure the intracellular ROS levels during adipogenesis in the presence or absence of Trolox and apocynin.

iv. To measure extracellular ROS levels during adipogenesis in the presence or absence of Trolox and apocynin.

v. To investigate the effect of exogenous H_2O_2 addition on adipogenesis in the presence or absence of Trolox and apocynin.

References

1. Kanda Y, Hinata T, Won S, Watanabe Y. Reactive oxygen species mediate adipocyte differentiation in mesenchymal stem cells. Life Sci. 2011;89(7–8):250–8.
2. Stephens JM. The fat controller : adipocyte development. PLoS Biol. 2012;10(11):e1001436.
3. Negash S, Agyemang C, Matsha TE, Peer N, Erasmus RT, Kengne AP. Differential prevalence and associations of overweight and obesity by gender and population group among school learners in South Africa: a cross-sectional study. BMC Obes. 2017;4(1):29.
4. Obesity and overweight [Internet]. World Health Organization; [cited 2017 Apr 25]. Available from: http://www.who.int/en/news-room/fact-sheets/detail/obesity-and-overweight
5. The Department of Health:South Africa. South African demographic and health survey 2016. Statistics South Africa. 2017.
6. Han TS, Sattar N, Lean M. ABC of obesity. Assessment of obesity and its clinical implications. BMJ. 2006;333(7570):695–8.
7. Kushner RF. Clinical assessment and management of adult obesity. Circulation. 2012;126(24):2870–7.
8. Global database on body mass index [Internet]. World Health Organization. [cited 2017 Nov 15]. Available from: http://apps.who.int/bmi/index.jsp?introPage=intro_3.html
9. Patel P, Abate N. Body fat distribution and insulin resistance. Nutrients. 2013;5(6):2019–27.
10. Adeboye B, Bermano G, Rolland C. Obesity and its health impact in Africa: a systematic review. Cardiovasc J Afr. 2012;23(9):512–21.
11. Reilly SM, Saltiel AR. Adapting to obesity with adipose tissue inflammation. Nat Rev Endocrinol. 2017;13(11):633–43.
12. The Department of Health:South Africa. Strategy for prevention and control of obesity in South Africa. 2015.
13. Marseglia L, Manti S, D'Angelo G, Nicotera A, Parisi E, Di Rosa G, et al. Oxidative stress in obesity: a critical component in human diseases. Int J Mol Sci. 2015;16(1):378–400.
14. Aroor AR, DeMarco VG. Oxidative stress and obesity: the chicken or the egg? Diabetes. 2014;63(7):2216–8.
15. de Villiers D, Potgieter M, Ambele MA, Adam L, Durandt C, Pepper MS. The role of reactive oxygen species in adipogenic differentiation. In: Advances in Experimental Medicine and Biology. Springer, Boston, MA; 2017. p. 125–44.

16. Fernández-Sánchez A, Madrigal-Santillán E, Bautista M, Esquivel-Soto J, Morales-González Á, Esquivel-Chirino C, et al. Inflammation, oxidative stress, and obesity. Int J Mol Sci. 2011;12(5):3117–32.

17. Liu G-S, Chan EC, Higuchi M, Dusting GJ, Jiang F, Hospital Q. Redox mechanisms in regulation of adipocyte differentiation: beyond a general stress response. Cells. 2012;1(4):976–93.

18. Castro JPJP, Grune T, Speckmann B, Access O. The two faces of reactive oxygen species (ROS) in adipocyte function and dysfunction. Biol Chem. 2016;397(8):709–24.

19. Hamad I, Arda NN, Pekmez M, Karaer S, Temizkan G. Intracellular scavenging activity of Trolox (6hydroxy2,5,7,8tetramethylchromane2carboxylic acid) in the fission yeast, Schizosaccharomyces pombe. J Nat Sci Biol Med. 2016;1(1):16–21.

20. Lü J, Lin PH, Yao Q, Chen C. Chemical and molecular mechanisms of antioxidants : experimental approaches and model systems. J Cell Mol Med. 2010;14(4):840–60.

21. Noor S. An overview of oxidative stress and antioxidant defensive system. Open Access Sci Reports. 2012;1(8):1177–88.

22. Youn U-YY, Shon M-SS, Kim G-NN, Katagiri R, Harata K, Ishida Y, et al. Antioxidant and anti-adipogenic activities of chestnut (Castanea crenata) byproducts. Food Sci Biotechnol. 2016;25(4):1169–74.

23. Lee YJ, Kim DB, Lee JS, Cho JH, Kim BK, Choi HS, et al. Antioxidant activity and anti-adipogenic effects of wild herbs mainly cultivated in Korea. Molecules. 2013;18(10):12937–50.

24. Yoo S-R, Seo C-S, Kim O-S, Shin H-K, Jeong S-J. Anti-adipogenic and antioxidant effects of the traditional Korean herbal formula Samchulgeonbi-tang: an in vitro study. Int J Clin Exp Med. 2015;8(6):8698–708.

25. Gesta S, Kahn CR. White adipose tissue. In: Symonds ME, editor. Adipose Tissue Biology. Springer, Cham; 2017. p. 149–99.

26. Scioli MG, Bielli A, Gentile P, Mazzaglia D, Cervelli V, Orlandi A. The biomolecular basis of adipogenic differentiation of adipose-derived stem cells. Int J Mol Sci. 2014;15:6517–26.

27. Luo L, Liu M. Adipose tissue in control of metabolism. J Endocrinol. 2016;231(3):R77–99.

28. Ehrlund A, Acosta JR, Björk C, Hedén P, Douagi I, Arner P, et al. The cell-type specific transcriptome in human adipose tissue and influence of obesity on adipocyte progenitors. Sci Data. 2017;4:170164.

29. Lee M-J. Hormonal regulation of adipogenesis. Compr Physiol. 2017;7:1151–95.

30. Ahima RS. Adipose tissue as an endocrine organ. Obesity. 2006;14:242S–249S.

31. Malina RM, Bouchard C, Bar-Or O. Growth, maturation, and physical activity. 2nd

ed. Champaign, IL: Human Kinetics; 2004.

32. Rosen ED, Spiegelman BM. What we talk about when we talk about fat. Cell. 2013;156(1–2):20–44.

33. Park A, Kim KW, Bae K-H. Distinction of white, beige and brown adipocytes derived from mesenchymal stem cells. World J Stem Cells. 2014;6(1):33–42.

34. Esteve Rafols M. Adipose tissue: cell heterogeneity and functional diversity. Endocrinol Nutr. 2014;61(2):100–12.

35. Lee M-J, Wu Y, Fried SK. Adipose tissue heterogeneity: implication of depot differences in adipose tissue for obesity complications. Mol Aspects Med. 2013;34(1):1–11.

36. Kershaw EE, Flier JS. Adipose tissue as an endocrine organ. J Clin Endocrinol Metab. 2004;89(6):2548–56.

37. Tang W, Zeve D, Suh JM, Bosnakovski D, Kyba M, Hammer RE, et al. White fat progenitor cells reside in the adipose vasculature. Science. 2008;322(5901):583–6.

38. Guimarães-Camboa N, Evans SM. Are perivascular adipocyte progenitors mural cells or adventitial fibroblasts? Cell Stem Cell. 2017;20(5):587–9.

39. Tchkonia T, Lenburg M, Thomou T, Giorgadze N, Frampton G, Pirtskhalava T, et al. Identification of depot-specific human fat cell progenitors through distinct expression profiles and developmental gene patterns. AJP Endocrinol Metab. 2006;292(1):E298–307.

40. Tchkonia T, Giorgadze N, Pirtskhalava T, Thomou T, DePonte M, Koo A, et al. Fat depot–specific characteristics are retained in strains derived from single human preadipocytes. Diabetes. 2006;55(9):2571–8.

41. Sanchez-Gurmaches J, Hung C-M, Guertin DA. Emerging complexities in adipocyte origins and identity. Trends Cell Biol. 2016;26(5):313–26.

42. Guimarães-Camboa N, Cattaneo P, Sun Y, Moore-Morris T, Gu Y, Dalton ND, et al. Pericytes of multiple organs do not behave as mesenchymal stem cells in vivo. Cell Stem Cell. 2017;20(3):345–359.e5.

43. Vishvanath L, Long JZ, Spiegelman BM, Gupta RK. Do adipocytes emerge from mural progenitors? Cell Stem Cell. 2017;20(5):585–6.

44. Ali AT, Hochfeld WE, Myburgh R, Pepper MS. Adipocyte and adipogenesis. Eur J Cell Biol. 2013;92:229–36.

45. Kahn CR. Can we nip obesity in its vascular bud? Science. 2008;322(5901):542–3.

46. Majka SM, Fox KE, Psilas JC, Helm KM, Childs CR, Acosta AS, et al. De novo generation of white adipocytes from the myeloid lineage via mesenchymal intermediates is age, adipose depot, and gender specific. Proc Natl Acad Sci U S

A. 2010;107(33):14781–6.

47. Crossno JT, Majka SM, Grazia T, Gill RG, Klemm DJ. Rosiglitazone promotes development of a novel adipocyte population from bone marrow-derived circulating proge. J Clin Invest. 2006;116(12):3220–8.

48. Billon N, Iannarelli P, Monteiro MC, Glavieux-Pardanaud C, Richardson WD, Kessaris N, et al. The generation of adipocytes by the neural crest. Development. 2007;134(12):2283–92.

49. Sowa Y, Imura T, Numajiri T, Takeda K, Mabuchi Y, Matsuzaki Y, et al. Adipose stromal cells contain phenotypically distinct adipogenic progenitors derived from neural crest. PLoS One. 2013;8(12):e84206.

50. Gregoire FM, Smas CM, Sul HS. Understanding adipocyte differentiation. Physiol Rev. 1998;78(3):783–809.

51. Otto TC, Lane MD. Adipose development: from stem cell to adipocyte. Crit Rev Biochem Mol Biol. 2005;40(4):229–42.

52. Ruiz-Ojeda FJ, Ruperez AI, Gomez-Llorente C, Gil A, Aguilera CM. Cell Models and their application for studying adipogenic differentiation in relation to obesity: a review. Int J Mol Sci. 2016;17(7).

53. Moseti D, Regassa A, Kim WK. Molecular regulation of adipogenesis and potential anti-adipogenic bioactive molecules. Int J Mol Sci. 2016;17(1):1–24.

54. Jiang Y, Jo A-Y, Graff JM. Snapshot: adipocyte life cycle. Cell. 2012;150(1):234–234.e2.

55. Ambele MA, Dessels C, Durandt C, Pepper MS. Genome-wide analysis of gene expression during adipogenesis in human adipose-derived stromal cells reveals novel patterns of gene expression during adipocyte differentiation. Stem Cell Res. 2016;16(3):725–34.

56. Symonds ME, editor. Adipose tissue biology. New York: Springer; 2012.

57. Farmer SR. Transcriptional control of adipocyte formation. Cell Metab. 2006;4(4):263–73.

58. Tang Q-Q, Otto TC, Lane MD. Commitment of C3H10T1/2 pluripotent stem cells to the adipocyte lineage. Proc Natl Acad Sci. 2004;101(26):9607–11.

59. Gupta RK, Mepani RJ, Kleiner S, Lo JC, Khandekar MJ, Cohen P, et al. Zfp423 expression identifies committed preadipocytes and localizes to adipose endothelial and perivascular cells. Cell Metab. 2012;15(2):230–9.

60. Hammarstedt A, Hedjazifar S, Jenndahl L, Gogg S, Grunberg J, Gustafson B, et al. WISP2 regulates preadipocyte commitment and PPAR activation by BMP4. Proc Natl Acad Sci. 2013;110(7):2563–8.

61. McBeath R, Pirone DM, Nelson CM, Bhadriraju K, Chen CS. Cell shape, cytoskeletal tension, and RhoA regulate stem cell lineage commitment. Dev Cell.

2004;6(4):483–95.

62. Pairault J, Green H. A study of the adipose conversion of suspended 3T3 cells by using glycerophosphate dehydrogenase as differentiation marker. Proc Natl Acad Sci U S A. 1979;76(10):5138–42.

63. Saben J, Thakali KM, Lindsey FE, Zhong Y, Badger TM, Andres A, et al. Distinct adipogenic differentiation phenotypes of human umbilical cord mesenchymal cells dependent on adipogenic conditions. Exp Biol Med. 2014;239(10):1340–51.

64. Zhao X-Y, Chen X-Y, Zhang Z-J, Kang Y, Liao W-M, Yu W-H, et al. Expression patterns of transcription factor PPARγ and C/EBP family members during in vitro adipogenesis of human bone marrow mesenchymal stem cells. Cell Biol Int. 2015;39(4):457–65.

65. Marquez MP, Alencastro F, Madrigal A, Jimenez JL, Blanco G, Gureghian A, et al. The role of cellular proliferation in adipogenic differentiation of human adipose tissue-derived mesenchymal stem cells. Stem Cells Dev. 2017;26(21):1578–95.

66. Entenmann G, Hauner H. Relationship between replication and differentiation in cultured human adipocyte precursor cells. Am J Physiol. 1996;270(4 Pt 1):C1011-6.

67. Scott MA, Nguyen VT, Levi B, James AW. Current methods of adipogenic differentiation of mesenchymal stem cells. Stem Cells Dev. 2011;20(10):1793–804.

68. Lowe CE, Rahilly O, Rochford JJ. Adipogenesis at a glance. J Cell Sci. 2011;124(16):2681–6.

69. Zhang J-W, Klemm DJ, Vinson C, Lane MD. Role of CREB in transcriptional regulation of CCAAT/enhancer-binding protein beta gene during adipogenesis. J Biol Chem. 2004;279(6):4471–8.

70. Reusch JE, Colton LA, Klemm DJ. CREB activation induces adipogenesis in 3T3-L1 cells. Mol Cell Biol. 2000;20(3):1008–20.

71. Tang QQ, Lane MD. Adipogenesis: from stem cell to adipocyte. Annu Rev Biochem. 2012;81(1):715–36.

72. Siersbæk R, Nielsen R, Mandrup S. PPARγ in adipocyte differentiation and metabolism – novel insights from genome-wide studies. FEBS Lett. 2010;584(15):3242–9.

73. Rosen ED, Hsu C, Wang X, Sakai S, Freeman MW, Gonzalez FJ, et al. C/EBPa induces adipogenesis through PPARg: a unified pathway. Genes Dev. 2002;(16):22–6.

74. Wu Z, Rosen ED, Brun R, Hauser S, Adelmant G, Troy AE, et al. Cross-regulation of C/EBP alpha and PPAR gamma controls the transcriptional pathway of adipogenesis and insulin sensitivity. Mol Cell. 1999;3(2):151–8.

75. Birsoy K, Chen Z, Friedman J. Transcriptional regulation of adipogenesis by KLF4.

Cell Metab. 2008;7(4):339–47.

76. Oishi Y, Manabe I, Tobe K, Tsushima K, Shindo T, Fujiu K, et al. Krüppel-like transcription factor KLF5 is a key regulator of adipocyte differentiation. Cell Metab. 2005;1(1):27–39.

77. Pei H, Yao Y, Yang Y, Liao K, Wu J-R. Krüppel-like factor KLF9 regulates PPARγ transactivation at the middle stage of adipogenesis. Cell Death Differ. 2011;18(2):315–27.

78. Mori T, Sakaue H, Iguchi H, Gomi H, Okada Y, Takashima Y, et al. Role of kruppel-like factor 15 (KLF15) in transcriptional regulation of adipogenesis. J Biol Chem. 2005;280(13):12867–75.

79. Kim JB, Wright HM, Wright M, Spiegelman BM. ADD1/SREBP1 activates PPAR gamma through the production of endogenous ligand. Proc Natl Acad Sci U S A. 1998;95(8):4333–7.

80. Banerjee S Sen, Feinberg MW, Watanabe M, Gray S, Haspel RL, Denkinger DJ, et al. The Krüppel-like factor KLF2 inhibits peroxisome proliferator-activated receptor-gamma expression and adipogenesis. J Biol Chem. 2003;278(4):2581–4.

81. Wu Z, Wang S. Role of kruppel-like transcription factors in adipogenesis. Dev Biol. 2013;373(2):235–43.

82. Tong Q, Dalgin G, Xu H, Ting CN, Leiden JM, Hotamisligil GS. Function of GATA transcription factors in preadipocyte-adipocyte transition. Science. 2000;290(5489):134–8.

83. Hudak CS, Sul HS. Pref-1, a gatekeeper of adipogenesis. Front Endocrinol (Lausanne). 2013;4:79.

84. Wang Y, Kim K-A, Kim J-H, Sul HS. Pref-1, a preadipocyte secreted factor that inhibits adipogenesis. J Nutr. 2006;136(12):2953–6.

85. Andersen C, Rayalam S, Della-Fera MA, Baile CA. Phytochemicals and adipogenesis. BioFactors. 2010;36(6):415–22.

86. Rayalam S, Della-Fera MA, Baile CA. Phytochemicals and regulation of the adipocyte life cycle. J Nutr Biochem. 2008;19(11):717–26.

87. Ibrahimi A, Sfeir Z, Magharaie H, Amri EZ, Grimaldi P, Abumrad NA. Expression of the CD36 homolog (FAT) in fibroblast cells: effects on fatty acid transport. Proc Natl Acad Sci U S A. 1996;93(7):2646–51.

88. Burkhardt AM, Zlotnik A. Translating translational research: mouse models of human disease. Cell Mol Immunol. 2013;10(5):373–4.

89. Kawaguchi N, Toriyama K, Nicodemou-Lena E, Inou K, Torii S, Kitagawa Y. De novo adipogenesis in mice at the site of injection of basement membrane and basic fibroblast growth factor. Cell Biol. 1998;95:1062–6.

90. Sharma P, Jha AB, Dubey RS, Pessarakli M. Reactive oxygen species, oxidative

damage, and antioxidative defense mechanism in plants under stressful conditions. J Bot. 2012;2012:1–26.

91. Nonell S, Flors C, editors. Singlet oxygen. The Royal Society of Chemistry; 2016. 1-21 p.

92. Abdal Dayem A, Hossain MK, Lee S Bin, Kim K, Saha SK, Yang G-M, et al. The role of reactive oxygen species (ROS) in the biological activities of metallic nanoparticles. Int J Mol Sci. 2017;18(1):120.

93. Rizzo AM, Berselli P, Zava S, Montorfano G, Negroni M, Corsetto P, et al. Endogenous antioxidants and radical scavengers. In: Giardi MT, Rea G, Berra B, editors. Bio-farms for nutraceuticals: functional food and safety control by biosensors. Boston, MA: Springer, Boston, MA; 2010. p. 52–67.

94. Atashi F, Modarressi A, Pepper MS. The role of reactive oxygen species in mesenchymal stem cell adipogenic and osteogenic differentiation: a review. Stem Cells Dev. 2015;24(10):1150–63.

95. Devasagayam TPA, Tilak JC, Boloor KK, Sane KS, Ghaskadbi SS, Lele RD. Free radicals and antioxidants in human health : current status and future prospects. J Assoc Physicians India. 2004;52:794–804.

96. Zuo L, Zhou T, Pannell BK, Ziegler AC, Best TM. Biological and physiological role of reactive oxygen species - the good, the bad and the ugly. Acta Physiol. 2015;214(3):329–48.

97. Birben E, Sahiner UM, Sackesen C, Erzurum S, Kalayci O. Oxidative stress and antioxidant defense. World Allergy Organ J. 2012;5(1):9–19.

98. Brandes RP, Weissmann N, Schröder K. Free radical biology and medicine nox family NADPH oxidases : molecular mechanisms of activation. Free Radic Biol Med. 2014;76:208–26.

99. Maraldi T. Natural compounds as modulators of NADPH oxidases. Oxid Med Cell Longev. 2013;2013:271602.

100. Meitzler JL, Antony S, Wu Y, Juhasz A, Liu H, Jiang G, et al. NADPH oxidases: a perspective on reactive oxygen species production in tumor biology. Antioxid Redox Signal. 2014;20(17):2873–89.

101. Skonieczna M, Hejmo T, Poterala-Hejmo A, Cieslar-Pobuda A, Buldak RJ. NADPH oxidases (NOX): insights into selected functions and mechanisms of action in cancer and stem cells. Oxid Med Cell Longev. 2017;2017:1–15.

102. Marchi S, Giorgi C, Suski JM, Agnoletto C, Bononi A, Bonora M, et al. Mitochondria-ros crosstalk in the control of cell death and aging. J Signal Transduct. 2012;2012:329635.

103. Venditti P, Stefano L Di, Meo S Di. Mitochondrial metabolism of reactive oxygen species. Mitochondrion. 2013;13(2):71–82.

104. St-Pierre J, Buckingham JA, Roebuck SJ, Brand MD. Topology of superoxide production from different sites in the mitochondrial electron transport chain. J Biol Chem. 2002;277(47):44784–90.

105. Circu ML, Aw TY. Reactive oxygen species, cellular redox systems, and apoptosis. Free Radic Biol Med. 2010;48(6):749–62.

106. Dikalov S. Cross talk between mitochondria and NADPH oxidases. Free Radic Biol Med. 2011;51(7):1289–301.

107. Engelking LR. Oxidative phosphorylation. In: Textbook of Veterinary Physiological Chemistry. 3rd ed. Boston: Academic Press; 2015. p. 219–24.

108. Ohnishi ST, Ohnishi T, Muranaka S, Fujita H, Kimura H, Uemura K, et al. A possible site of superoxide generation in the complex I segment of rat heart mitochondria. J Bioenerg Biomembr. 2005;37(1):1–15.

109. Zickermann V, Kerscher S, Zwicker K, Tocilescu MA, Radermacher M, Brandt U. Architecture of complex I and its implications for electron transfer and proton pumping. Biochim Biophys Acta - Bioenerg. 2009;1787(6):574–83.

110. Masoro EJ, Austad SN. Handbook of the biology of aging. 7th ed. Austad EJM and SN, editor. San Diego: Academic Press; 2011.

111. Liu Y, Fiskum G, Schubert D. Generation of reactive oxygen species by the mitochondrial electron transport chain. J ofNeurochemistry. 2002;80:780–7.

112. Lenaz G. Mitochondria and reactive oxygen Species. Which role in physiology and pathology? In: Scatena R, Bottoni P, Giardina B, editors. Advances in Mitochondrial Medicine. Dordrecht: Springer Netherlands; 2012. p. 93–136.

113. Chen Q, Vazquez EJ, Moghaddas S, Hoppel CL, Lesnefsky EJ. Production of Reactive Oxygen Species by Mitochondria. 2003;278(38):36027–31.

114. Ribas V, García-Ruiz C, Fernández-Checa JC, Garcia-Ruiz C, Fernandez-Checa JC. Glutathione and mitochondria. Front Pharmacol. 2014;5:151.

115. Bai J, Cederbaum AI. Mitochondrial catalase and oxidative injury. Neurosignals. 2001;10(3–4):189–99.

116. Block K, Gorin Y, Abboud HE. Subcellular localization of Nox4 and regulation in diabetes. Proc Natl Acad Sci. 2009;106(34):14385–90.

117. Case AJ, Li S, Basu U, Tian J, Zimmerman MC. Mitochondrial-localized NADPH oxidase 4 is a source of superoxide in angiotensin II-stimulated neurons. Am J Physiol Circ Physiol. 2013;305(1):H19–28.

118. Irshad M, Chaudhuri PS. Oxidant-antioxidant system: role and significance in human body. Indian J Exp Biol. 2002;40(11):1233–9.

119. Halliwell B. Antioxidants in human health and disease. Annu Rev Nutr. 1996;16(1):33–50.

120. Sharma P, Singh RP. Evaluation of antioxidant activity in foods with special reference to TEAC method. Am J Food Technol. 2013;8(2):83–101.

121. Davies KJA. Oxidative stress , antioxidant defenses , and damage removal , repair , and replacement systems. IUBMB Life. 2000;50(4–5):279–89.

122. Lobo V, Patil A, Phatak A, Chandra N. Free radicals, antioxidants and functional foods: Impact on human health. Pharmacogn Rev. 2010;4(8):118.

123. Noguchi N, Watanabe A, Shi H. Diverse functions of antioxidants. Free Radic Res. 2000;33(6):809–17.

124. Young IS, Woodside J V. Antioxidants in health and disease. J Clin Pathol. 2001;54:176–86.

125. Nimse SB, Pal D. Free radicals, natural antioxidants, and their reaction mechanisms. RSC Adv. 2015;5(35):27986–8006.

126. Niki E. Role of vitamin E as a lipid-soluble peroxyl radical scavenger: in vitro and in vivo evidence. Free Radic Biol Med. 2014;66:3–12.

127. Albertini R, Abuja PM. Prooxidant and antioxidant properties of Trolox C, analogue of vitamin E, in oxidation of low-density lipoprotein. Free Radic Res. 1999;30(3):181–8.

128. Huang D, Boxin OU, Prior RL. The chemistry behind antioxidant capacity assays. J Agric Food Chem. 2005;53(6):1841–56.

129. Penn JS, Tolman BL, Bullard LE. Effect of a water-soluble vitamin E analog, Trolox C, on retinal vascular development in an animal model of retinopathy of prematurity. Free Radic Biol Med. 1997;22(6):977–84.

130. Lúcio M, Nunes C, Gaspar D, Ferreira H, Lima JLFC, Reis S. Antioxidant activity of vitamin E and Trolox: understanding of the factors that govern lipid peroxidation studies in vitro. Food Biophys. 2009;4(4):312–20.

131. Davies MJ, Fornit LG, Willson RL. Vitamin E analogue Trolox C e.s.r. and pulse-radiolysis studies of free-radical reactions. Biochem J. 1988;255:513–22.

132. Wattamwar PP, Hardas SS, Butterfield DA, Anderson KW, Dziubla TD. Tuning of the pro-oxidant and antioxidant activity of trolox through the controlled release from biodegradable poly(trolox ester) polymers. J Biomed Mater Res - Part A. 2011;99 A(2):184–91.

133. Fagundes DS, Gonzalo S, Arruebo MP, Plaza MA, Murillo MD. Melatonin and Trolox ameliorate duodenal LPS-induced disturbances and oxidative stress. Dig Liver Dis. 2010;42(1):40–4.

134. Sun J, Ming L, Shang F, Shen L, Chen J, Jin Y. Apocynin suppression of NADPH oxidase reverses the aging process in mesenchymal stem cells to promote osteogenesis and increase bone mass. Sci Rep. 2015;5:18572.

135. Sun Y, Gong F, Yin J, Wang X, Wang X, Sun Q, et al. Therapeutic effect of apocynin

through antioxidant activity and suppression of apoptosis and inflammation after spinal cord injury. Exp Ther Med. 2017;13(3):952–60.

136. Edwin van den Worm. Investigations on apocynin, a potent NADPH oxidase inhibitor [dissertation]. Utrecht: Utrecht University; 2001.

137. Rehman A ur, Dugic E, Benham C, Lione L, Mackenzie LS. Selective inhibition of NADPH oxidase reverses the over contraction of diabetic rat aorta. Redox Biol. 2014;2:61–4.

138. Sharma N, Nehru B. Apocyanin, a microglial NADPH oxidase inhibitor prevents dopaminergic neuronal degeneration in lipopolysaccharide-induced parkinson's disease model. Mol Neurobiol. 2016;53(5):3326–37.

139. Heumuller S, Wind S, Barbosa-Sicard E, Schmidt HH, Busse R, Schroder K, et al. Apocynin is not an inhibitor of vascular NADPH oxidases but an antioxidant. Hypertension. 2008;51(2):211–7.

140. Mehta SK, Gowder SJT. Members of antioxidant machinery and their functions. In: Gowder SJT, editor. Basic principles and clinical significance of oxidative Stress. Rijeka: IntechOpen; 2015. p. 59–86.

141. Gummersbach C, Hemmrich K, Kröncke KD, Suschek C V., Fehsel K, Pallua N. New aspects of adipogenesis: radicals and oxidative stress. Differentiation. 2009;77(2):115–20.

142. Higuchi M, Dusting GJ, Peshavariya H, Jiang F, Hsiao ST-F, Chan EC, et al. Differentiation of human adipose-derived stem cells into fat involves reactive oxygen species and forkhead box O1 mediated upregulation of antioxidant enzymes. Stem Cells Dev. 2013;22(6):878–88.

143. Lee H, Lee YJ, Choi H, Ko EH, Kim J. Reactive oxygen species facilitate adipocyte differentiation by accelerating mitotic clonal expansion. J Biol Chem. 2009;284(16):10601–9.

144. Wang X, Hai C. Redox modulation of adipocyte differentiation: hypothesis of "redox chain" and novel insights into intervention of adipogenesis and obesity. Free Radic Biol Med. 2015;89:99–125.

145. Hou Y, Xue P, Bai Y, Liu D, Woods CG, Yarborough K, et al. Nuclear factor erythroid-derived factor 2-related factor 2 regulates transcription of CCAAT/enhancer-binding protein β during adipogenesis. Free Radic Biol Med. 2012;52(2):462–72.

146. Saitoh Y, Xiao L, Mizuno H, Kato S, Aoshima H, Taira H, et al. Novel polyhydroxylated fullerene suppresses intracellular oxidative stress together with repression of intracellular lipid accumulation during the differentiation of OP9 preadipocytes into adipocytes. Free Radic Res. 2010;44(9):1072–81.

147. Tormos K V., Anso E, Hamanaka RB, Eisenbart J, Joseph J, Kalyanaraman B, et al. Mitochondrial complex III ROS regulate adipocyte differentiation. cell metab. 2011;14(4):537–44.

148. Kim JH, Kim S-H, Song SY, Kim W-S, Song SU, Yi T, et al. Hypoxia induces adipocyte differentiation of adipose-derived stem cells by triggering reactive oxygen species generation. Cell Biol Int. 2014;38(1):32–40.

149. Carrière A, Carmona MC, Fernandez Y, Rigoulet M, Wenger RH, Pénicaud L, et al. Mitochondrial reactive oxygen species control the transcription factor CHOP-10/GADD153 and adipocyte differentiation: a mechanism for hypoxia-dependent effect. J Biol Chem. 2004;279(39):40462–9.

150. Schröder K, Wandzioch K, Helmcke I, Brandes RP. Nox4 acts as a switch between differentiation and proliferation in preadipocytes. Arterioscler Thromb Vasc Biol. 2009;29(2):239–45.

151. Drehmer DL, de Aguiar AM, Brandt AP, Petiz L, Cadena SMSC, Rebelatto CK, et al. Metabolic switches during the first steps of adipogenic stem cells differentiation. Stem Cell Res. 2016;17(2):413–21.

152. Turker I, Zhang Y, Zhang Y, Rehman J. Oxidative stress as a regulator of adipogenesis. FASEB J. 2007;21(6):A1053–A1053.

153. Furukawa S, Fujita T, Shimabukuro M, Iwaki M, Yamada Y, Nakajima Y, et al. Increased oxidative stress in obesity and its impact on metabolic syndrome. J Clin Invest. 2004;114(12):1752–61.

154. Mouche S, Mkaddem S Ben, Wang W, Katic M, Tseng Y-HH, Carnesecchi S, et al. Reduced expression of the NADPH oxidase NOX4 is a hallmark of adipocyte differentiation. Biochim Biophys Acta - Mol Cell Res. 2007;1773(7):1015–27.

155. Mitchell JB, Xavier S, DeLuca AM, Sowers AL, Cook JA, Krishna MC, et al. A low molecular weight antioxidant decreases weight and lowers tumor incidence. Free Radic Biol Med. 2003;34(1):93–102.

156. Kraus NA, Ehebauer F, Zapp B, Rudolphi B, Kraus BJ, Kraus D. Quantitative assessment of adipocyte differentiation in cell culture. Adipocyte. 2016;5(4):351.

Chapter 2: General Materials and Methods

2.1 Isolation of ASCs from lipoaspirates and solid fat

In this study, cryopreserved human adipose-derived stromal/stem cells (ASCs) isolated in previous studies in our laboratory as well as freshly isolated ASCs were used. ASCs were isolated from human adipose tissue as previously described by Zuk and colleagues (2001) and Bunnell and colleagues (2008) with minor modifications[1,2]. These studies were approved by the Ethics Committee, Faculty of Health Sciences, University of Pretoria, Pretoria, South Africa, study numbers 421/2013 and 414/2015. The current study was also approved by the Ethics Committee Faculty of Health Sciences, University of Pretoria, Pretoria, South Africa, study number 134/2017.

ASCs were isolated either from lipoaspirates or solid fat tissue samples. Isolation procedures were carried out in a laminar air flow cabinet under sterile conditions. Fat tissue used was obtained from patients who had undergone liposuction or abdominoplasty procedures following written informed consent (see Appendix C). A total of four ASC cultures were used in the study, three cultures were obtained from solid fat tissue samples and one was from a lipoaspirate sample. The isolation procedure for solid adipose tissue involved an additional step, which was to separate solid fat tissue attached to the skin surface. Thereafter, the fat tissue was cut up into smaller pieces using scalpel blade and forceps to obtain a finely minced fat sample. Thereafter the finely minced fat sample and lipoaspirates samples then followed the same isolation procedure.

Approximately 25 ml of lipoaspirate or minced solid fat tissue was transferred to 50 ml centrifuge tubes (Falcon® Conical centrifuge tubes: Corning Incorporated, New York, USA). This was followed by a washing step where the tubes were topped up with PBS supplemented with 2% PenStrep (Gibco® by Life Technologies). This mixture was then centrifuged (Sorvall ST 16R Refrigerated Centrifuge, Thermo Fisher Scientific, Germany) for 3 minutes at 1660 x g. The oil layer and PBS were aspirated and the fat tissue transferred into a new 50 ml tube. This washing step was repeated 2 to 3 times depending on the amount of blood contamination. After washing, freshly prepared 0.1% sterile type

1 collagenase (Gibco® by Life Technologies, New York, USA) was added in a 1:1 volume ratio to fat tissue in 50 ml centrifuge tubes. This was incubated for 45 minutes (up to 2 hours for solid adipose tissue) in a rotating incubator (ProBlot™ Hybridization Oven, Labnet International, New Jersey, USA) at a temperature of 37 ºC. Following incubation, tubes were centrifuged at 738 x g for 5 minutes, followed by shaking to resuspend the cell pellet and another round of centrifugation. Thereafter, adipose tissue fragments and collagenase solution were aspirated leaving behind a cell pellet in a small volume of the collagenase (about 5 ml). The cell pellet was then resuspended in the remaining collagenase solution and filtered through a 70 µm cell strainer to remove any remaining tissue.

Collagenase activity was then neutralized by adding complete DMEM medium in a 1:1 volume ratio with the collagenase (Gibco® by Life Technologies, Paisly, UK) (DMEM medium + 10% FBS + 2% PenStrep). This mixture was topped up with PBS containing 2% PenStrep and centrifuged at 266 x g for 5 minutes. The supernatant was then aspirated and the cell pellet resuspended in VersaLyse™ (Beckman Coulter, Krefeld, Germany) for 10 minutes to lyse any residual red blood cells. After the VersaLyse™ step, the cell pellet was washed twice by adding PBS containing 2% PenStrep and then centrifuged at 266 x g for 5 minutes.

After washing, supernatant was aspirated and cell pellet was resuspended in complete DMEM medium followed by filtration through a 70 µm strainer to remove tissue debris. The resulting cell suspension is referred to as the stromal vascular fraction (SVF). Thus, SVF refers to the cellular component of adipose tissue, excluding mature adipocytes. SVF consists of ASCs, endothelial cells, pre-adipocytes, macrophages, smooth muscle cells, lymphocytes, and pericytes among others[3]. A cell count of the SVF was done by transferring 100 µl of cell suspension to a flow cytometry tube, followed by 100 µl of Flow Count™ (Beckman Coulter) fluorospheres and 2 µl of Vybrant® DyeCycle™ Ruby (VDC Ruby) (Thermo Fisher Scientific, USA) to ensure that only nucleated cells are counted. VDC Ruby is a fluorescent cell permeable DNA dye that can be used to stain for cell nuclei[4]. Counts were obtained using a Gallios flow cytometer (Beckman Coulter, Miami,

USA). Cells were then plated in 75 cm^2 cell culture flasks (Greiner Bio-One GmbH, Frickenhausen, Germany) at a seeding density of 50 000 cells/cm^2 and incubated at 37 ºC, 5% CO_2. See Appendix A for absolute cell count calculation.

These cells were then labelled using an anonymized labelling code used as standard practice in our laboratory. For example, A141117-01 A P0 F0 or SA141117-01 A P0 F0 as shown in Figure 2.1.

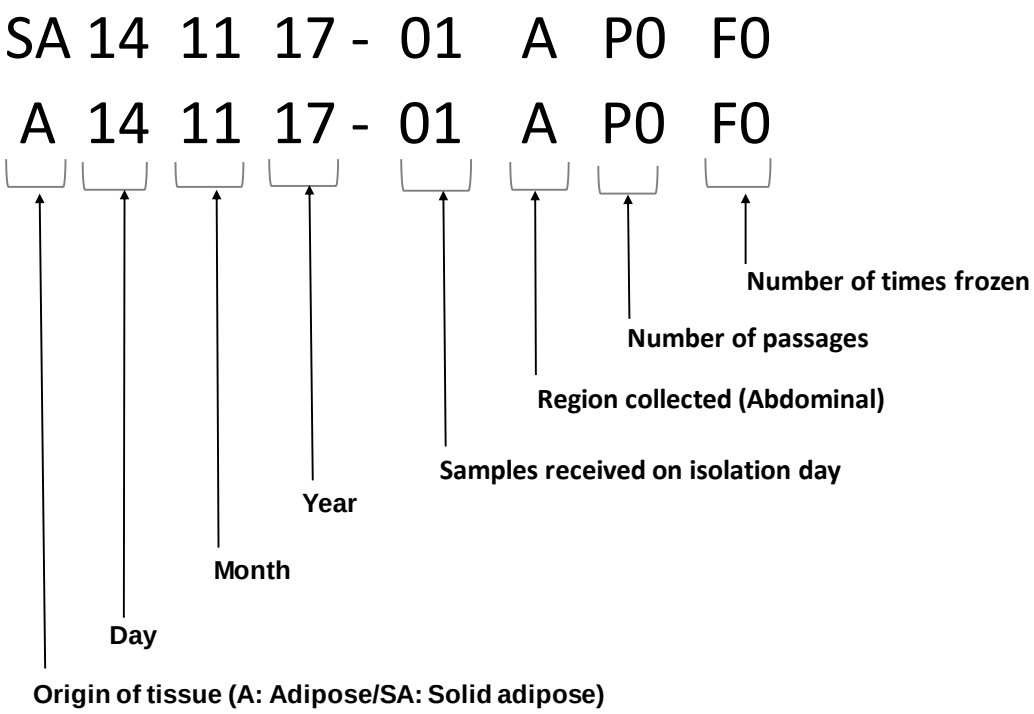

Figure 2.1 Criteria used to identify ASC cultures.
ASC cultures were identified by tissue origin, isolation date, number of donors on day, collection region, passage number and number of times frozen.

After 72 hours of incubation, cultures were washed twice with complete DMEM to remove non-adherent cells. Thereafter cultures were maintained in complete DMEM until the cells were confluent. Medium changes were done every three to four days. Figure 2.2 shows a summary of the ASC isolation procedure.

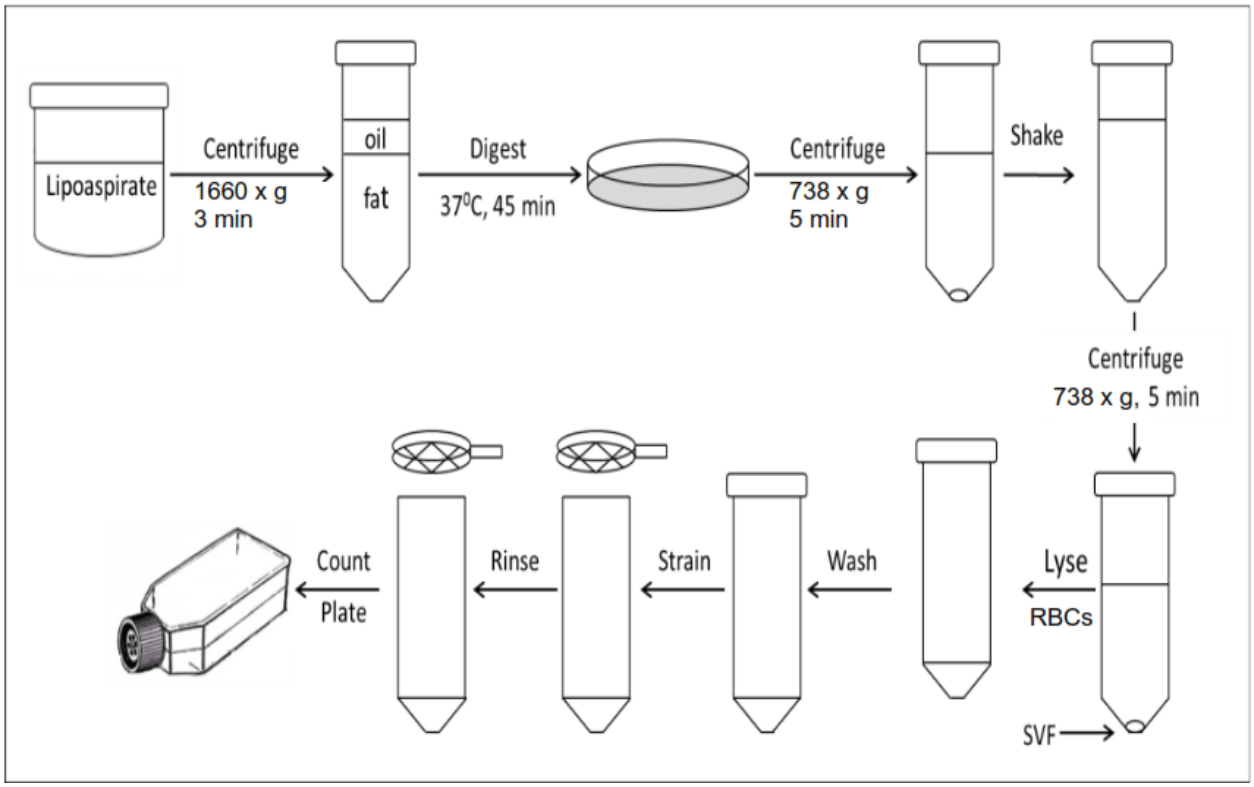

Figure 2.2 Processing of adipose tissue and isolation of adipose-derived stromal/stem cells. Lipoaspirate samples were processed by enzymatic digestion and the stromal vascular fraction (SVF) collected. ASCs from the SVF were allowed to adhere to tissue culture flasks and non-adherent cells were washed away after 24 hours. RBCs – red blood cells

2.2 Expansion of adipose derived stromal/stem cells

The experimental procedures used in this study required large numbers of cells. For this reason, the isolated ASCs were first expanded to obtain enough cells for the experiments. Once the previously seeded SVF cells (in 75 cm^2 cell culture flasks) reached 90 to 100% confluence, they were expanded by sub culturing in several flasks for 3 to 4 rounds. This was done by aspirating the cell culture medium followed by the addition of 0.25% trypsin-EDTA (1X, GIBCO by Life Technologies™, Grand Island, NY, USA) to detach ASCs from the culture flask surface. After 15 minutes incubation at 37 ºC and 5% CO_2, the flasks were checked using a microscope to ensure that all cells detached from the cell surface. Thereafter, 4 ml of complete DMEM media was added to cell culture flask to neutralize the trypsin. The cell suspensions were then transferred to 50 ml centrifuge tubes and topped up with complete DMEM medium followed by centrifuging at 300 x g for 5 minutes.

This wash step was repeated once more. The resulting cell pellet was resuspended in complete DMEM and cell counts were performed on the Gallios flow cytometer. Absolute cell counts were calculated as previously described. After obtaining cell counts, ASCs were re-seeded in 75 cm^2 cell culture flasks at a density of 5 000 cells/cm^2. Whenever previously cultured cells were trypsinised and re-seeded, the passage number increased by one e.g. Passage 0 (P0) became P1. In this study, ASCs were used at passages P3 and P4.

Any remaining cells were cryopreserved in DMEM supplemented with 10% DMSO for future use. Aliquots of 1 to 2 million cells in 1 ml freezing media, consisting of complete DMEM supplemented with 10% DMSO, were transferred to cryovials labelled with sample ID, cell number and date. Samples were placed in Coolcell® Freezing containers (BioCision, California, USA) and stored in a freezer at -80 ºC for 24 hours. The cells were then transferred to a dewar and cryopreserved in liquid nitrogen.

The cultured ASCs were maintained in DMEM medium without pyruvate (Gibco by Life Technologies, Paisly, UK). DMEM without pyruvate was used because downstream experiments in this study involved the measurement of reactive oxygen species (ROS) in ASCs. Pyruvate is a ROS scavenger that may influence the outcome of results in this study if present in culture medium[5,6]. Medium changes were done once every three to four days.

This procedure for expansion and maintenance of cells was carried out for all the four different cultures used until sufficient numbers of cells needed to perform all the experimental conditions at the same passage were obtained. ASCs were then seeded in 6-well plates (Greiner Bio-One GmbH, Frickenhausen, Germany) at a density of 5 000 cells/cm^2 for use in investigating the different experimental treatments. The methods used in these experiments are discussed in section 2.4.

2.3 Flow cytometric characterization of ASCs

Phenotypic characterisation of ASCs was done before seeding ASCs in 6- and 12-well plates to ensure that cells used adhered to the ASCs recommended immunophenotype. A six colour antibody immunophenotype panel was adopted as per the criteria set out by the International Federation for Adipose Therapeutics and Science (IFATS) and International Society of Cellular Therapy (ISCT)[7,8]. A volume of 100 µl cell suspension was added to a flow cytometry tube, followed by addition of 5 µl antibody solutions of CD34-PC7 (Beckman Coulter), CD45-KO (Beckman Coulter), CD73-FITC (BD Biosciences), CD90-BV421 (Molecular Probes by Life Technologies), CD36-APC (Molecular Probes by Life Technologies) and CD44-APC/CY7 (BioLegend, CA, USA) (Table 2.1.) This was then incubated for 20 minutes in the dark at room temperature. Thereafter, 700 µl PBS was added to the flow cytometry tube after which the cells were analysed on the Gallios flow cytometer. A second flow cytometry tube which contained 100 µl of cell suspension without any antibodies was prepared to serve as an unstained negative control. The negative control tube served as a baseline onto which positive detection limits were set for the stained sample. Results were expressed as the mean ± SD of four independent ASC cultures except for CD34 and CD36 which were representative of 2 independent ASC cultures. This was because the antibody reagent ran out and surface staining for two cultures was not done for these two markers.

2.3.1 Flow cytometer setup and data analysis

Instrument start-up was performed and Flow Check Pro™ (Beckman Coulter, Miami, USA) was acquired to verify laser alignment and instrument performance. Acquisition protocols were set up on the Gallios flow cytometer for the various experiments. The setup of each protocol is discussed in the respective methodology sections. All flow cytometry protocols used in this study were set to acquire either 5 000 events, with a second stop criterion of not exceeding an acquisition time of 5 minutes for each sample. Following data acquisition on the Gallios flow cytometer, data analysis was done using the Kaluza analysis software version 2.0 (Beckman Coulter, Miami, USA). Table 2.1 shows the excitation lasers and detection (emission) channels for the different fluorochromes.

Table 2.1 The excitation and emission spectrums, lasers and detectors used for all fluorochrome and/or dyes used in the study.

Reagent	Excitation Laser	Emission wavelength	Filter	Detection Channel
CD73-FITC	Blue: 488 nm	520 nm	525/40	FL1
CD34-PC7		770 nm	755LP	FL5
Nile Red		>528 nm	575/30	FL2
MitoSOX™ Red		580 nm		
CD36-APC	Red: 638 nm	660 nm	620/20	FL6
CellROX® Deep Red		665 nm		
CD44-APC/CY7		785 nm	755LP	FL8
CD90-BV421	Violet: 405 nm	421 nm	450/40	FL9
DAPI		461 nm		
CD45-KO		528 nm	550/40	FL10

FITC: Fluorescein isothiocyanate, **PC7:** Phycoerythrin-Cyanin 7, **APC:** Allophycocyanin, **APC/CY7:** Allophycocyanin/Cy7, **BV421:** Brilliant Violet™ 421, **DAPI:** 4′,6-diamidino-2-phenylindole, **KO:** Krome Orange

2.3.1.1 Setup and gating strategy followed for ASC phenotypic characterization

Simultaneous multicolour staining was performed to determine the ASC immunophenotypic profile. Since ASC phenotypic characterisation was being done as a simultaneous multicolour panel, colour compensation was necessary to correct for spectral overlap (spillover). Spectral overlap occurs when fluorescence from a fluorochrome is detected in a detector designed to measure signal from another channel. A previously designed ASC phenotype panel routinely used by researchers and post-graduate students in our research group was utilised in this study. The colour compensation matrix used was created using cells stained with individual antibodies to correct for spectral overlap. Compensation settings were then kept constant for the duration of the experimental runs in the study. Colour compensation set up was done by other students in our research group. Figure 2.3 shows an extract of the colour compensation matrix used in this study.

Spillover (%)										
	FL1	**FL2**	**FL3**	**FL4**	**FL5**	**FL6**	**FL7**	**FL8**	**FL9**	**FL10**
FL1		0.00	0.00	0.00	0.00	0.00	0.00	0.00	0.00	25.12
FL2	7.37		0.00	0.00	0.00	0.00	0.00	0.00	0.00	18.72
FL3	0.00	0.00		0.00	0.00	0.00	0.00	0.00	0.00	0.00
FL4	0.00	0.00	0.00		0.00	0.00	0.00	0.00	0.00	0.00
FL5	0.00	54.26	0.00	0.00		62.07	0.00	0.00	0.00	6.90
FL6	0.00	49.75	0.00	0.00	0.00		0.00	4.00	0.00	8.00
FL7	0.00	0.00	0.00	0.00	0.00	0.00		0.00	0.00	0.00
FL8	0.00	0.00	0.00	0.00	0.00	0.00	0.00		0.00	0.00
FL9	0.00	0.00	0.00	0.00	0.00	0.00	0.00	0.00		0.00
FL10	0.00	0.00	0.00	0.00	0.00	0.00	0.00	0.00	5.00	

Figure 2.3 Compensation matrix showing compensation settings used in the study.
The compensation matrix shows the spillover percentages that comprised the colour compensation settings applied in this study.

To determine the ASC immunophenotype the following gating strategy was performed. A forward scatter (FS) vs side scatter (SS) density plot was created first to select for intact cells and exclude debris and dead cells. FS discriminates cells/particles by size whereas SS discriminates based on intracellular granularity/complexity of the cells or particles. Debris and dead cells tend to have lower FS levels and are usually located at the bottom left hand corner of the FS/SS density plot (Figure 2.4).

Thereafter, the principles of sequential gating (Figure 2.5) were applied to determine what percentage of ASCs adhere to the suggested ASC immunophenotype. Sequential gating refers to a systematic, successive gating strategy that can be used to identify specific subsets of cell populations[9].

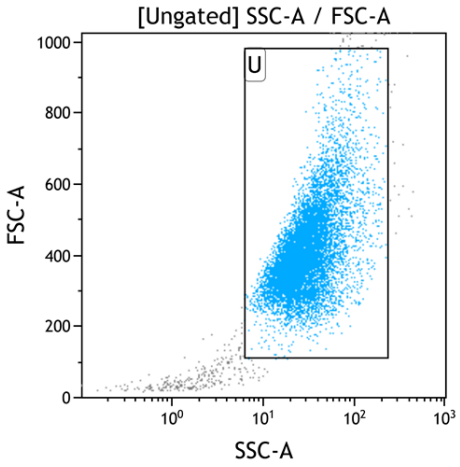

Figure 2.4 Gating strategy applied for excluding debris and dead cells.
A FS vs SS density plot was created to distinguish cell populations. Debris and dead cells lying at the bottom left hand corner of the plot were removed from analysis by drawing a region around the cells of interest as shown above.

To apply the principles of sequential gating (Figure 2.5), two parameter density plots displaying two fluorochromes one on each axis were created to determine the co-expression of surface markers. The two parameter plots were split into four quadrants to enable visualisation of four distinct subpopulations within the ASCs as shown in Figure 2.6. Cells falling into the upper left quadrant were negative for the x-axis fluorochrome and positive for y-axis fluorochrome, whereas ASCs in the lower left quadrant represented cells negative for both the x and y axis fluorochromes. Cells in the upper right quadrant were positive for both the x and y axis fluorochromes, while ASCs in the lower right quadrant were positive for the x-axis fluorochrome and negative for the y-axis fluorochrome.

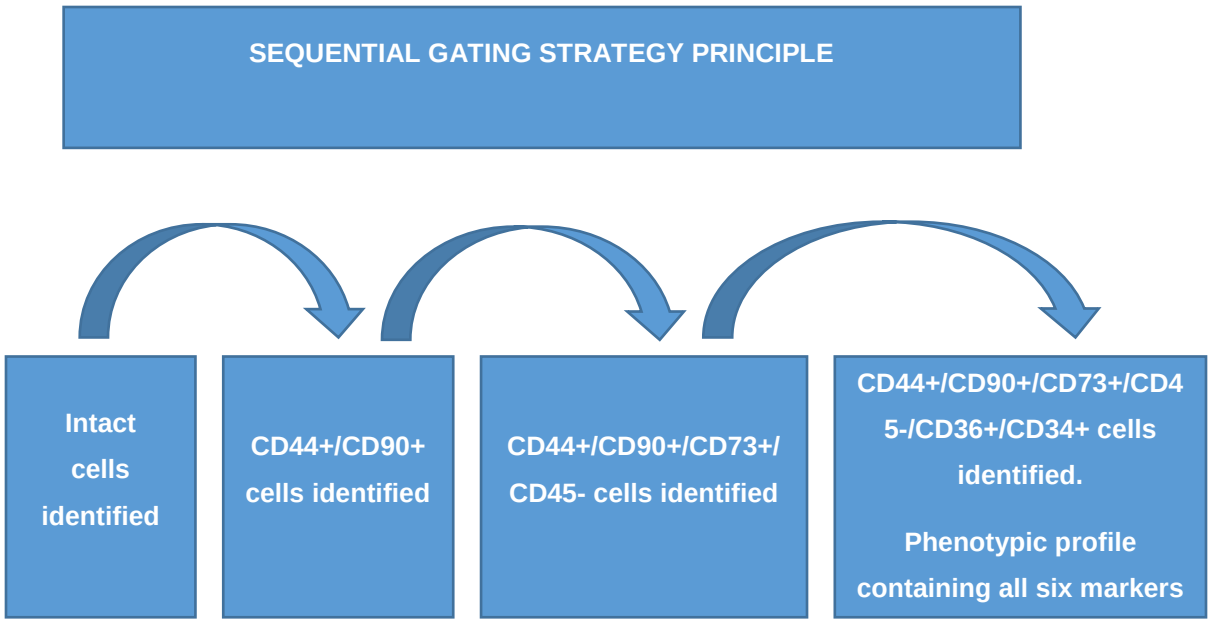

Figure 2.5 Sequential gating strategy principle applied to determine the intact ASC immunophenotype.
The first gating startegy identified ASC CD44/CD90 expression, followed by a second gating startegy which indicated ASC CD44/CD90/CD73/CD45 expression and lastly a third gating strategy identifying ASC CD44/CD90/CD73/CD45/CD36/CD34 expression.

Following the selection of intact cells using FS vs SS density plot (Figure 2.4). The first two parameter density plot was created to identify intact cells that expressed CD90 and CD44 (Figure 2.6A). Having identified CD44+/CD90+ cells, the next step was to determine the percentage of the CD44+/CD90+ cells that expressed CD45 and CD73. This was done using a second two parameter density plot (CD45 vs CD73) which was gated on CD90+/CD44+ ASCs (Figure 2.6B). This density plot now indicated the CD90/CD44/CD73/CD45 expression profiles of the ASCs. Thereafter a third two parameter density plot showing CD34 vs CD36 and gated on CD90+/CD44+/CD73+/CD45- ASCs was created (Figure 2.6C). This density plot indicated the CD90/CD44/CD73/CD45/CD36/CD34 expression profiles of the ASCs and thus the immunophenotypic profile of all six markers.

Unstained control ASCs were used to set the region limits (as shown in Figure 2.6), in order to allow for the detection of positive fluorochrome staining. Positive expression of fluorochromes was indicated by fluorescence shift from the lower left quadrant (Figure

2.7). According the IFATS and ISCT, to be classified as ASCs cells should be positive for CD73, CD105, CD44, CD90, CD36 (weakly positive), CD34 (variable) and negative for CD45[7,8]. The expression of CD34 has been reported to be subsequently lost during cell culture. In addition various studies have also reported that the expression levels of CD34 vary in cultured ASCs[7,8,10].

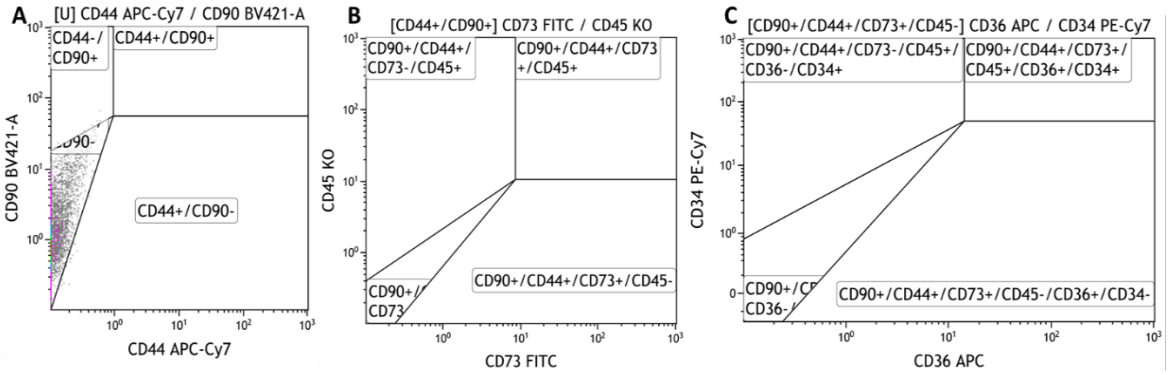

Figure 2.6 Unstained surface marker expression profiles.
Unstained ASCs were used to set the region limits, allowing for the detection of positive fluorochrome staining. **(A)** represents CD90/CD44 expression profiles, **(B)** shows CD90/CD44/CD73/CD45 ASC expression profiles and **(C)** represents CD90/CD44/CD73/CD45/CD36/CD34 expression profiles.

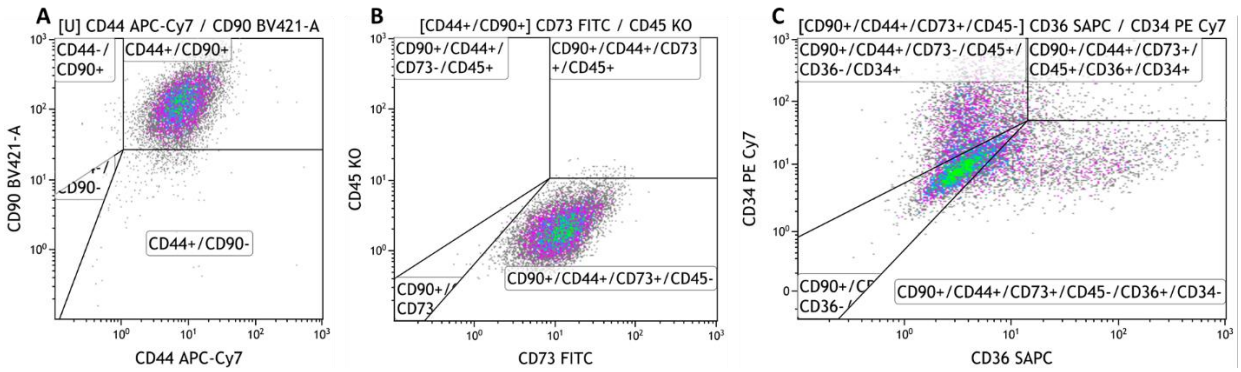

Figure 2.7 Positive surface marker expression profiles.
Example of an ASC culture positively stained with surface marker antibodies showing the relative expression profiles of CD90/CD44/CD73/CD45/CD34/CD36. **(A)** shows CD90/CD44 expression profiles, **(B)** shows CD90/CD44/CD73/CD45 ASC expression profiles whereas **(C)** represents CD90/CD44/CD73/CD45/CD36/CD34 expression profiles.

2.4 Treatments and differentiation of ASCs

Following isolation, expansion and characterization of ASCs, adipogenic quantification, ROS measurement assays and fluorescent microscopy imaging were performed. For adipogenic quantification and ROS measurements, ASCs were seeded in 6-well plates and in 12-well plates for fluorescent microscopy imaging. Figure 2.8 and Figure 2.9 show the experimental layout for the 6- well plates. Figure 2.10 shows the experimental layout for the 12-well plate used.

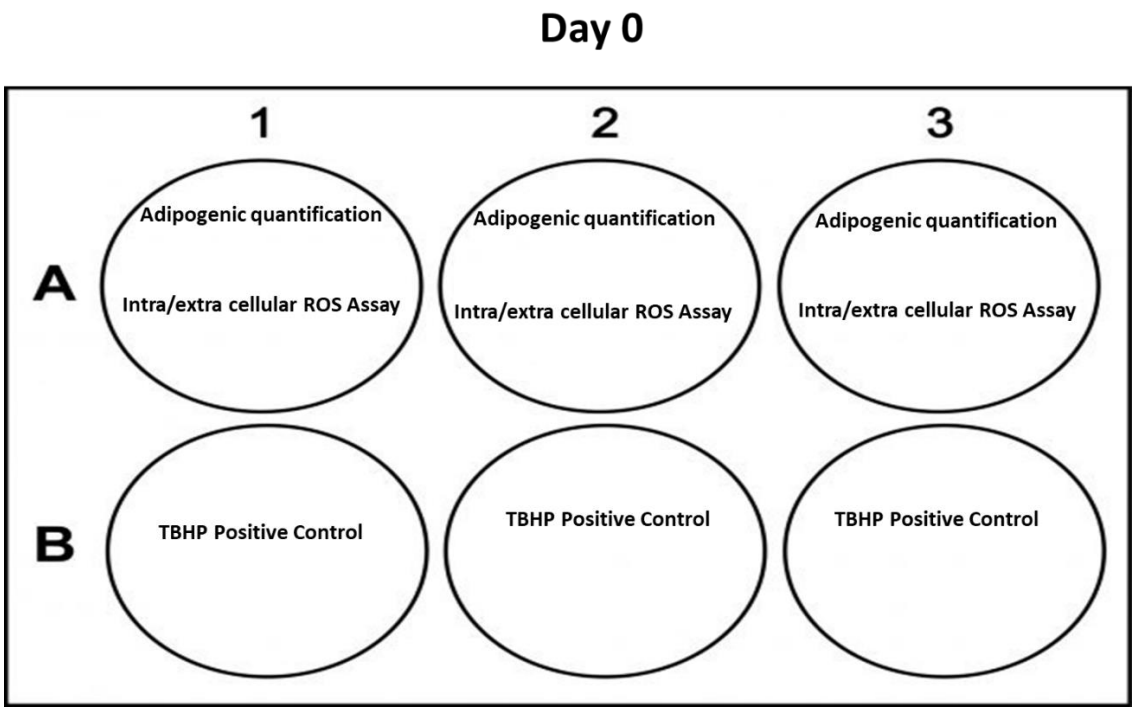

Figure 2.8 Experimental 6-well plate layout for Day 0.
Three wells were seeded for day 0 baseline adipogenic quantification, intra and extracellular ROS assays measurements. The other three well were seeded for the intracellular ROS assay TBHP positive control.

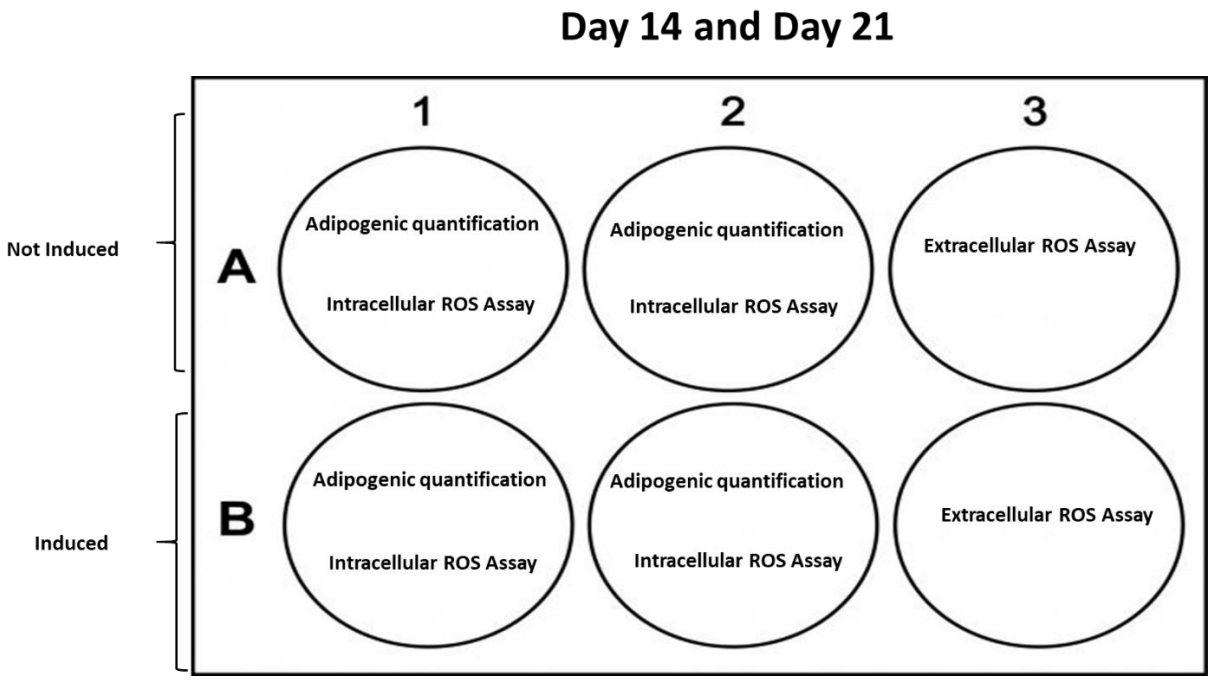

Figure 2.9 Experimental 6-well plate layout for day 14 and day 21.
For each of the treatment conditions a day 14 and day 21 plate was set up as shown above for the induced and non-induced ASC cultures. Two wells each were reserved for adipogenic quantification and intracellular ROS assays, whereas wells in column 3 were reserved for extracellular ROS measurements.

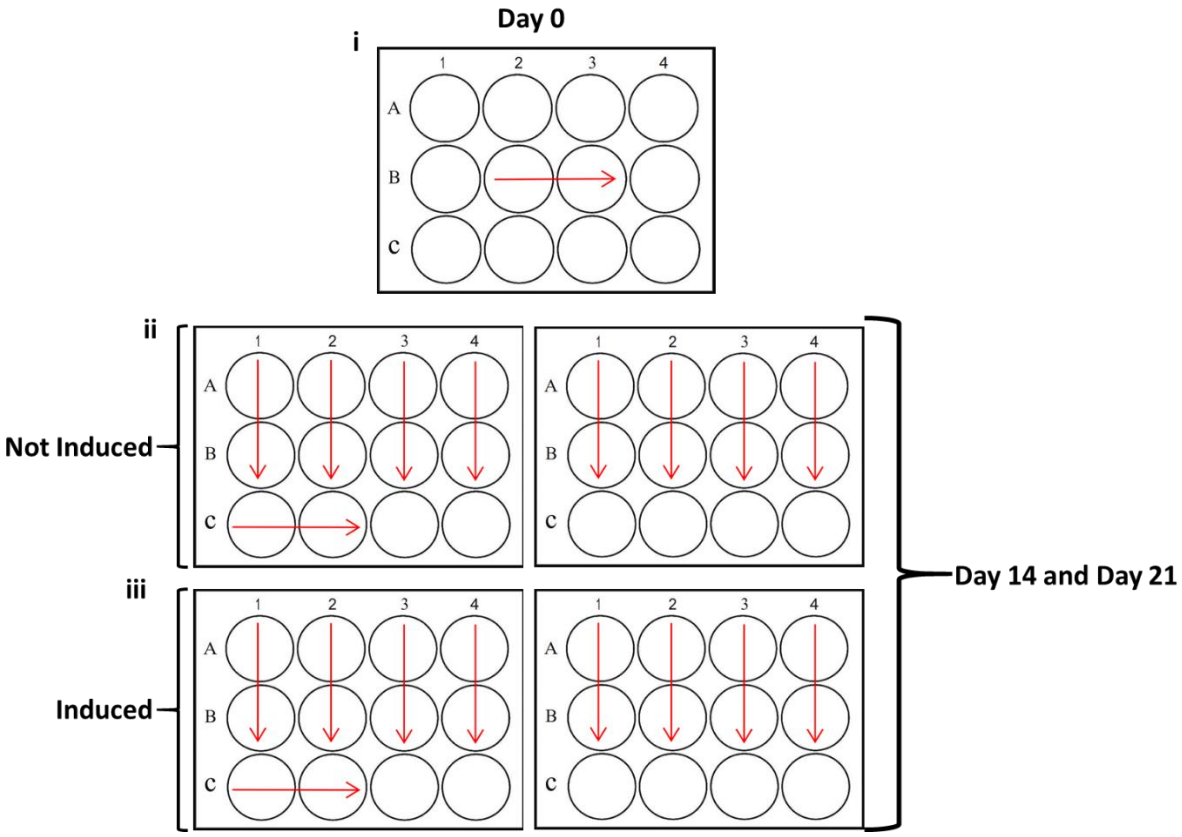

Figure 2.10 Experimental 12-well plate layout for fluorescent microscopy imaging.
Two wells (shown by the red arrows) were seeded for day 0 baseline imaging (**i**). Day 14 time point plate set up was as shown (**ii and iii**), two 12-well plate each for induced and non-induced ASCs cultures. The day 21 time point had the same plate layout. Each of the nine treatment conditions is represented by the arrows, ASCs were seeded in two wells for each of the treatment condition.

The detailed experimental procedures for ASCs seeded in 6-well and 12-well plates were as follows: ASCs were seeded in 6- and 12-well plates at a density of 5 000 cells/cm^2 in complete DMEM medium without pyruvate (Figures 2.8 to 2.10). ASCs were then incubated at 37 °C and 5% CO_2 until they reached 90 to 100% confluency. Change of medium was done once every three to four days. Approximately 4 days before the expected day of cells reaching 90 to 100% confluency, medium was changed to DMEM without pyruvate and without phenol red. This was done because phenol red interfers with florescence and flow cytometry measurements[11]. From this point onwards, complete DMEM referes to complete DMEM without pyruvate and without phenol red unless otherwise specified. Once the ASCs reached 90 to 100% confluency in the 6-well and 12-

well plates, they were then subjected to different treatments and induced to differentiate as follows:

2.4.1 Adipocyte differentiation

Medium in three of the wells in a 6-well plate (one plate per condition per time point) was changed to adipogenic induction medium containing complete DMEM supplemented with adipogenic induction medium which consisted of 1 μM dexamethasone (Sigma-Aldrich), 0.5 mM 3-isobutyl-methylxanthine (Sigma-Aldrich), 200 μM indomethacin (Sigma-Aldrich), 10 μg/ml human insulin (Sigma-Aldrich) while the remaining three wells were maintained in complete DMEM medium and served as non-induced controls. Adipogenic induced and non-induced ASC cultures were then incubated in their respective culture media for 0, 14 and 21 days. Four independent ASC cultures were used. Two wells in each 6-well plate (one induced and non-induced) were reserved for the extracellular ROS assay (Figure 2.9). Following adipogenic induction, medium was changed once every two days. Lipid formation in differentiated ASCs was measured on day 0, 14 and 21 post adipogenic induction using the Gallios flow cytometer.

2.4.2 Trypsinisation of ASCs

At the respective time points post induction, ASCs were trypsinised from 6-well plates. Medium was aspirated from the respective wells, followed by the addition of 500 µl trypsin-EDTA (Gibco®) and incubated for 15 minutes. Once dislodged, this cell suspension was neutralized with 500 µl of complete DMEM medium. This cell suspension was then transferred to separate 15 ml tubes, one for induced cells and the other for non-induced cells using a disposable Pasteur pipette. The volume of this cell suspension was then topped up to 4 ml with complete DMEM medium.

Thereafter, appropriate volumes of the resulting cell suspension was split into different aliquots each for the following assays:

i. Nile Red adipogenic quantification
ii. 7-AAD viability
iii. CellRox® Deep Red intracellular ROS measurement

iv. MitoSOX™ Red Mitochondrial ROS measurement

2.4.3 Flow cytometric adipogenic quantification

On day 0, 14 and 21 post differentiation, flow cytometric quantification of adipogenesis was done using the Gallios flow cytometer. ASCs were trypsinised from the 6-well plates as described in Chapter 2 section 2.42. Following trypsinisation, 1 ml of the cell suspension was stained with Nile Red and DAPI stain. Cells were treated with Nile Red stain to a final concentration of 0.02 µg/ml and with 5 ng/ml DAPI final concentration. This suspension was then incubated at 37 °C for 30 minutes followed by flow cytometric analysis immediately. Care was taken to handle cells gently and no additional washing steps were included to prevent release of intracellular lipid droplets by differentiated adipocytes. Adipocytes are known to be fragile cells that need to be handled with care. Nile Red stain was chosen for use in this study instead of the widely-used Oil Red O stain because Oil Red O is relatively cell impermeable and does not penetrate live cells. Thus, use of Oil Red O is mainly limited to analysis of dead cells, the dye is also non-fluorescent and therefore unsuitable for flow cytometry[12]. Whereas Nile Red stain can be used quantitatively via flow cytometry to stain either live or dead adipocytes[13,14].

2.4.3.1 Elimination of dead cells

In flow cytometry, it is critical to identify and remove data points representing dead cells to ensure accuracy of results[15]. DAPI is a DNA binding dye that will only penetrate cells with compromised membranes, an indicator of cell death. Once the dye enters the cell it binds to DNA and fluoresces. The fluorescent cells represent dead cells and can therefore be gated out. To ensure that data analysis was done only on viable cells with intact membranes. The following gating strategy was implemented using Kaluza analysis software: Gating strategies were set using day 0 non-induced, untreated ASCs which served as the negative control. These settings were then applied to the rest of the conditions throughout the differentiation period to detect any changes in either Nile Red composition or intracellular ROS levels.

First level gating was done to identify viable ASCs and this was done by creating a side scatter Log vs DAPI FL9 density plot (Figure 2.11A). A region was then drawn on the DAPI dim population which represented viable ASCs. The DAPI bright cells to the right of the DAPI FL9 plot represented dead cells and were gated out as shown on Figure 2.11A Thereafter, a forward scatter (FS) vs side scatter (SS) Log density plot was created and this was gated on the viable cells (Figure 2.11B). This was to exclude debris as well as any remaining dead cells. Dead cells and debris tend to have lower FS levels and are usually located at the bottom left corner of the FS/SS density plot. A region was drawn on the intact cells leaving out the debris as shown in Figure 2.11B and these cells were identified as ASCs.

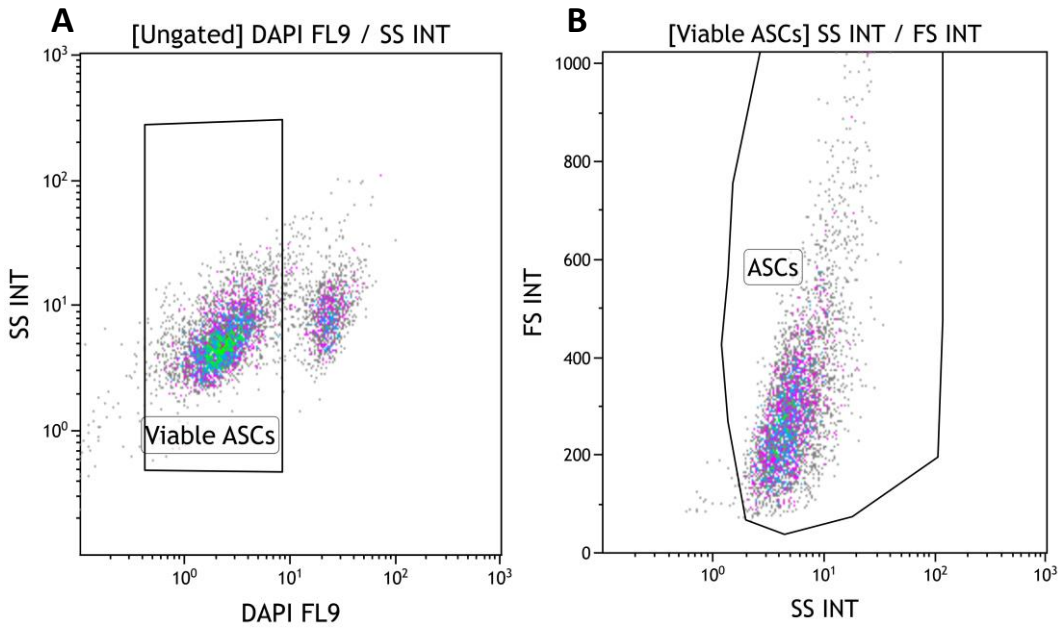

Figure 2.11 Gating strategy for viable and intact ASCs.
Non-induced, untreated ASCs at day 0 were used to set the gating controls. Only viable cells were used for data analysis, dead cells and debris were removed from analysis. DAPI bright cells represented dead cells and were excluded from analysis (**A**). Debris and remaining dead cells were excluded using the FS vs SS density plot (**B**).

2.4.3.2 Setup and gating strategy followed for Nile Red quantification

To detect the proportion of cells that differentiated to adipocytes a SS Log vs Nile Red (FL2) density plot on viable ASCs was created. A region was drawn around the Nile Red (FL2) bright cells as shown on Figure 2.12 and these cells represented Nile Red positive cells. A shift to the right of the Nile Red (FL2) density plot signified an increase in lipid content and thus constituted differentiated cells.

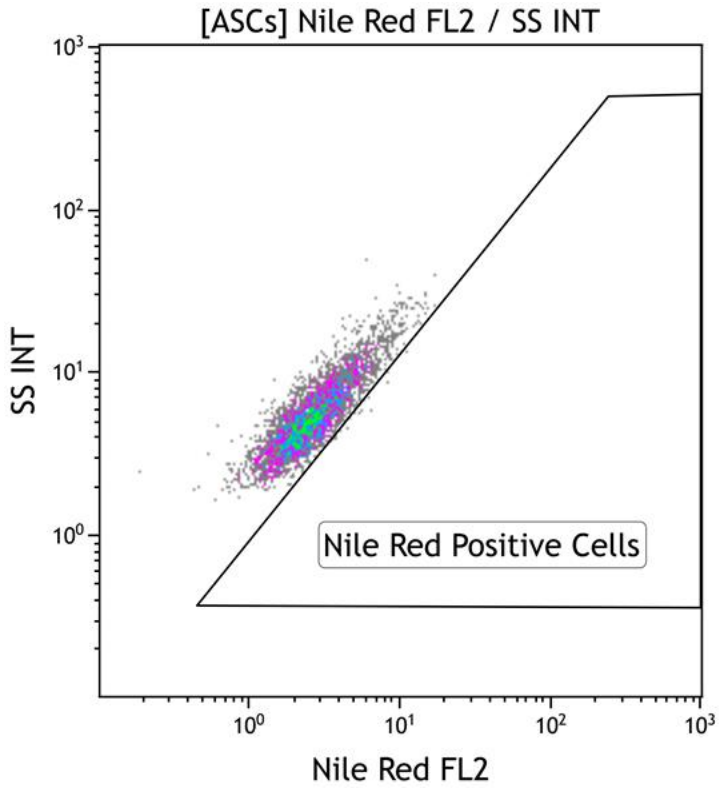

Figure 2.12 Gating strategy to detect the percentage of cells that differentiated into adipocytes. Adipogenic differentiation is represented by Nile Red positive cells in the Nile Red FL2 region

2.4.4 Treatment of ASCs with vehicle control

ASCs in this condition served as the untreated negative control. On reaching 90 to 100% confluency, complete medium was replaced with adipogenic induction medium (medium supplemented with 0.2% ethanol) for the induced ASC cultures. Medium was supplemented with 0.2% ethanol because the ROS scavengers Trolox and apocynin were dissolved in ethanol. Non-induced ASC cultures were maintained in complete DMEM

medium (medium supplemented with 0.2% ethanol). The cultures were then induced to differentiate as described in section 2.4.1.

2.4.5 Treatment of ASCs with Trolox and apocynin

On reaching 90 to 100% confluency, complete medium was replaced with adipogenic induction medium (medium supplemented with either 10 µM Trolox or 100 µM apocynin) for the induced ASC cultures. Non-induced ASC cultures were maintained in complete DMEM medium (medium supplemented with either 10 µM Trolox or 100 µM apocynin). The cultures were then induced to differentiate as described in section 2.4.1. Trolox and apocynin were maintained in the respective culture media throughout the set differentiation periods.

2.4.6 Treatment of ASCs with hydrogen peroxide

To mimic the effects of oxidative stress conditions, cells were pretreated with 20 µM H_2O_2 for 24 hours as well as prolonged treatment with 20 µM H_2O_2 throughout the set differentiation periods. The value of 20 µM H_2O_2 was derived from literature as well as from a previous study conducted by an MSc student from our research group[16].

2.4.6.1 Pretreatment of ASCs with hydrogen peroxide

On reaching 90 to 100% confluency, medium supplemented with 20 µM H_2O_2 was added to ASC cultures (induced and non-induced) in complete medium and incubated for 24 hours at 37 °C and 5% CO_2. After 24 hours, the medium containing H_2O_2 was removed and then replaced with adipogenic induction medium supplemented with 0.2% ethanol (vehicle control) for the induced ASC cultures. The induced ASC cultures were then differentiated as described in section 2.4.1. The non-induced ASC cultures were maintained in complete medium supplemented also with 0.2% ethanol (vehicle control). The degree of adipocyte differentiation was assessed on days 0, 14 and 21 post adipogenic induction.

2.4.6.2 Pretreatment of ASCs with hydrogen peroxide followed by addition of Trolox and apocynin

On reaching 90 to 100% confluency, medium supplemented with 20 µM H_2O_2 was added to ASC cultures (induced and non-induced) in complete medium and incubated for 24 hours at 37 ºC and 5% CO_2. After 24 hours, the medium containing H_2O_2 was removed and then replaced with adipogenic induction medium (medium supplemented with either 10 µM Trolox or 100 µM apocynin) for the induced ASC cultures. Non-induced ASC cultures were maintained in complete DMEM medium (media supplemented with either 10 µM Trolox or 100 µM apocynin). The induced ASC cultures were then differentiated as described in section 2.4.1. Trolox and apocynin were maintained in the respective culture media throughout the set differentiation periods.

2.4.6.3 Prolonged treatment of ASCs with hydrogen peroxide

On reaching 90 to 100% confluency, complete medium was replaced with adipogenic induction medium supplemented with 20 µM H_2O_2 and 0.2% ethanol (vehicle control) for the induced ASC cultures. Non-induced ASC cultures were maintained in complete DMEM medium supplemented with 20 µM H_2O_2 and 0.2% ethanol (vehicle control). The induced ASC cultures were then differentiated as described in section 2.4.1. The H_2O_2 and vehicle control were maintained throughout the differentiation periods. The degree of adipocyte differentiation was assessed on days 0, 14 and 21 post adipogenic induction.

2.4.6.4 Prolonged treatment of ASCs with hydrogen peroxide followed by addition of Trolox and apocynin

On reaching 90 to 100% confluency, complete medium was replaced with adipogenic induction medium supplemented with either 20 µM H_2O_2 and 10 µM Trolox or 20 µM H_2O_2 and 100 µM apocynin for the induced ASC cultures. Non-induced ASC cultures were maintained in complete DMEM medium supplemented with either 20 µM H_2O_2 and 10 µM Trolox or 20 µM H_2O_2 and 100 µM apocynin. The induced ASC cultures were then differentiated as described in section 2.4.1. The H_2O_2, apocynin and Trolox were maintained throughout the set differentiation periods. The degree of adipocyte differentiation was assessed on days 0, 14 and 21 post adipogenic induction.

2.5 Flow cytometric quantification of intracellular ROS measurements

Intracellular ROS measurements were performed using the CellROX® Deep Red assay reagent and the MitoSOX™ Red mitochondrial superoxide indicator reagent (Invitrogen by Thermo Fisher Scientific, Eugene, Oregon USA). At day 0, 14 and 21 post adipogenic induction, induced and non-induced ASCs were trypsinised from 6-well plates as described in Chapter 2, section 2.42. After trypsinisation non-induced and induced ASCs were pooled into separate 15 ml tubes and volume topped up to 4 ml with complete DMEM medium.

One ml and 500 µl of the respective cell suspension was transferred into labelled flow cytometry tubes for the CellROX® Deep Red and MitoSOX™ Red assays respectively. For the tert-butyl hydroperoxide (TBHP) CellROX® Deep Red positive control, 1 ml of day 0 cell suspension was first treated with 100 µM TBHP for 30 minutes at 37 ºC before subjected to the same procedure as for test samples. CellROX® Deep Red and MitoSOX™ Red reagents were added to cell suspension to a final concentration of 5 µM followed by the addition of DAPI (5 ng/ml). This mixture was then incubated in the dark at 37 ºC for 30 minutes, washed twice with PBS and then resuspended in 1 ml of complete DMEM medium for immediate analysis using the Gallios flow cytometer.

2.5.1 Setup and gating strategy followed for intracellular ROS measurements

For the CellROX® Deep Red assay, a SS Log vs CellROX® FL6 density plot was created to detect total intracellular ROS levels (Figure 2.13A). A SS Log vs MitoSOX™ FL2 was created for mitochondrial ROS detection (Figure 2.13B). Mean fluorescence intensity (MFI) was the parameter used to assess intracellular ROS levels. MFI represents the quantity of a parameter per event, in other words the fluorescence intensity per cell, and is expressed as relative fluorescent units. In this case MFI represents the average amount of ROS present per given cell. All cells stained positive with the CellROX® Deep Red reagent, thus a region was drawn around all cells as shown in Figure 2.13A and the MFI of the selected cells was used. Interestingly we observed a MitoSox Red negative and a MitoSox Red positive population. Thus, for MitoSox Red we reported the MFI of the cells that stained positive for MitoSOX Red. For the MFI, a region was drawn around the

proportion of cells that stained positively with MitoSOX™ Red reagent as shown in Figure 2.13B. A shift in cells to the right of MitoSOX™ FL2 density plot indicated an increase in the percentage of cells staining positively with MitoSOX™ Red reagent. The MFI corresponding to the selected positively stained cells was used.

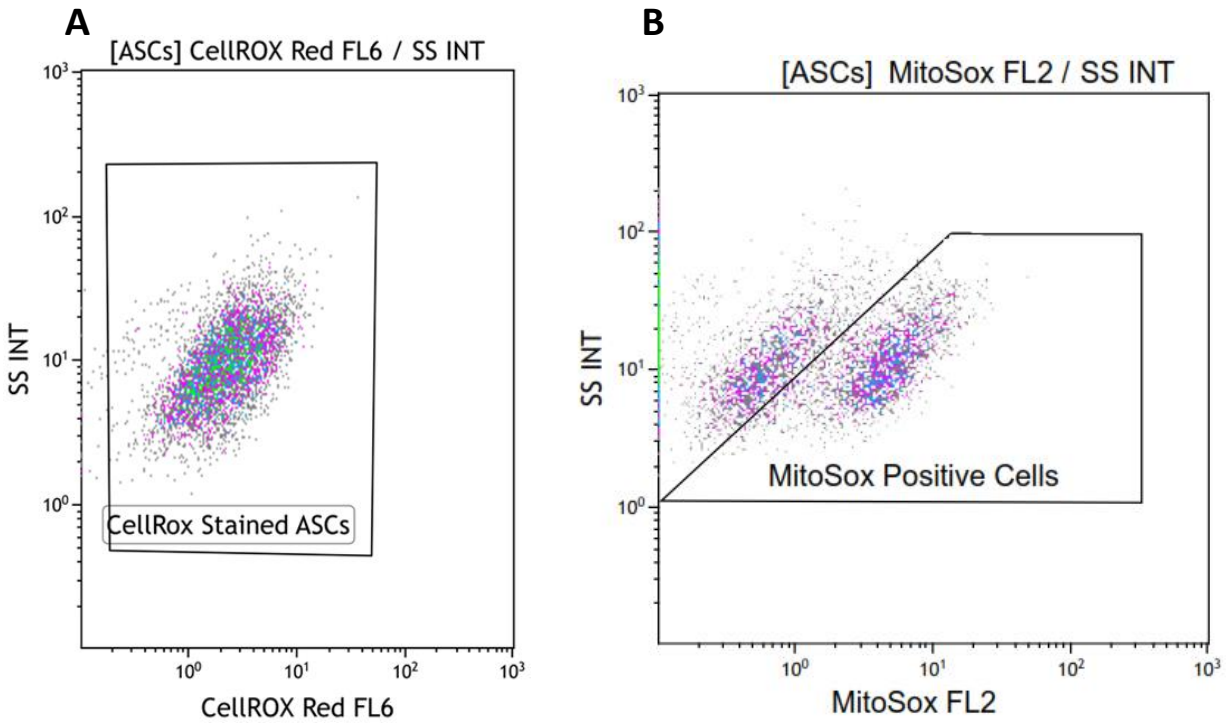

Figure 2.13 Gating strategy to detect intracellular ROS levels in differentiating ASCs
Total intracellular cytoplasmic ROS levels were measured from the MFI of the cells in the CellRox Red FL6 region (**A**). Mitochondrial ROS levels were represented by MitoSox Positive cells in the MitoSox FL2 region (**B**).

References

1. Zuk PA, Zhu M, Mizuno H, Huang J, Futrell JW, Katz AJ, et al. Multilineage cells from human adipose tissue: implications for cell-based therapies. Tissue Eng. 2001;7(2):211–28.

2. Bunnell BA, Flaat M, Gagliardi C, Patel B, Ripoll C. Adipose-derived stem cells: Isolation, expansion and differentiation. Methods. 2008;45(2):115–20.

3. Bora P, Majumdar AS. Adipose tissue-derived stromal vascular fraction in regenerative medicine: a brief review on biology and translation. Stem Cell Res Ther. 2017;8(1):145.

4. Pieper IL, Radley G, Chan CHH, Friedmann Y, Foster G, Thornton CA. Quantification methods for human and large animal leukocytes using DNA dyes by flow cytometry. Cytom Part A. 2016;89(6):565–74.

5. Long LH, Halliwell B. Artefacts in cell culture: pyruvate as a scavenger of hydrogen peroxide generated by ascorbate or epigallocatechin gallate in cell culture media. Biochem Biophys Res Commun. 2009;388(4):700–4.

6. Ramos-Ibeas P, Barandalla M, Colleoni S, Lazzari G. Pyruvate antioxidant roles in human fibroblasts and embryonic stem cells. Mol Cell Biochem. 2017;429(1–2):137–50.

7. Oberbauer E, Steffenhagen C, Wurzer C, Gabriel C, Redl H, Wolbank S. Enzymatic and non-enzymatic isolation systems for adipose tissue-derived cells: current state of the art. Cell Regen. 2015;4(7).

8. Baer PC. Adipose-derived mesenchymal stromal/stem cells: an update on their phenotype in vivo and in vitro. World J Stem Cells. 2014;6(3):256–65.

9. Lugli E, Roederer M, Cossarizza A. Data analysis in flow cytometry: the future just started. Cytometry A. 2010;77(7):705–13.

10. Bourin P, Bunnell BA, Casteilla L, Dominici M, Katz AJ, March KL, et al. Stromal cells from the adipose tissue-derived stromal vascular fraction and culture

expanded adipose tissue-derived stromal/ stem cells: a joint statement of the International Federation for Adipose Therapeutics (IFATS) and Science and the International S. Cytotherapy. 2013;15(6):641–8.

11. Wu D, Yotnda P. Production and Detection of Reactive Oxygen Species (ROS) in Cancers. J Vis Exp. 2011;(57):e3357.

12. Boumelhem BB, Assinder SJ, Bell-Anderson KS, Fraser ST. Flow cytometric single cell analysis reveals heterogeneity between adipose depots. Adipocyte. 2017 Apr 3;6(2):112–23.

13. Majka SM, Miller HL, Helm KM, Acosta AS, Childs CR, Kong R, et al. Analysis and isolation of adipocytes by flow cytometry. 1st ed. Vol. 537, Methods in Enzymology. Elsevier Inc.; 2014. 281-296 p.

14. Aldridge A, Kouroupis D, Churchman S, English A, Ingham E, Jones E. Assay validation for the assessment of adipogenesis of multipotential stromal cells-a direct comparison of four different methods. Cytotherapy. 2013;15(1):89–101.

15. Life Technologies Corporation. Dead Cell Identification in Flow Cytometry. BioProbes. 2011;26(64):26–8.

16. Miard S, Dombrowski L, Carter S, Boivin L, Picard F. Aging alters PPARγ in rodent and human adipose tissue by modulating the balance in steroid receptor coactivator-1. Aging Cell. 2009;8(4):449–59.

Chapter 3: Isolation, expansion and characterization of adipose-derived stromal/stem cells

3.1 Introduction

Stem cells have generated great interest in the research and clinical fields and they have the potential to be applied in many areas. Stem cells hold great promise in regenerative medicine for use as cell based therapies mainly owing to their multilineage differentiation potential. Several clinical trials have been conducted using stem cells as cell based therapies for the treatment of various diseases such as acute myocardial infarction, liver cirrhosis and stroke[1–3]. Mesenchymal stromal/stem cells (MSCs) are adult stem cells that were initially isolated from the bone marrow. Bone marrow derived MSCs (BM-MSCs) can be differentiated into chondrocytes, adipocytes and osteocytes. However, the use of BM-MSCs is limited because of the relatively complex and painful isolation procedures. Also, cell yields from bone marrow aspirates are generally very low making the bone marrow a less ideal site for MSC isolation[1,4]. Interestingly, it was later discovered that MSCs could be isolated from almost all tissue types particularly umbilical cord, liver, adipose tissue, placenta, dental tissues among others[1,5].

Stem cells are often required in large numbers for use in most research and clinical applications. Thus, tissue sources which are easily accessible by minimally invasive procedures, and which provide high cell numbers with multilineage differentiation capacity will be an attractive option[2,3,6–8]. Adipose tissue is a readily and easily accessible tissue that can be obtained in relative abundance from surgical wastes following liposuction and abdominoplasty procedures. Acquiring stem cells from adipose tissue, considered as biological waste, is generally considered ethically acceptable and the isolated stem cells have good regenerative capacity. Consequently, adipose tissue is an attractive source of stem cells for most tissue engineering and regenerative medicine applications, thus, supporting the use of adipose tissue as the source for isolating stem cells[2,4,7].

To confirm that cells isolated from fat tissue are representative of stem cells, the International Federation for Adipose Therapeutics and Science (IFATS) together with

the International Society for Cellular Therapy (ISCT) guidelines were adopted. Under these criteria stem cells should be plastic adherent, positive for cell surface markers CD13, CD29, CD44, CD73, CD90 and CD105. Whilst, CD36 and CD34 are unstable positive markers present at variable levels. The cells should also be negative for the markers CD31, CD45, and CD235a. In addition, the cells also need to possess trilineage differentiation capacity into adipocytes, chondrocytes and osteoblasts[9–11]. Thus, this chapter therefore describes the procedures used in the isolation of ASCs from human lipoaspirate samples as well as the expansion and characterisation procedures used to ensure that isolated cells adhered to the IFATS and ICTS guidelines.

3.2 Materials and Methods

Isolation, expansion and characterization of ASCs was performed as described in Chapter 2, sections 2.1 to 2.3 respectively.

3.3 Results

3.3.1 Isolation and expansion of ASCs

As per the IFATS and ISCT guidelines, adherence to plastic is a defining characteristic feature of ASCs. A proportion of the SVF cells were observed to adhere to the plate surface within 24 hours of incubation, on initial contact with plate surface, the cells had a spherical morphology. This was however lost with prolonged incubation period as the cells were observed to spread out forming a characteristic spindle shaped morphology resembling that of fibroblasts. Spherical shaped adherent cells were also observed but these were present in lower numbers. Further incubation promoted cell proliferation and the cells grew to confluency. Different ASC cultures exhibited different growth rates and thus time taken to reach confluency.

3.3.2 Characteristics of the cell cultures used in this study

The passage number, number of freezing cycles the cells were exposed to and time to confluency (per given passage) are summarized in Table 3.1. A total number of four ASC cultures from different donors were used in the study. Three of these were obtained from

solid adipose tissue, while one was from a lipoaspirate sample. The average time taken by adherent ASCs to reach confluency across the cultures at the different passages (P1 and P2) was 14.5 ± 4.62 days (Table 3.1).

Table 3.1 Characteristics of the different cultures.

Culture	Passage	Frozen	Time to confluency (days)	Average time to confluency per culture (days)
SA060218-01 A P1/P2 F0	1	0	19	19.5
	2		20	
A141117-01 A P1/P2 F1	1	1	7	7
	2		7	
SA230118-01 A P1/P2 F0	1	0	19	15
	2		11	
SA211117-01 A P1/P2 F0	1	0	13	16.5
	2		20	

3.3.3 Characterisation of ASCs

A six-colour antibody panel CD90/CD44/CD73/CD45/CD36/CD34 was used to characterise the immunophenotype of ASCs before seeding them in 6-well plates to investigate the different experimental treatments. Immunophenotyping showed that most ASCs were CD90+CD44+CD73+CD45- (98.25 ± 1.11%). The surface marker CD45 is a common leukocyte antigen that is expressed on original mature leukocytes. The average CD45 expression observed in the ASC cultures was 0.32 ± 0.21%. Different ASC subpopulations were observed in this study. Differences in the expression profiles of CD34 and CD36 contributed to this. Based on our gating strategy, the following four different ASC immunophenotypic profiles were revealed from the findings:

i. CD90+CD44+CD73+CD45-CD34-CD36- (34.14 ± 8.15%)
ii. CD90+CD44+CD73+CD45-CD34-CD36+ (31.30 ± 8.70%)
iii. CD90+CD44+CD73+CD45-CD34+CD36- (30.73 ± 1.54%)
iv. CD90+CD44+CD73+CD45-CD36+CD34+ (3.83 ± 0.98%)

3.4 Discussion

In this study, we have employed procedures that have been optimised in our laboratory to isolate ASCs from human adipose tissue for the purposes of investigating the effects of ROS scavengers on adipogenesis. Literature has shown that there is no standardised procedure for isolating ASCs from fat tissue samples. These differences in ASC isolation procedures between different laboratories have made inter-laboratory comparison of isolated ASCs difficult. The IFATS and ISCT have therefore established guidelines to assist in the standardisation of ASC characterisation. Following these guidelines, the ASCs isolated in this study were simultaneously stained with the monoclonal antibodies CD73, CD90, CD44, CD36, CD34 and CD45. This study therefore reports a combined ASC CD90, CD44, CD73, CD45, CD36, CD34 phenotype. Isolated ASCs in culture revealed four immunophenotypes which all fulfilled the IFATS and ISCT criteria. Thus, isolated cells to be used for downstream experimental procedures were ASCs.

Heterogeneity is one of the hallmarks of isolated ASCs. The four different subpopulations of cells as shown by the different immunophenotypic profiles highlight the heterogenous nature of these isolated cells. The observed variation in the expression of CD34 and CD36 is not surprising as it has been reported that the expression levels of these markers varies in cultured ASCs[9–11]. The four different subpopulations detected were CD34+CD36-, CD34-CD36+, CD34-CD36- and CD34+CD36+ cells, which all expressed CD73, CD44, CD90 but not CD45. CD34 is a transmembrane phosphoglycoprotein that is expressed mostly on haematopoietic stem and progenitor cells and is traditionally used as a negative marker of ASCs. It has previously been observed that all cells at P0 (adherent fraction of SVF) express CD34, but expression of CD34 is subsequently lost during cell culture over time with increase in cell passaging[12].

CD36 on the other hand is a transmembrane glycoprotein implicated in many biological processes including uptake of free long chain fatty acids. CD36 is expressed in many cell types such as platelets, monocytes, adipocytes as well as ASCs[13,14]. As per IFATS and ISCT guidelines, CD36 should be dimly expressed in ASCs and together with CD34 their expression profiles in ASCs is variable[10,15]. In line with this study, other investigators have

also reported on the heterogeneity of ASCs. Notably in studies by Baer and colleagues (2013), they detected the presence of CD34+CD36- and CD34-CD36+ ASC subpopulations which showed co-expression of CD73, CD90 and CD105 at passages 2 to 4. In addition, in their experiments they did not detect the presence of a double positive CD34+CD36+ subpopulation, which is almost similar to what we observed in this study, as we only detected a small proportion of this CD34+CD36+ double positive subpopulation (3.83 ± 0.98%). However, in contrast with this study Baer and colleagues (2013) did not report on the double negative CD34-CD36- subpopulation[16]. Flow cytometric analysis of ASCs at passages 1 and 2 in experiments by Pancho-pena and colleagues (2011) also revealed the expression of CD34 and CD36 as well as co expression of other surface markers CD44, CD90, CD105 and CD29 among others[17]. In addition, studies by Durandt and colleagues (2016) also showed that a subpopulation of ASCs had a higher expression of the surface marker CD36[13].

The observed existence of different ASC subpopulations is most likely due to several different factors. ASC cultures were established from donors who differ in age, ethnicity, gender, body mass indices as well as presence of disease. These factors most probably have an influence on cell surface marker expression[18]. Donor variability may also account for differences in inter laboratory results. In addition, the other possible reasons for the ASC heterogeneity maybe due to ASC isolation procedures as well as cell culture conditions. Isolation procedures and cell culture conditions have also been described to possibly influence the expansion of selected subpopulations as well as affect the cell differentiation potential[18].

In summary, the findings from this study show that isolated cells to be used for downstream experiments were of the ASCs phenotype. Bourin and colleagues (2013) recommended the use of at least two positive and two negative markers for phenotypic characterization, additional markers can be included to strengthen the results[10]. We recommend including some additional markers for immunophenotypic characterization of ASCs in the future. In addition, assessing for trilineage differentiation into the adipogenic,

chondrogenic and osteogenic lineages would be of great importance to fully compliment the characterisation of these cells.

References

1. Zhao RC, editor. Essentials of mesenchymal stem cell biology and its clinical translation. Dordrecht: Springer Dordrecht; 2013.

2. Yu G, Wu X, Dietrich MA, Polk P, Scott LK, Andrey A, et al. Yield and characterization of subcutaneous human adipose-derived stem cells by flow cytometric and adipogenic mRNA analyses. Cytotherapy. 2015;12(4):538–46.

3. Mailey B, Hosseini A, Baker J, Young A, Alfonso Z, Hicok K, et al. Adipose-derived stem cells: methods for isolation and applications for clinical use. In: C. K, editor. Stem Cells and Tissue Repair. New York: Humana Press, New York; 2014. p. 161–81.

4. Zuk PA, Zhu M, Ashjian P, De Ugarte DA, Huang JI, Mizuno H, et al. Human adipose tissue is a source of multipotent stem cells. Mol Biol Cell. 2002;13(12):4279–95.

5. Ullah I, Subbarao RB, Rho GJ. Human mesenchymal stem cells - current trends and future prospective. Biosci Rep. 2015;35(2):e00191.

6. Bunnell BA, Flaat M, Gagliardi C, Patel B, Ripoll C. Adipose-derived stem cells: Isolation, expansion and differentiation. Methods. 2008;45(2):115–20.

7. Krähenbühl SM, Grognuz A, Michetti M, Raffoul W, Applegate LA. Enhancement of human adipose-derived stem cell expansion and stability for clinical use ClinMed. Int J Stem Cell Res Ther. 2015;2(1).

8. Gimble J, Guilak F. Adipose-derived adult stem cells: isolation, characterization, and differentiation potential. Cytotherapy. 2003;5(5):362–9.

9. Baer PC. Adipose-derived mesenchymal stromal/stem cells: an update on their phenotype in vivo and in vitro. World J Stem Cells. 2014;6(3):256–65.

10. Bourin P, Bunnell BA, Casteilla L, Dominici M, Katz AJ, March KL, et al. Stromal cells from the adipose tissue-derived stromal vascular fraction and culture expanded adipose tissue-derived stromal/ stem cells: a joint statement of the

International Federation for Adipose Therapeutics (IFATS) and Science and the International S. Cytotherapy. 2013;15(6):641–8.

11. Oberbauer E, Steffenhagen C, Wurzer C, Gabriel C, Redl H, Wolbank S. Enzymatic and non-enzymatic isolation systems for adipose tissue-derived cells: current state of the art. Cell Regen. 2015;4(7).

12. Eto H, Suga H, Matsumoto D, Inoue K, Aoi N, Kato H, et al. Characterization of structure and cellular components of aspirated and excised adipose tissue. Plast Reconstr Surg. 2009;124(4):1087–97.

13. Durandt C, van Vollenstee FA, Dessels C, Kallmeyer K, de Villiers D, Murdoch C, et al. Novel flow cytometric approach for the detection of adipocyte subpopulations during adipogenesis. J Lipid Res. 2016;57(4):729–42.

14. Park YM. CD36, a scavenger receptor implicated in atherosclerosis. Exp Mol Med. 2014;46(6):e99.

15. Hamid AA, Idrus RBH, Saim AB, Somasumdaram S, Chua K-H. Characterization of human adipose-derived stem cells and expression of chondrogenic genes during induction of cartilage differentiation. Clinics. 2012;67(2):99–106.

16. Baer PC, Kuçi S, Krause M, Kuçi Z, Zielen S, Geiger H, et al. Comprehensive phenotypic characterization of human adipose-derived stromal/stem cells and their subsets by a high throughput technology. Stem Cells Dev. 2013;22(2):330–9.

17. Pachón-Peña G, Yu G, Tucker A, Wu X, Vendrell J, Bunnell BA, et al. Stromal stem cells from adipose tissue and bone marrow of age-matched female donors display distinct immunophenotypic profiles. J Cell Physiol. 2011;226(3):843–51.

18. Baer PC, Geiger H. Adipose-derived mesenchymal stromal/stem cells: tissue localization, characterization, and heterogeneity. Stem Cells Int. 2012;2012:11 pages.

Chapter 4: Effects of ROS scavengers on adipogenesis

4.1 Introduction

Adipogenesis is a developmental process in which precursor stem cells form fully differentiated lipid filled mature adipocytes[1,23]. This process is mediated by numerous factors that comprise of transcription factors, hormones, cell cycle proteins, small molecules among other factors[2,4–6]. Adipogenesis is a time dependent process occurring through different stages[7]. Reactive oxygen species (ROS) have been described to play a role during the transition from stem cell to adipocyte[7–10]. In cells, NADPH oxidase (NOX) and mitochondria are the main sources of ROS producing mainly hydrogen peroxide (H_2O_2) and superoxide ($O_2^{\bullet-}$)[8,11,12]. Enhancement of adipogenesis can result in increased adipose tissue mass, which in turn leads to obesity[7]. Obesity is a global health crisis that is associated with physiological changes ultimately leading to the development of metabolic syndrome[13].

Obesity is characterised by high levels of ROS in adipose tissue and this generated ROS has been implicated in enhancing adipogenesis[7]. Effective therapeutic solutions for obesity and related complications remain to be identified or developed. Counteracting ROS during adipogenesis may help provide ways to supress adipogenesis and in turn obesity. Antioxidants are an example of substances that can be used to prevent or reduce ROS. Numerous enzymatic and non-enzymatic (endogenously or exogenously derived) antioxidants have been described to be involved in regulating adipogenesis as well as obesity in many *in vitro* and *in vivo* studies[7,11,14]. In this study, the antioxidants Trolox and apocynin were used as ROS scavengers during the adipogenic differentiation of isolated primary human adipose-derived stromal/stem cells (ASCs). Adipogenic quantification was assessed by flow cytometric analysis of Nile Red stained cells. Use of flow cytometry allows for a quantitative analysis of adipogenic differentiation, allowing for rapid acquisition of many cells at the single cell level[15–17]. The alternative is to make use of qualitative analysis using microscopy after cells are stained with a lipid-specific dye such as Oil Red O[17]. Only a limited number of cells are analysed with microscopy and the ability

to analyse many cells results in more accurate reporting of the fraction (percentage) of cells that differentiated into adipocytes.

The role of ROS in the process of adipogenesis remains largely unknown, and the effects of the ROS scavengers Trolox and apocynin on adipogenesis have not been extensively described in literature. This chapter therefore investigates the influence of Trolox and apocynin treatment on adipogenic differentiation in human ASCs *in vitro*.

4.2 Materials and Methods

4.2.1 Selection of an appropriate concentration of ROS scavenger

The concentration of the ROS scavanger Trolox used for downstream experiments was 10 µM. The MTT 3-(4,5-dimethylthiazol-2-yl)-2,5-diphenyltetrazolium bromide (Sigma-Aldrich) and the Sulforhodamine B (SRB) (Sigma-Aldrich) assays were used to determine the concentration of Trolox to use during a previous study in our laboratory. In this study Trolox at various concentrations was also tested on cell cultures over a period of 21 days using the MTT and SRB assays. Both the SRB and MTT assays were used in order to increase the reliability and validity of our viability results. The MTT assay is a widely used cell viability assay, that relies on cellular metabolic activity to convert colourless tetrazolium to purple formazan[18]. However, certain compounds e.g. plant extracts, antioxidants, phytoestrogens etc. can cross react with tetrazolium leading to false positives[19,20]. The SRB assay is based on total cellular protein content measurements as opposed to cellular metabolic functionality and is thus not affected by these interfering substances[19]. As a result, in this study the SRB assay was chosen as a confimatory assay. ASCs were seeded in 12-well plates (Thermo Scientific™) at a density of 5 000 cells/cm^2 (9 500 cells per well) and incubated at 37 °C, 5% CO_2 till they reached 90 to 100% confluency. They were then treated with the following concentrations of Trolox: 0, 2.5, 5, 10, 20 and 40 µM for 21 days. Viability assessments were done at day 0, 1, 7, 14 and 21 post treatment, respectively.

4.2.1.1 MTT Assay

At each respective time point, the MTT assay was done according to the manufacture's instructions with slight modifications[21]. Stock MTT solution was made up by dissolving MTT in PBS (pH 7.4) at 5 mg/ml and filtered using a 0.22 µm filter. A volume of 50 µl MTT solution was added to all wells in a 12-well plate and the plates were incubated in the dark at 37°C for 4 hours. The supernatant was removed and the cells were allowed to dry in the dark overnight (until they were visibly dry). The formazan blue crystals were solubilized by adding dimethyl sulfoxide (DMSO;Sigma-Aldrich) to all the wells. The plates were then swirled gently until all formazan crystals were completely dissolved. Thereafter, a 100 µl aliquot of each sample was transferred to a 96-well plate, and the optical density (OD) of each well was measured at a wavelength of 570 nm against a reference wavelength of 630 nm using a microplate spectrophotometer (Power Wave X;BioTek Instruments, Winooski, VT, USA). The percentage cell viability was calculated as follows:

Equation 4.1

$$\frac{\text{mean OD}_{\text{Sample}} - \text{mean OD}_{\text{Blank}}}{\text{mean OD}_{\text{Control}} - \text{mean OD}_{\text{Blank}}} \times 100\ \%$$

4.2.1.2 SRB Assay

The SRB colourimetric assay was followed as described in the protocol by Vichai and Kirtikara (2006) with slight modifications[18]. Without removing the cell culture medium, 250 µl cold 50% (w/v) trichloroacetic acid (TCA) was added to each well in a 12-well plate. This was followed by incubating the plates at 4 ºC for 1 hr. Following incubation, cells were gently washed four times with distilled water and left to dry overnight. The ASC cultures were then stained for 30 minutes with 500 µl of 0.4 % (w/v) SRB dye dissolved in 1% acetic acid. Unbound dye was removed by washing four times with 1% (v/v) acetic acid, and left to dry overnight. Protein-bound dye was solubilized with 10 mM Tris base solution (pH 10.5) [tris(hydroxymethyl) aminomethane] and plates were swirled gently till SRB was completely dissolved. Thereafter, a 100 µl aliquot of each sample was transferred to a 96-well plate, and the OD of each well was measured at a wavelength of 565 nm against a reference wavelength of 690 nm using a microplate spectrophotometer

(Power Wave X;BioTek Instruments, Winooski, VT, USA). The percentage of growth inhibition was calculated as follows:

Equation 4.2

100 - % of control cell growth

$$\% \text{ of control cell growth} = \frac{\text{mean } OD_{sample} - \text{mean } OD_{day\ 0}}{\text{mean } OD_{negative\ control} - \text{mean } OD_{day\ 0}}$$

4.2.2 Treatment and adipogenic differentiation of ASCs

Isolation of ASCs from fat tissue, expansion and characterisation were performed as described in Chapter 2, section 2.1 to 2.3. Following the selection of the appropriate concentration of ROS scavenger, experiments to quantify ASC adipogenic differentiation under different treatments were set up were set up as described in Chapter 2 section 2.4.

4.2.3 ASC viability assessment during adipogenesis

Following adipogenic differentiation under the different treatment conditions, ASC viability was assessed. Various factors, including cell culture conditions and sample preparation may compromise viability of the samples. Thus, it is important to establish the sample viability during analysis of the samples. 7-aminoactinomycin D (7-AAD) (Beckman Coulter) was used to assess the viability of ASCs during the differentiation period. Viable ASCs possess intact cell membranes and can exclude penetration by non-permeable fluorescent dyes, such as 7-AAD and propidium iodide. Compromised cell membranes provide less resistance to above-mentioned dyes crossing the cell membranes[22]. Viability assessments were carried out at day 0, 14 and 21 post induction. At the respective time points, ASCs were trypsinised from 6-well plates as described in Chapter 2 section 2.42. Thereafter 500 µl of the cell suspension was transferred into a labelled flow cytometry tube, followed by addition of 5 µl of 7-AAD. This was then incubated in the dark for 30 minutes at 37 ºC. Thereafter cell suspension was analysed on the Gallios flow cytometer. 7-AAD was excited by the 488 nm blue laser and fluorescence emission was detected in

the FL4 (695/30 BP filter) channel. Data generated was analysed using the Kaluza analysis 2.0 software. Four biological replicates were analysed in the experiments.

4.2.4 Flow cytometric adipogenic quantification

Flow cytometric quantification of adipogenesis was performed as described in Chapter 2 section 2.43.

4.2.5 Flow cytometer setup and data analysis

Instrument start-up, protocol set up and gating strategies employed are as described in Chapter 2, section 2.3.1 and 2.4.3.2.

4.2.6 Fluorescence microscopy staining procedure

On day 0, 14 and 21 post induction, medium was aspirated from wells and replaced with fresh complete medium for both induced and non-induced wells. Complete DMEM without pyruvate and without phenol red was used. Thereafter ASCs were simultaneously stained with a final concentration of 0.1 µg/ml Nile Red stain and 2.5 µM VDC violet (Thermo Fisher Scientific/Life technologies; Waltham, MA, USA). This was followed by incubating for 20 minutes at 37 °C, 5% CO_2. Medium was then aspirated, followed by washing twice with PBS. One (1 ml) PBS was added to each well after the washing steps were completed.

Fluorescence images were captured at 20X magnification using an AxioVert A1 inverted fluorescence microscope (Carl Zeiss, Gottigen, Germany) equipped with an AxioCam Cm1 camera (Carl Zeiss, Gottigen, Germany). Images were captured in single channels and then subsequently overlaid using Zen 2.3 (blue edition) software, Carl Zeiss Microscopy GmbH, Cottigen, Germany. The first image was captured using Filter Set 9 (Excitation Band Pass 450-490 nm; Emission Long Pass 515 nm; Carl Zeiss, Cottigen, Germany) to visualise lipid droplets. The second image was captured using Filter Set 49 (Excitation Green filter 365 nm; Emission Band Pass 445/50 nm; Carl Zeiss, Cottigen, Germany) to visualize cell nuclei. Images were enhanced, but not manipulated, post-

acquisition using Zen 2.3 (blue edition) software, Carl Zeiss Microscopy GmbH, Cottigen, Germany.

4.2.7 Statistical analysis

Flow cytometry data was analysed using the Kaluza software was exported to Microsoft excel spread sheets. Statistical analysis was then performed using GraphPad Prism version 6 (GraphPad Software Inc., San Diego, USA). The non-parametric Kruskal-Wallis test was used to test for differences among the means. Follow up Dunn's multiple comparisons test was applied to determine where differences occurred between the groups. The non-parametric Mann-Whitney test was also used in testing for significant difference between two data sets. Data was generated from four donor ASC cultures and expressed as the mean ± standard deviation (SD) of all replicates. Differences were considered statistically significant at $p \leq 0.05$.

4.3 Results

4.3.1 Selection of an appropriate concentration of ROS scavenger

From previous preliminary work in our laboratory, a concentration of 10 µM Trolox was shown to be non-toxic to cells in culture. We again performed the MTT and SRB assays to validate the safety of 10 µM Trolox on cells in culture over 21 days. Trolox at 10 µM concentration had no effect on cell viability throughout the 21 day incubation period (data not shown). As a result, the concentration of 10 µM was again chosen for use in this study. Apocynin was used at a concentration of 100 µM and this value was derived from literature[23]. Dose response experiments using the MTT and SRB assays were not done for apocynin due to resource constrains.

4.3.2 ASC viability assessment during adipogenesis

The sample viability obtained for the respective experimental conditions is summarized in Table 4.1. No statistical significance was observed between the treatment conditions and control ASCs during all the respective experimental conditions. A slight decrease in the viability of non-induced ASCs on day 21 was observed ranging from 86.77 ± 9.58%

to 91.04 ± 4.19% compared to 95.74 ± 2.20% on day 0 across all the different treatment conditions throughout the differentiation period. The slight decrease in ASC viability on day 21 particularly with non-induced ASCs is most likely due to cells becoming over confluent with prolonged periods in cell culture. Non-induced controls were seeded at the same concentration as induced ASCs and cultured over a 21-day period. Confluency in cell culture has been reported to reduce mitotic index and eventually leading to cell death[24].

In accordance to the guidelines set by the International Federation for Adipose Therapeutics and Science (IFATS) together with the International Society for Cellular Therapy (ISCT) in defining ASCs, the cell viability should be greater than 90%[25]. Cells maintained high levels of viability throughout the experimental procedures. The mean viability of ASCs for all the time points and treatment conditions tested throughout the differentiation period was 93.28 ± 4.21% (Table 4.1). Thus, ASCs remained viable throughout the experimental procedures.

Table 4.1 ASC percentage viability during adipogenesis under various treatment conditions.

Experimental Condition	Treatment	Percentage viability (%)			
		Non-induced		Induced	
		Day 14	Day 21	Day 14	Day 21
Effects of ROS scavengers on ASC viability during adipogenesis	ASCs Only	93.04 ± 2.91	89.68 ± 6.23	96.28 ± 0.81	94.06 ± 2.88
	ASCs + 10 µM Trolox	93.85 ± 1.76	90.40 ± 5.99	95.96 ± 1.00	94.87 ± 3.53
	ASCs + 100 µM Apocynin	93.11 ± 2.84	90.52 ± 3.90	96.31 ± 0.98	95.52 ± 1.92
Effects of H_2O_2 treatment on ASC viability during adipogenesis	ASCs + 20 µM $preH_2O_2$	92.83 ± 3.05	88.13 ± 6.31	95.92 ± 0.97	93.08 ± 3.51
	ASCs + 20 µM $proH_2O_2$	92.28 ± 4.58	90.18 ± 4.43	96.46 ± 1.62	94.78 ± 2.52
Effects of H_2O_2 pre-treatment and ROS scavenger addition on ASC viability during adipogenesis.	ASCs + 20 µM $preH_2O_2$ + 10 µM Trolox	93.41 ± 3.08	89.08 ± 7.83	95.23 ± 1.14	93.63 ± 3.13
	ASCs + 20 µM $preH_2O_2$ + 100 µM Apocynin	92.11 ± 3.65	86.77 ± 9.58	95.28 ± 0.95	93.59 ± 4.68
Effects of H_2O_2 prolonged treatment and ROS scavenger addition on ASC viability during adipogenesis	ASCs + 20 µM $proH_2O_2$ + 10 µM Trolox	93.65 ± 2.83	91.04 ± 4.19	96.01 ± 1.66	94.33 ± 2.10
	ASCs + 20 µM $proH_2O_2$ + 100 µM Apocynin	93.86 ± 2.12	88.92 ± 6.24	96.67 ± 0.83	94.79 ± 2.52

4.3.3 Effects of serial passage on adipogenesis in ASCs

In previous adipogenesis studies by a former master's student from our research group, adipogenic differentiation in ASCs was investigated using ASCs at passage 7 (P7) to quantify adipogenic differentiation on day 14 and ASCs at between P10 and P14 to quantify adipogenic differentiation on day 21. The addition of adipogenic induction medium to ASCs at P7 and to ASCs between P10 and P14 increased the percentage of Nile Red positive cells from 0.38 ± 0.17% to 5.62 ± 2.37% on day 14 and from 0.46 ± 0.29% to 2.12 ± 0.59% on day 21 when comparing the induced versus the non-induced cultures (Figure 4.1). This reflected a statistically significant 14.8- and 4.6-fold increase in the percentage of Nile Red positive cells on day 14 ($p=0.0022$) and day 21 ($p=0.0022$) respectively.

The result obtained from that study showed the percentage of Nile Red positive ASCs decreased significantly (p=0.0022) from 5.62 ± 2.37% on day 14 to 2.12 ± 0.59% on day 21 (Figure 4.1). This indicates that an increase in cell passage number from P7 on day 14 to between P10 and P14 on day 21, resulted in a significant decrease in adipogenic differentiation capacity of the cells. These observations are supported by experiments from Safwani and colleagues (2014), in which they reported that the adipogenic differentiation potential of human ASCs decreased after P10[26].

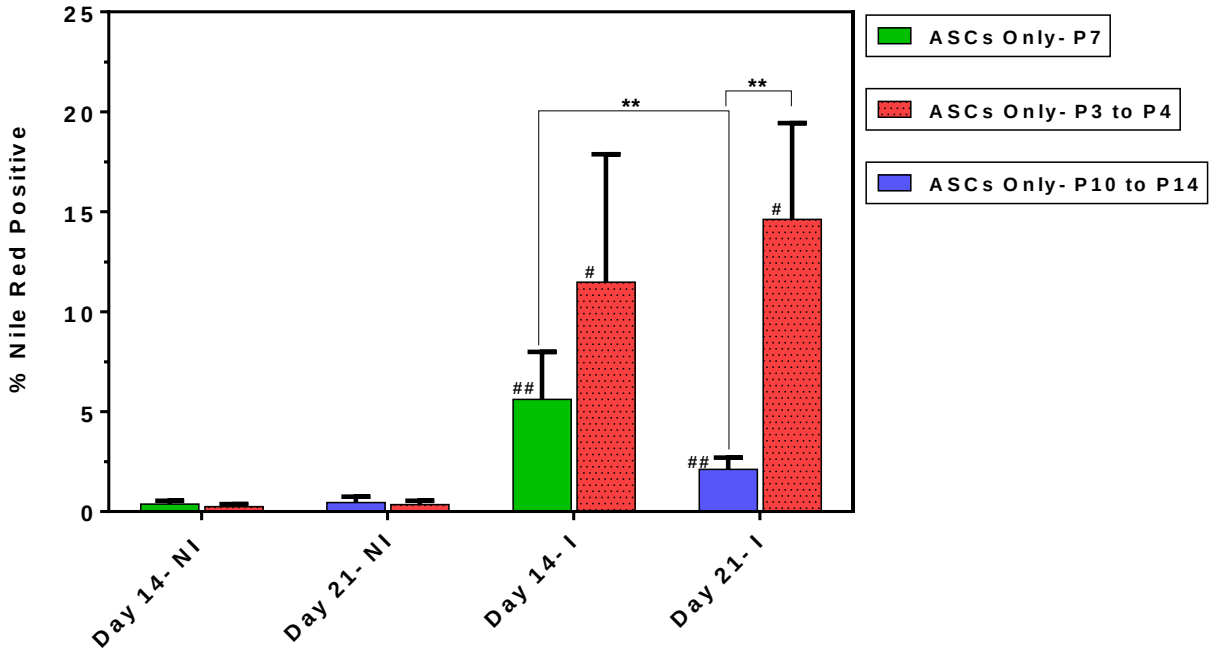

Figure 4.1 Effects of serial passage on ASCs adipogenesis.
The graph shows adipogenic differentiation of ASCs at different passages. Adipogenic quantification was performed on day 14 using ASCs at P7 (green bars) and on day 21 using ASCs at passages between P10 and P14 (blue bars) in the previous study by a former master's student. While in this current study adipogenesis was performed using cells at P3 and P4 (red bars with dots) on day 14 and 21. The addition of adipogenic induction media to ASCs significantly increased adipogenesis on day 14 and day 21, respectively. There was a decrease in the percentage of Nile Red positive ASCs when comparing induced ASCs at P7 on day 14 and induced ASCS at between P10 and P14 on day 21 from the previous study. While in this current study the percentage of Nile Red positive ASCs (P3 and P4) showed an increase from day 14 to day 21. In previous study n = 2 while current study n=4. **NI**: Non-induced; **I**: Induced. (Data was generated from a preliminary study by a former master's student). # Represents statistical significance from the respective non-induced ASC cultures. ***** Represents statistical significance as indicated by the lines.

The data generated in the preliminary study above by the previous investigator therefore suggested that the increase in passage number resulted in a significant decrease in the adipogenic differentiation potential of ASCs *in vitro.* Based on the results obtained in the previous study we used cells consistently at much lower passages (P3 and P4) on day 14 and 21 and increased the number of biological replicates (from n=2 to n=4). Furthermore, adipogenic differentiation experiments in the previous study were run at different times and not as one single experimental setup. In this current study ASC adipogenic differentiation experiments were thus performed as one single experiment. Other investigators in our laboratory have observed that the adipogenic differentiation capacity of ASCs decreases with increased passage number (personal communication, Dr C Durandt; unpublished data). We thus decided to use lower passages in this study to ensure that the relative effect of extracellular H_2O_2 and antioxidant treatments on the differentiation are investigated at optimal adipogenic differentiation (Figure 4.2).

The addition of adipogenic induction medium to ASCs at P3 and P4 increased the percentage of Nile Red positive cells from 0.25 ± 0.13% to 11.48 ± 6.40% on day 14 and from 0.35 ± 0.19% to 14.62 ± 4.82% on day 21 when comparing the induced versus the non-induced cultures (Figures 4.1 and 4.2). This reflected a statistically significant 45.9- and 41.8-fold increase in the percentage of Nile Red positive cells on day 14 ($p=0.0286$) and day 21 ($p=0.0286$) respectively. In effect, we have therefore shown that the percentage of adipogenic differentiation non-significantly ($p=0.1143$) increased from 5.62 ± 2.37% (ASCs at P7 in previous study) to 11.48 ± 6.40% (ASCs at P3 and P4 in the current study) on day 14. While on day 21, the percentage of adipogenic differentiation significantly ($p=0.0095$) increased from 2.12 ± 0.59% (ASCs at P10 to P14 in previous study) to 14.62 ± 4.82% (ASCs at P3 and P4 in the current study) (Figure 4.1).

4.3.4 Effects of ROS scavengers on adipogenesis in ASCs

ASCs between P3 and P4 previously seeded in 6-well plates were treated with the ROS scavengers Trolox and apocynin at 10 µM and 100 µM respectively, and then induced to differentiate in the presence of these scavengers. ASCs only (without ROS scavenger treatment) served as controls to investigate the effects of ROS scavenger addition on

ASC differentiation on day 0, 14 and 21 post adipogenic induction. The addition of Trolox to adipogenic induced ASCs decreased the percentage of Nile Red positive ASCs from 11.48 ± 6.4% in ASCs only to 10.41 ± 4.84% on day 14 and from 14.62 ± 4.82% in ASCs only to 13.22 ± 3.71% on day 21 (Figure 4.2A). This reflected a 1.1- and 1.2-fold decrease in the percentage of Nile Red positive ASCs on day 14 and day 21 respectively, which was however not statistically significant (p=0.9999 on day 14 and p=0.8286 on day 21).

Adipogenic differentiation was also assessed quantitatively using the mean fluorescence intensity (MFI) which represents the average quantity of lipids per given cell and is expressed as relative mean fluorescence intensity. The addition of Trolox to induced ASCs increased the MFI from 36.89 ± 18.10 in ASCs only to 41.05 ± 18.37 on day 14 and from 55.40 ± 30.46 in ASCs only to 68.14 ± 36.41 on day 21 (Figure 4.2B). This reflected a 1.1- and 1.2-fold increase in the MFI on day 14 and day 21 respectively, which was however not statistically significant (p=0.6571 on both day 14 and day 21).

On the other hand, apocynin addition to adipogenic induced ASCs slightly increased the percentage of Nile Red positive ASCs by 1.1-fold from 11.48 ± 6.4% in ASCs only to 12.69 ± 1.64% on day 14 (Figure 4.2A). Whereas on day 21, apocynin addition slightly decreased the percentage Nile Red positive ASCs by 1.2-fold from 14.62 ± 4.82% in ASCs only to 12.47 ± 5.33%. None of these observed changes with apocynin treatment on day 14 (p=0.4857) and on day 21 (p=0.6571) was statistically significant. Whereas apocynin addition to induced ASCs decreased the MFI from 36.89 ± 18.10 in ASCs only to 34.49 ± 19.01 on day 14, indicating no fold change in the MFI (Figure 4.2B). Whilst on day 21, apocynin addition increased the MFI from 55.40 ± 30.46 in ASCs only to 61.45 ± 38.86 reflecting a 1.1-fold change. None of these observed changes in MFI with apocynin treatment on day 14 and on day 21 (p=0.8286) was statistically significant.

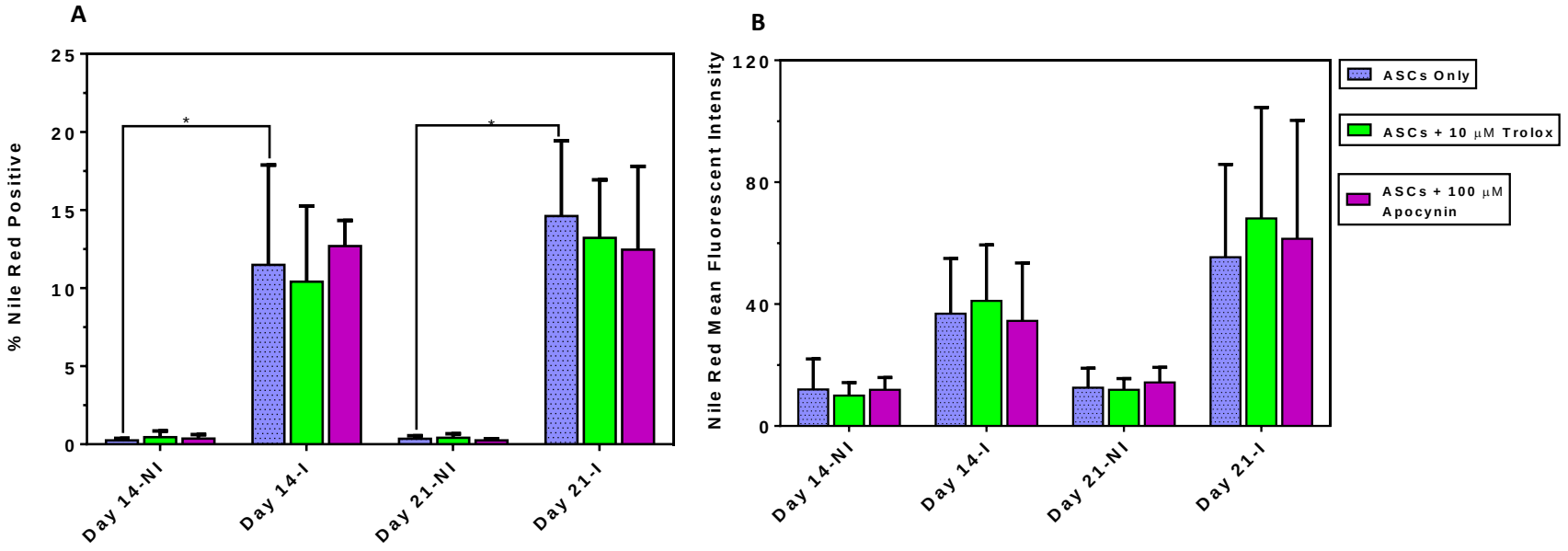

Figure 4.2 Percentages and MFI showing the effects of ROS scavengers on adipogenesis in ASCs.
(A) shows the percentage adipogenic differentiation of cells whilst **(B)** represents the respective MFI of the differentiating cells. The addition of adipogenic induction media to ASCs significantly increased adipogenesis on day 14 and day 21, respectively **(A)**. Treatment of ASCs with Trolox and apocynin followed by adipogenic differentiation had no effect on the percentage of Nile Red positive cells **(A)** as well as the MFI **(B)** on day 14 and day 21 when compared to ASCs only. ASCs incubated with complete DMEM only served as the non-induced controls. n = 4. NI: Non-induced; I: Induced. * $p < 0.05$

4.3.5 Effect of extracellular H_2O_2 addition on adipogenesis in ASCs

To investigate the effects of extracellular ROS on adipogenesis, ASCs were either pre-treated with 20 µM H_2O_2 for 24 hours and induced to differentiate (pre-treated ASCs) or were induced to differentiate in the presence of 20 µM H_2O_2 throughout the differentiation period (prolong treated ASCs). ASCs only (without H_2O_2 treatment) cultures served as controls. In pre-treated ASCs, the percentage of Nile Red positive ASCs increased slightly by 1.2- fold on day 14 (from 11.48 ± 6.4% in ASCs only to 13.86 ± 4.27%) while there was no fold change in the percentage of Nile Red positive ASCs on day 21 (from 14.62 ± 4.82% in ASCs only to 14.91 ± 5.58% on day 21) as shown in Figure 4.3A. There was no statistically significant difference in the percentage of Nile Red positive ASCs observed with H_2O_2 pre-treated ASCs on day 14 ($p=0.4857$) and day 21 ($p>0.9999$) when compared to control ASCs only. Whilst pre-treatment of ASCs with 20 µM H_2O_2 decreased the MFI by 1.2- fold (from 36.89 ± 18.10 in ASCs only to 31.79 ± 13.79) on day 14. On day 21 the MFI increased from 55.40 ± 30.46 in ASCs only to 58.36 ± 29.33, reflecting no fold change. There was no statistically significant difference in the MFI on day 14 ($p=0.6571$) and day 21 ($p=0.8286$) when compared to control ASCs only (Figure 4.3B).

On the other hand, prolonged treated ASCs showed a 1.4-fold increase in the percentage of Nile Red positive ASCs on day 14 (from 11.48 ± 6.4% in ASCs only to 15.76 ± 3.13%) while there was also no change on day 21 (from 14.62 ± 4.82% in ASCs only to 15.40 ± 4.05%) (Figure 4.3A). The kinetics of adipogenic differentiation were fastest with prolonged treatment of ASCs on day 14 while there was no further increase on day 21. There was however no statistically significant difference in the percentage of Nile Red positive ASCs on day 14 ($p=0.3429$) and on day 21 ($p=0.6571$) when compared to control ASCs only. With prolonged treatment, the MFI decreased by 1.1- fold on day 14 (from 36.89 ± 18.10 in ASCs only to 32.90 ± 12.49) while there was no fold change on day 21, MFI decreased from 55.40 ± 30.46 in ASCs only to 52.79 ± 28.46. No statistically significant difference in the MFI was observed on day 14 ($p>0.9999$) and day 21 ($p=0.8286$) when compared to control ASCs only (Figure 4.3B).

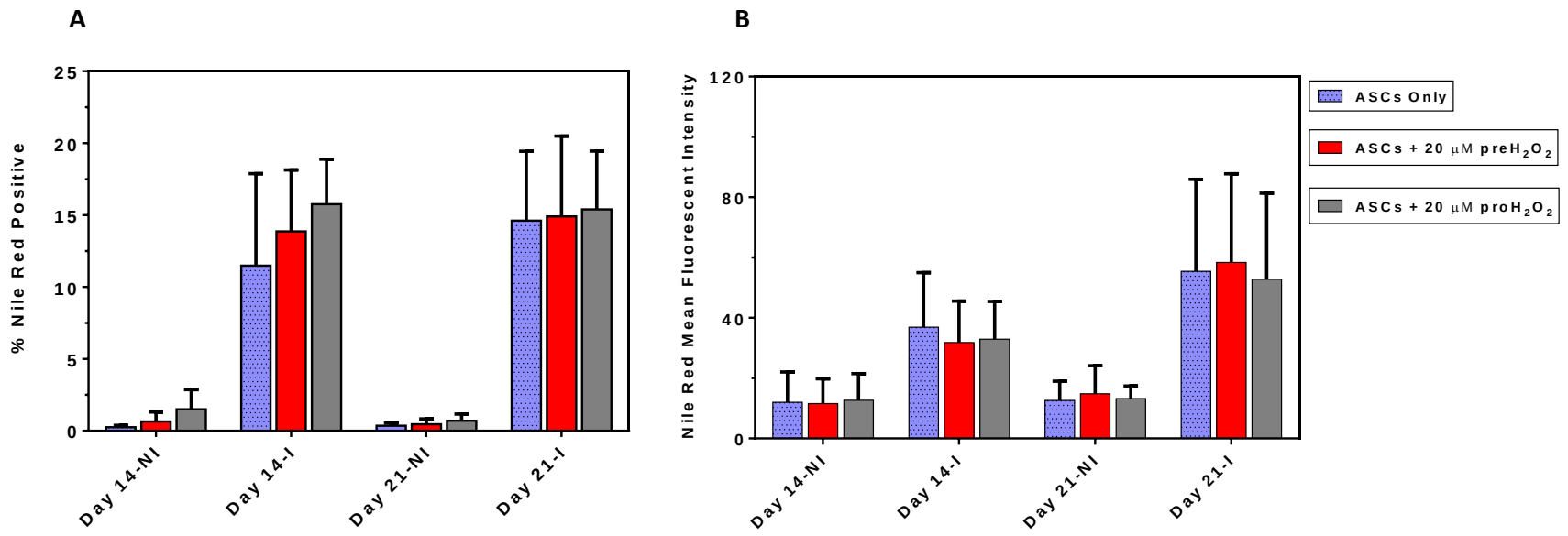

Figure 4.3. Percentages and MFI showing the effects of extracellular H_2O_2 treatment on ASCs adipogenesis.
(A) shows the percentage adipogenic differentiation of cells whilst **(B)** represents the respective MFI of the differentiating cells. The treatment of ASCs with 20 µM H_2O_2 for either 24 hours (pre-treated ASCs) or throughout the differentiation period (prolonged treated ASCs), enhances adipogenesis. The increase in adipogenesis of ASCs between the different treatment conditions was more pronounced on day 14 of differentiation. The kinetics of adipogenic differentiation was fastest in prolonged treated ASCs and did not increase further after day 14 **(A)**. Extracellular H_2O_2 treatment of ASCs had no effect on the MFI of the differentiated cells. n = 4. NI: Non-induced; I: Induced.

4.3.6 Effect of ROS scavengers on H_2O_2 treated ASCs during adipogenesis

Having shown that extracellular H_2O_2 treatment increased the kinetics of adipogenesis in ASCs, the effects of ROS scavengers on both H_2O_2 pre- and prolong treated ASCs was investigated. The control consisted of ASCs treated in the same way as the experiment but without the addition of scavengers.

4.3.5.1 Effect of ROS scavengers on adipogenesis of H_2O_2 pre-treated ASCs

The addition of Trolox to H_2O_2 pre-treated ASCs followed by adipogenic differentiation decreased the percentage of Nile Red positive ASCs by 1.2- fold on day 14 (from 13.86 ± 4.27% in the ASC control to 11.61 ± 6.13%) while there was no fold change on day 21 (from 14.91 ± 5.58% in the ASC control to 14.15 ± 5.59%) (Figure 4.4A). There was no statistically significant difference in the percentage of Nile Red positive ASCs on day 14 ($p=0.4857$) and day 21 ($p=0.6571$) when compared to the ASC control. Trolox addition to pre-treated ASCs increased the MFI by 1.3- fold on day 14 (from 31.79 ± 13.71 in the ASC control to 41.09 ± 17.05). Whilst on day 21 the MFI increased by 1.2- fold (from 58.36 ± 29.33 in the ASC control to 67.60 ± 34.87). This increase in MFI with Trolox addition was however not statistically significant on day 14 and day 21 (Figure 4.4B).

Conversely, the addition of apocynin to H_2O_2 pre-treated ASCs induced to differentiate, decreased significantly ($p=0.0286$) the percentage of Nile red positive ASCs by 1.5- fold on day 14 (from 13.86 ± 4.27% in the ASC control to 9.11 ± 0.92%). On the contrary, there was also no fold change in the percentage of Nile Red positive ASCs on day 21 (from 14.91 ± 5.58% in the ASC control to 15.04 ± 5.60%), which was not statistically significant ($p>0.9999$) when compared to the ASC control. The addition of apocynin to induced H_2O_2 pre-treated ASCs increased the MFI by 1.3- fold on day 14 (from 31.79 ± 13.71 in the ASC control to 37.39 ± 17.56). On day 21 apocynin addition to induced H_2O_2 pre-treated ASCs increased the MFI from 58.36 ± 29.33 in the ASC control to 57.94 ± 29.05. This reflected a no fold change in the MFI with apocynin addition. There was however, no statistically significant difference in the MFI on day 14 and day 21 ($p=0.6571$) (Figure 4.4B).

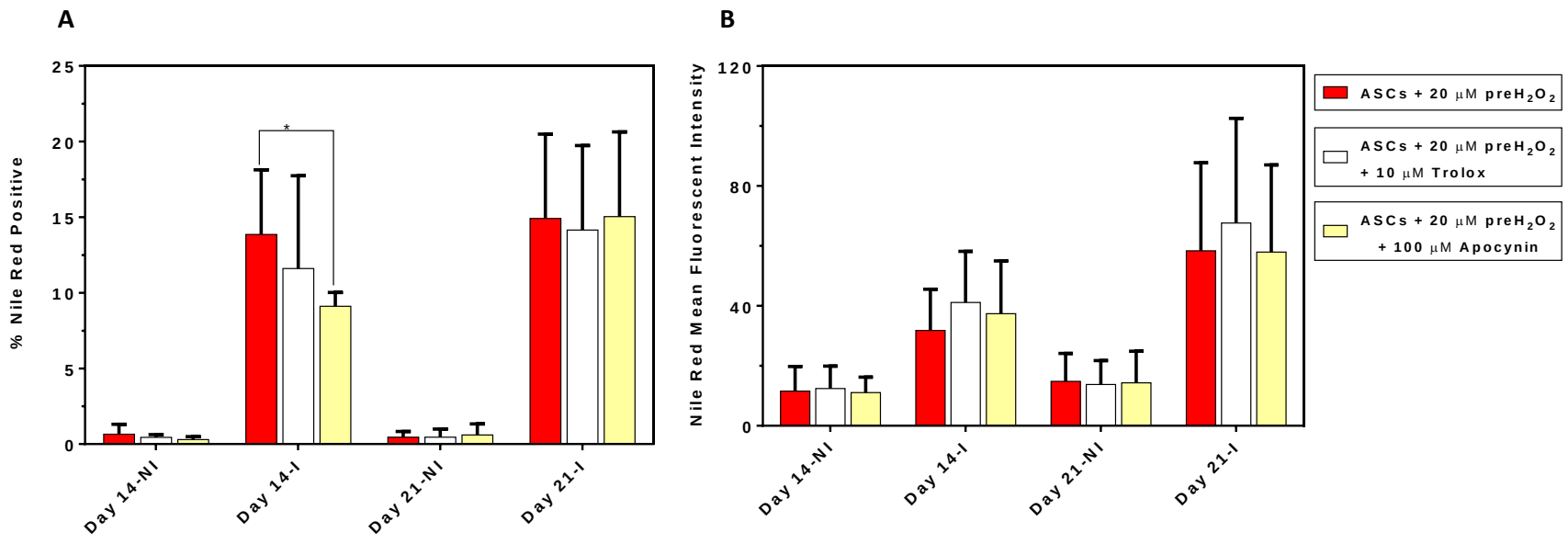

Figure 4.4 Percentages and MFI showing the effects of ROS scavengers on adipogenesis of H_2O_2 pre-treated ASCs.
(A) shows the percentage adipogenic differentiation of cells whilst **(B)** represents the respective MFI of the differentiating cells. Addition of Trolox to H_2O_2 pre-treated ASCs followed by adipogenic differentiation had no effect on the percentage of Nile Red positive cells on day 14 and day 21 when compared to H_2O_2 pre-treated ASCs only. However, the addition of apocynin significantly decreased adipogenesis on day 14 whereas there was no effect on adipogenesis on day 21 **(A)**. Trolox and apocynin addition to H_2O_2 pre-treated ASCs had no effect on the MFI of the differentiating cells **(B).** ASCs incubated with complete DMEM only served as the non-induced controls. n = 4. NI: Non-induced; I: Induced. * $p < 0.05$

4.3.5.2 Effect of ROS scavengers on adipogenesis of H_2O_2 prolonged treated ASCs

Trolox addition to H_2O_2 prolonged treated ASCs followed by adipogenic differentiation showed a negligible decrease (p=0.8286) in the percentage of Nile Red positive ASCs on day 14 (from 15.76 ± 3.13% in the ASC control to 15.49 ± 6.02%). On the contrary, day 21 showed a negligible increase in the percentage of Nile Red positive ASCs (from 15.40 ± 4.05% in the ASC control to 16.42 ± 5.91%), which was not statistically significant (p=0.8286) (Figure 4.5A). With Trolox addition to prolong treated ASCs, the MFI increased by 1.3- fold (from 32.90 ± 12.49 in the ASC control to 42.80 ± 21.11) on day 14 and by 1.2- fold (from 52.79 ± 28.46 in the ASC control to 62.38 ± 32.04) on day 21. There was no statistically significant difference in the MFI on day 14 and day 21 (p=0.4857) (Figure 4.5B).

The addition of apocynin to H_2O_2 prolonged treated ASCs followed by adipogenic differentiation decreased the percentage of Nile Red positive ASCs by 1.3- and 1.1-fold on day 14 (from 15.76 ± 3.13% in the ASC control to 12.01 ± 1.83%) and day 21 (from 15.40 ± 4.05% in the ASC control to 13.84 ± 4.58%) respectively (Figure 4.5A). The observed decrease in the percentage Nile Red positive ASCs with apocynin addition was however not statistically significant on day 14 (p=0.0571) and day 21 (p=0.3429). Whereas apocynin addition to prolonged treated ASCs increased the MFI by 1.3- fold on day 14 (from 32.90 ± 12.49 in the ASC control to 42.85 ± 25.17). On day 21 apocynin addition increased the MFI from 52.79 ± 28.46 in the ASC control to 54.68 ± 26.03 reflecting a no fold change. There was however no statistically significant difference in the MFI on day 14 and day 21 (p=0.6571) with apocynin addition compared to H_2O_2 prolonged treated ASCs only (Figure 4.5B).

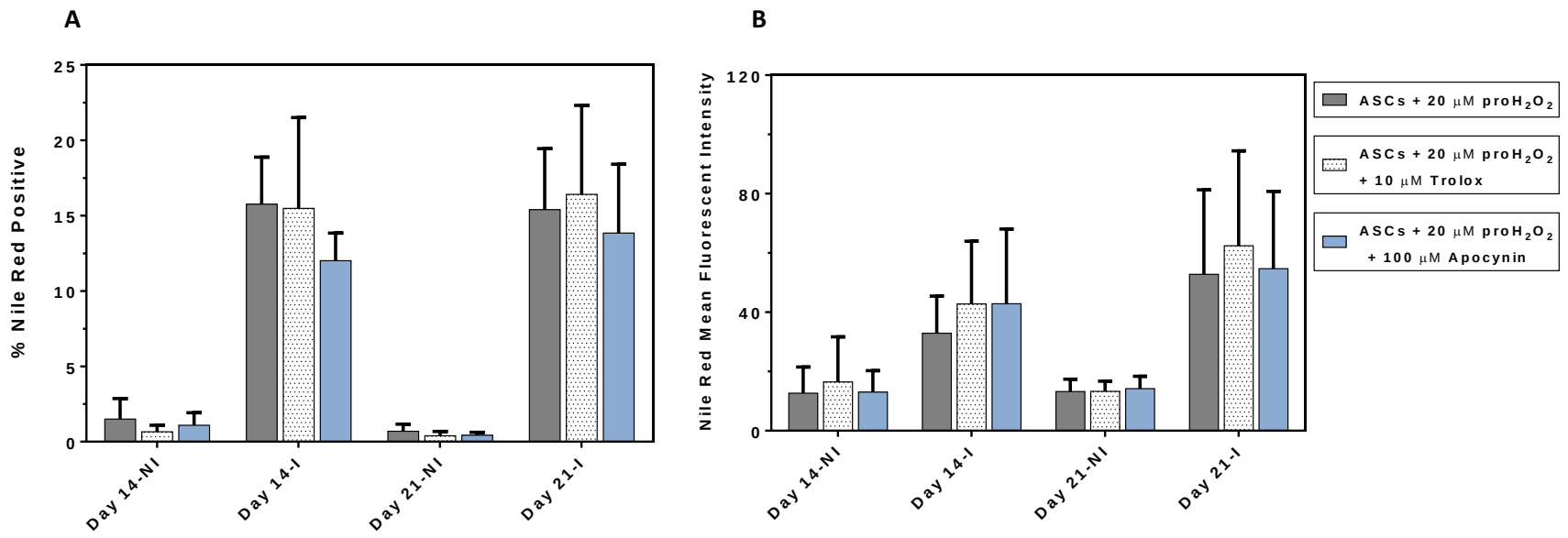

Figure 4.5 Percentages and MFI showing the effects of ROS scavengers on adipogenesis in H_2O_2 prolonged treated ASCs.
(A) shows the percentage adipogenic differentiation of cells whilst **(B)** represents the respective MFI of the differentiating cells. Trolox and apocynin addition to H_2O_2 prolonged treated ASCs followed by adipogenic differentiation showed no effect in the percentage of Nile Red positive cells on day 14 and day 21 when compared to H_2O_2 prolong treated ASCs only **(B)**. Trolox and apocynin addition to prolong treated ASCs had no effect on the MFI of the differentiating ASCs **(B)**. ASCs incubated with complete DMEM only served as the non-induced controls. n = 4. NI: Non-induced; I: Induced.

4.3.6 Fluorescence microscopy

Fluorescence microscopy images of both induced and non-induced ASC cultures for all the treatment conditions were captured. Cell nuclei stained blue and lipid droplets appeared as yellow-green small spherical bodies distributed throughout the cell. Induction of adipogenic differentiation induced lipid droplet formation and accumulation in ASCs however, only a proportion of the cells induced to differentiate accumulated lipid droplets (Figures 4.6 to 4.8). Non-induced ASCs incubated in complete DMEM medium only, also accumulated lipid droplets. These lipid droplets were however smaller and diffusely distributed around the cytoplasm (Figures 4.6 to 4.8). Fluorescence microscopy gave qualitative results, showing the presence or absence of lipid droplets only. Microscopy images did not show any visible changes in cell differentiation or lipid droplet accumulation in ASCs for all the treatment conditions. As such, this study will only show microscopy images representing adipogenic differentiation in ASCs only (Figure 4.6) and adipogenic differentiation of ASCs in the presence of either Trolox or apocynin on the different days of differentiation (Figure 4.7 and Figure 4.8 respectively).

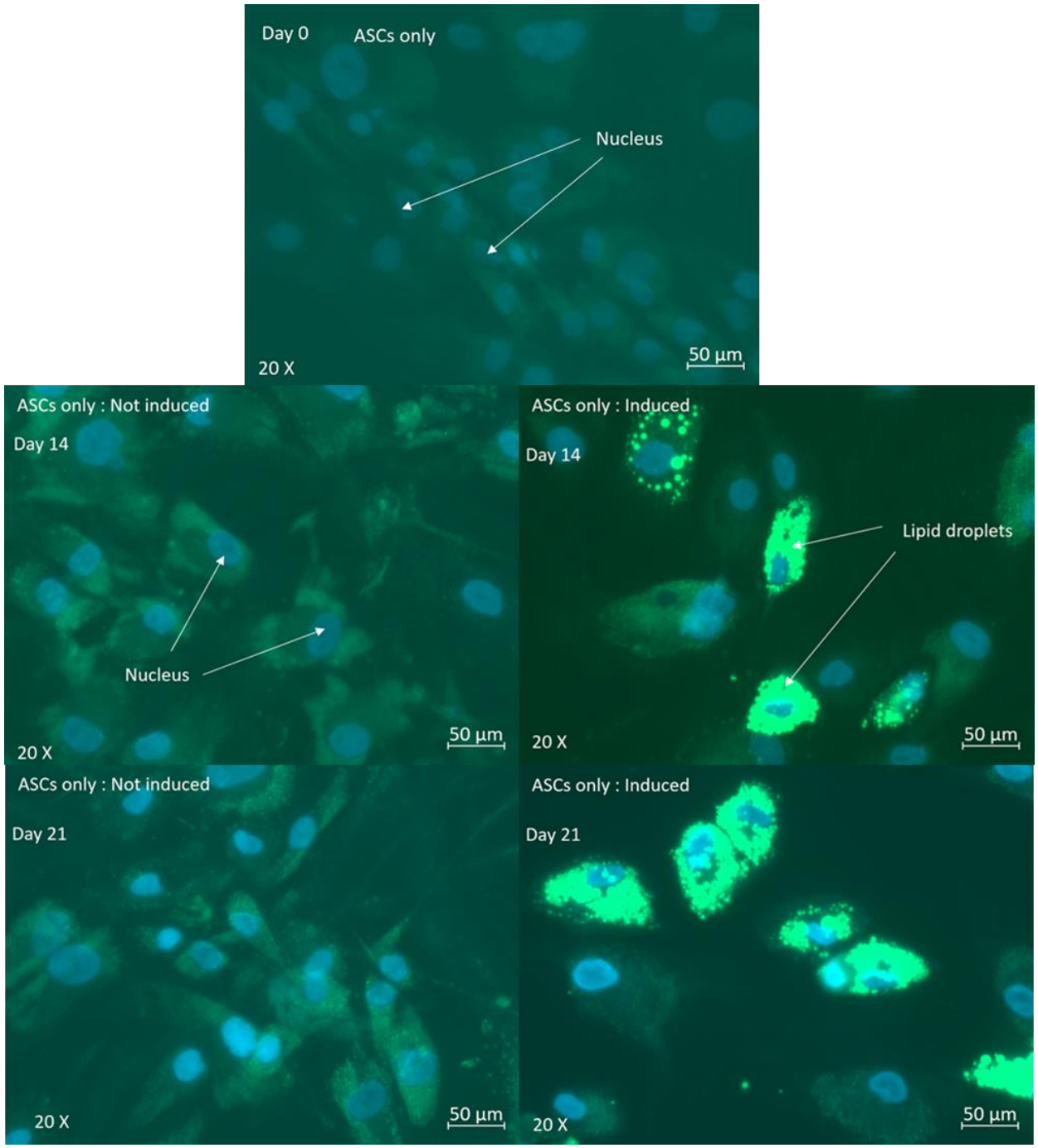

Figure 4.6 Fluorescence microscopy of ASC differentiation.
Images of induced and non-induced ASCs at day 0, 14 and 21 post adipogenic differentiation. Induced cultures on day 14 and 21 showed the presence lipid droplets accumulation, confirming cells underwent adipogenic differentiation. 20x magnification was used.

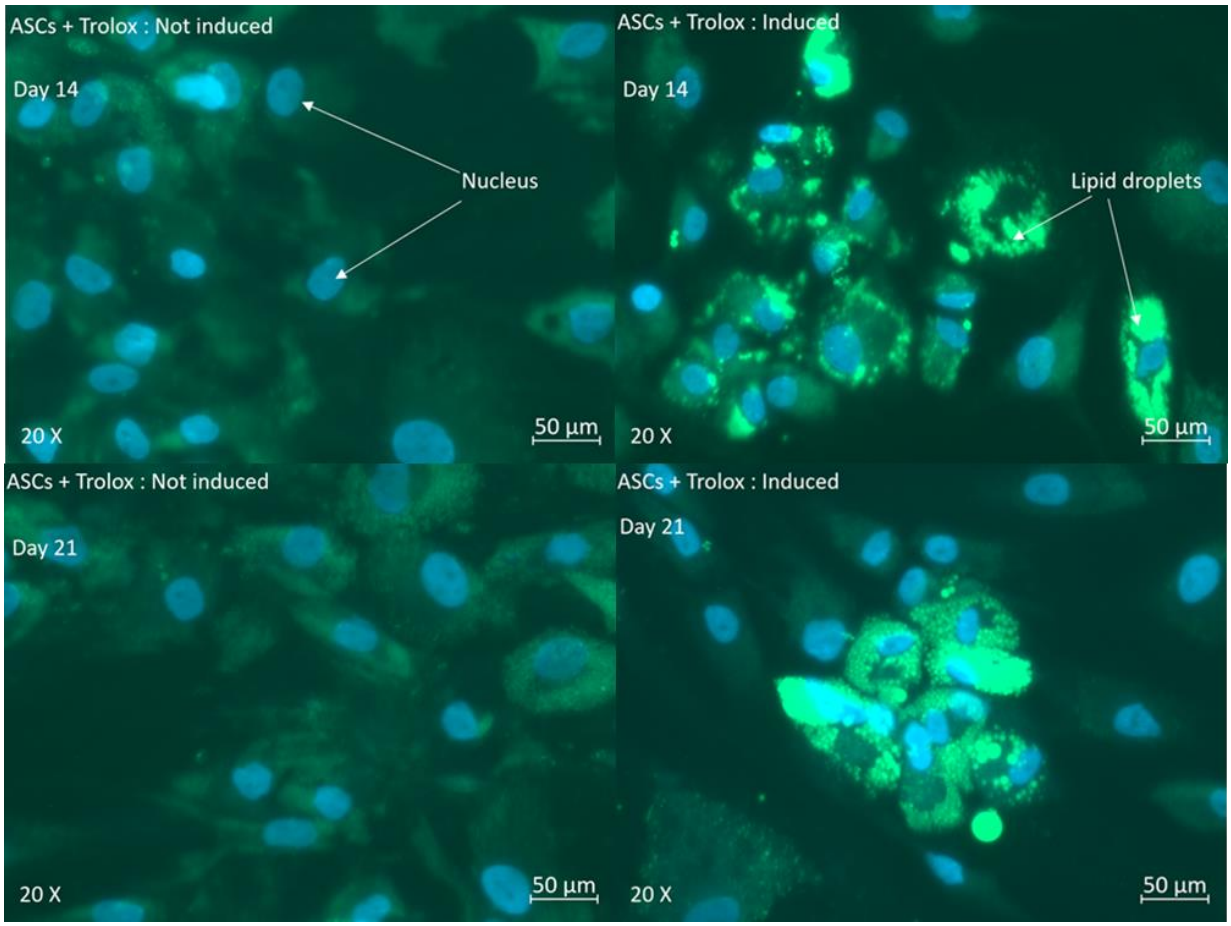

Figure 4.7 Fluorescence microscopy of differentiating ASCs treated with Trolox.
Images of induced and non-induced ASCs differentiated in the presence of 10 µM Trolox at day 14 and 21 post adipogenic differentiation. The presence of lipid droplet accumulation was evident in induced cultures on day 14 and 21 indicating cell differentiation in the presence of Trolox. 20x magnification was used.

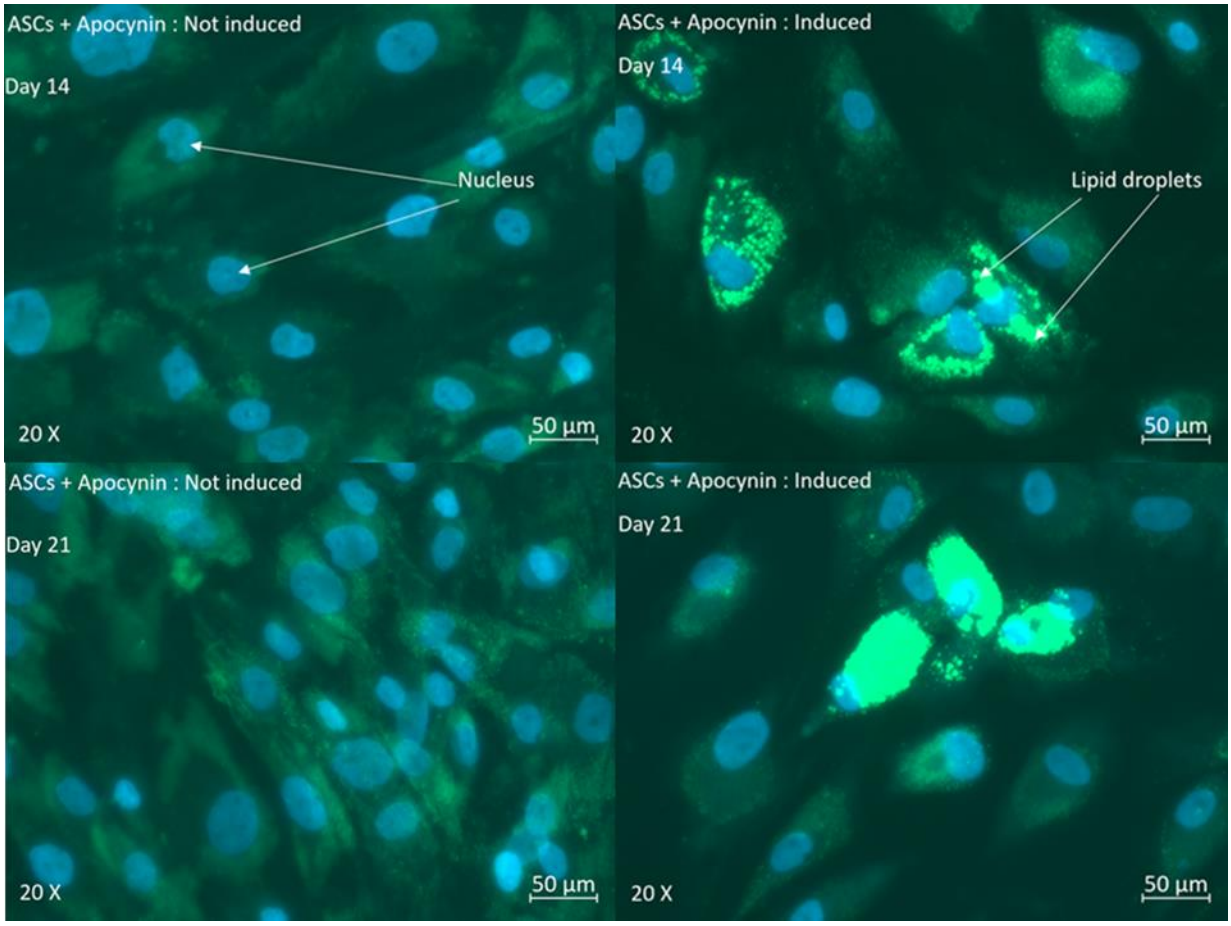

Figure 4.8 Fluorescence microscopy of differentiating ASCs treated with apocynin.
Images of induced and non-induced ASCs differentiated in the presence of 100 µM apocynin at day 14 and 21 post adipogenic differentiation showed lipid droplet accumulatio in induced culture. This confirms cell differentiated in the presence of apocynin. 20x magnification was used.

4.4 Discussion

Accelerated differentiation of adipocytes causes abnormal expansion of adipose tissue leading to obesity and other metabolic disorders[27]. The process of adipogenesis plays a major role in the formation and expansion of adipose tissue. Adipogenesis is a complex process that forms adipocytes and is regulated by an intricate network of chemical compounds among which include ROS[28]. However, the exact mechanisms governing the role played by ROS in adipogenesis remain largely unknown[8,29]. A deeper understanding of the different molecular players involved in adipocyte formation will help identify novel therapeutic targets in the fight against obesity and its comorbidities. Hence, this study investigated the influence of ROS and ROS scavengers on adipogenesis through the treatment of differentiating ASCs with the ROS scavengers Trolox and apocynin.

In this study, ASCs were induced to differentiation into the adipogenic lineage in the presence and absence of the ROS scavengers Trolox and apocynin. Using flow cytometric analysis, adipogenic differentiation was quantified based on Nile Red staining of the differentiated ASCs. The addition of Trolox to adipogenic differentiating ASCs resulted in no change in the percentage of Nile Red positive ASCs (differentiated ASCs) as well as in the MFI of the differentiating ASCs on day 14 and day 21 (Figure 4.2). In previous studies by other investigators, Trolox has been shown to have intracellular scavenging activity against H_2O_2, $O_2^{\bullet-}$, hydroxyl and peroxyl radicals[30,31]. Since ROS have been described to be involved in adipogenesis as well as in promoting adipogenesis. The addition of Trolox to differentiating ASCs was expected to result in an inhibition of adipogenesis in this study. However, lack of an effect in adipogenesis following Trolox addition suggests that Trolox does not supress adipogenesis in differentiating human ASCs. The findings also suggest that intracellular ROS are not involved in adipogenic differentiation.

There is very little information available in literature describing the role of Trolox on adipogenesis and this study is among the few that have investigated the influence of Trolox on adipogenic differentiation in human ASCs in relation to its ROS scavenging properties. In agreement with our findings, experiments by Alves and colleagues (2013)

revealed that Trolox addition to adipogenic differentiating BM-MSCs (at P3) for 21 days also did not have any discernible effect on adipogenic differentiation[32]. The antioxidant property of Trolox is well described in literature as it has been widely used in several studies as a positive control reference standard to measure the antioxidant properties of natural plant derived products[33,34]. Although in this study, there was no effect on adipogenesis following Trolox addition. There was however an observed slight non-significant decreasing trend in the percentage of Nile Red positive ASCs with Trolox addition (Figure 4.2A). Thus, the potential use of Trolox as a ROS scavenger to suppress adipogenesis still needs to be explored further, since Trolox could a beneficial substance in combating obesity.

ASCs were also induced to differentiation in the presence of apocynin for 14 and 21 days. This again resulted in no change in the percentage of Nile Red positive ASCs on day 14 and day 21 and in the MFI of the differentiating ASCs (Figure 4.2). Apocynin is a natural methoxy-substituted catechol that is used as a NADPH oxidase (NOX) inhibitor to block $O_2^{\bullet-}$ production in cells and is also a ROS scavenger[35–37]. The lack of an adipogenic effect following apocynin addition suggests that in human ASCs, apocynin does not inhibit adipogenesis. This could possibly suggest that NOX derived ROS are not involved in adipogenic differentiation of ASCs. The findings from this study are in contrast to experiments by Nakagawa-Yagi and colleagues (2012), who reported that apocynin (concentrations ranging from 10 to 100 µM) dose dependently increased adipogenic differentiation of human preadipocytes during the early phases of differentiation (7 days)[38].

The effects of apocynin on adipogenic differentiation in human ASCs have not been extensively described in literature. This study is among the few to describe how apocynin affects the different phases of adipogenic differentiation in human ASCs. However, the effects of apocynin on adipogenesis during the early and late phases of differentiation remain unclear and further studies are however needed to gain a deeper understanding on apocynin mechanism of action on this process.

The influence of extracellular H_2O_2 pre-treatment and prolonged treatment of ASCs undergoing adipogenic differentiation was also investigated in this study. H_2O_2 pre- and prolong treated ASCs showed enhanced adipogenic differentiation capacity with a more pronounced effect observed on day 14 compared to day 21. There was however no effect in the MFI with extracellular H_2O_2 treatment of adipogenic induced ASCs (Figure 4.3B). The constant supply of H_2O_2 to differentiating cells (prolonged treatment) resulted in an even greater enhancement effect with much faster adipogenic differentiation kinetics than pre-treated ASCs on day 14. The lack of statistical significance of the observed adipogenic enhancement effect with H_2O_2 treatment may have been due to the observed inherent variability between primary cultures which are donor dependent as indicated by the large error bars in the adipogenic differentiation graph or that the concentration of the extracellular H_2O_2 was not high enough to cause any statistically significant effect (Figure 4.3A).

However, the observed adipogenic enhancing trend with H_2O_2 treatment gave an indication that ROS possibly accelerated the process of adipogenesis. Furthermore, both H_2O_2 pre- and prolonged treated ASCs as well as the untreated control ASCs attained maximum differentiation on day 21, however, the kinetics of differentiation were fastest in the prolonged H_2O_2 treated cells, followed by H_2O_2 pre-treated cells as seen on day 14 (Figure 4.3A). In addition, the higher level of ASC adipogenic differentiation seen with prolonged exposure to H_2O_2 compared to pre-treatment on day 14, may suggest that ROS are required continuously during adipogenesis. Intriguingly, there was no further increase in adipogenesis with extracellular H_2O_2 treatment on day 21. It is most likely that the cells had already reached their maximal differentiation capacity. Another possible reason is that the cellular antioxidant defence mechanisms may have been activated to counter the effects of the extracellular H_2O_2 addition. This suggestion is supported in experiments by Higuchi and colleagues (2013), where they reported that adipogenic induction was accompanied by an activation of antioxidative enzymes which included SOD, catalase and glutathione peroxidase[39,40].

Having shown that extracellular H_2O_2 enhances adipogenesis, this study went on further to investigate the effect of ROS scavenger addition to H_2O_2 treated ASC adipogenic differentiation capacity. Trolox addition to adipogenic differentiating H_2O_2 pre-treated ASCs resulted in no effect on the percentage of Nile Red positive ASCs as well as in the MFI of the differentiating ASCs on day 14 and day 21 (Figure 4.4). This finding suggests that Trolox does not inhibit adipogenesis in human ASCs pre-treated with extracellular H_2O_2. Thus, also suggesting that, in H_2O_2 pre-treated ASCs Trolox lacks intracellular ROS scavenging activity against endogenously generated ROS, thereby does not supress adipogenesis.

The addition of apocynin to adipogenic induced H_2O_2 pre-treated ASCs significantly inhibited the percentage of Nile Red positive ASCs on day 14 whereas there was no change in adipogenesis on day 21 (Figure 4.4A). The effects of apocynin treatment on adipogenic differentiation in H_2O_2 treated ASCs *in vitro* has not been extensively described in literature. However, the findings from this study show that in H_2O_2 pre-treated ASCs, apocynin inhibits adipogenesis but only during the early phases of differentiation on day 14. This suggests that NOX derived ROS are involved in adipogenesis during the early phases of differentiation in cells that have been exposed to extracellular ROS such as in the case of oxidative stress condition. Lack of an effect by apocynin on day 21 of differentiation may suggests NOX derived ROS are not involved during the later phases of differentiation. Lack of an effect on the MFI following apocynin addition to H_2O_2 pre-treated ASCs (Figure 4.4B). Suggests that during the early phases of differentiation, apocynin only suppresses the number of cells that differentiate into the adipogenic lineage without affecting the amount of lipid droplet accumulation in the individual cells.

In ASCs treated with H_2O_2 for a prolonged period, the addition of Trolox resulted in no discernible difference in the percentage of Nile Red positive ASCs as well as in the MFI of the differentiating cells on day 14 and day 21 (Figure 4.5). Since Trolox is a direct scavenger of ROS, simultaneous addition of Trolox and H_2O_2 may have resulted in a direct cancellation effect of Trolox by H_2O_2 in the medium, thereby leaving very little or no Trolox in the medium to have an intracellular scavenging effect in the differentiating ASCs.

This observation supports findings by Sugahara and colleagues (2018) who reported that Trolox exhibits a free radical scavenging effect in a dose dependent manner when mixed in solutions containing ROS[31]. The results of this study thus suggest that Trolox has little to no adipogenic inhibition effect in ASCs induced to differentiate in the continuous presence of H_2O_2.

The addition of apocynin to H_2O_2 prolonged treated ASCs resulted in no change in the percentage of Nile Red positive ASCs as well as in the MFI of the differentiating cells on day 14 and day 21 (Figure 4.5). This finding suggests that in the continuous presence of extracellular H_2O_2 apocynin does not suppress adipogenesis in differentiating ASCs. Suggesting that NOX derived ROS are not involved during adipogenic differentiation of ASCs. However, although apocynin addition to differentiating ASCs in the continuous presence of H_2O_2 did not influence adipogenesis. A slight decreasing trend in adipogenesis was observed on day 14 and day 21 with apocynin addition (Figure 4.5A). This contrasted with Trolox where no trend was observed (Figure 4.5A). This finding suggests that apocynin may probably possess adipogenic inhibition properties in the presence of extracellular H_2O_2. Hence, additional studies are required to gain deeper insights into the possible mechanisms of action by apocynin in differentiating ASCs.

4.5 Conclusion

This study showed that the use of human ASCs at lower passages greatly improves adipogenic differentiation. This study demonstrated that apocynin is a possible inhibitor of adipogenesis particularly during the early phases of differentiation in H_2O_2 pre-treated ASCs. Adipogenic inhibition by apocynin implies that NOX derived ROS are likely to be involved in adipogenic regulation especially in conditions where the cells are exposed to extracellular ROS such as in oxidative stress. The findings from this study also showed that Trolox addition to adipogenic differentiating ASCs does not influence adipogenesis in the presence or absence of extracellular H_2O_2. This suggesting that intracellular ROS are not involved in adipogenic differentiation of ASCs. The effects of Trolox and apocynin in adipogenic differentiation of human ASCs have not been extensively described in literature. This study is one of the few that has evaluated the effects of Trolox and

apocynin in adipogenic differentiation of primary human ASCs in the presence and absence of short term and prolonged exposure to extracellular H_2O_2.

Application of the findings in this study could be limited by the lack of statistical significance in the different treatment conditions. This could be due to the concentration of ROS scavengers used not being high enough to produce a significant adipogenic inhibition effect. As such, experiments to determine the optimum concentrations of ROS scavengers exhibiting the maximum adipogenic inhibition effects without affecting cell viability need be conducted in the future. It is recommended that future studies also investigate the differential gene expression of adipocyte specific and antioxidative enzyme genes during adipogenesis to help decipher the possible mechanisms of action governing the interplay between ROS, ROS scavengers and adipogenesis. Above all the findings from this study suggest that apocynin could be a useful anti-adipogenic/anti-obesity agents particularly in the presence of extracellular ROS.

References

1. Gregoire FM, Smas CM, Sul HS. Understanding adipocyte differentiation. Physiol Rev. 1998;78(3):783–809.

2. Ali AT, Hochfeld WE, Myburgh R, Pepper MS. Adipocyte and adipogenesis. Eur J Cell Biol. 2013;92:229–36.

3. Lefterova MI, Lazar MA. New developments in adipogenesis. Trends Endocrinol Metab. 2009;20(3):107–14.

4. Jiang Y, Jo A-Y, Graff JM. Snapshot: adipocyte life cycle. Cell. 2012;150(1):234–234.e2.

5. Ambele MA, Dessels C, Durandt C, Pepper MS. Genome-wide analysis of gene expression during adipogenesis in human adipose-derived stromal cells reveals novel patterns of gene expression during adipocyte differentiation. Stem Cell Res. 2016;16(3):725–34.

6. Symonds ME, editor. Adipose tissue biology. New York: Springer; 2012.

7. Wang X, Hai C. Redox modulation of adipocyte differentiation: hypothesis of “redox chain” and novel insights into intervention of adipogenesis and obesity. Free Radic Biol Med. 2015;89:99–125.

8. de Villiers D, Potgieter M, Ambele MA, Adam L, Durandt C, Pepper MS. The role of reactive oxygen species in adipogenic differentiation. In: Advances in Experimental Medicine and Biology. Springer, Boston, MA; 2017. p. 125–44.

9. Lee D. Inhibitory effect of caffeic acid phenethyl on adipocyte differentiation through regulation of reactive oxygen species in the 3T3-L1 cell model. Free Radic Biol Med. 2018;120:S48–9.

10. Alcala M, Calderon-Dominguez M, Serra D, Herrero L, Ramos MP, Viana M. Short-term vitamin E treatment impairs reactive oxygen species signaling required for adipose tissue expansion, resulting in fatty liver and insulin resistance in obese mice. Peterson JM, editor. PLoS One. 2017;12(10):e0186579.

11. Kanda Y, Hinata T, Won S, Watanabe Y. Reactive oxygen species mediate adipocyte differentiation in mesenchymal stem cells. Life Sci. 2011;89(7–8):250–8.

12. Atashi F, Modarressi A, Pepper MS. The role of reactive oxygen species in mesenchymal stem cell adipogenic and osteogenic differentiation: a review. Stem Cells Dev. 2015;24(10):1150–63.

13. O. Lee, Y. Kwon, H. Hong, C. Park, B. Lee YK, Lee OH, Kwon YI, Hong HD, Park CS, Lee BY, et al. Production of reactive oxygen species and changes in antioxidant enzyme activities during differentiation of 3T3-L1 adipocyte. J Korean Soc Appl Biol Chem. 2009;52(1):70–5.

14. Hwang S, Kim J-K, Kim I-H, Lim Y-H. Inhibitory effect of ethanolic extract of Ramulus mori on adipogenic differentiation of 3T3-L1 cells and their antioxidant activity. J Food Biochem. 2018;42(2):e12469.

15. Durandt C, van Vollenstee FA, Dessels C, Kallmeyer K, de Villiers D, Murdoch C, et al. Novel flow cytometric approach for the detection of adipocyte subpopulations during adipogenesis. J Lipid Res. 2016;57(4):729–42.

16. Kraus NA, Ehebauer F, Zapp B, Rudolphi B, Kraus BJ, Kraus D. Quantitative assessment of adipocyte differentiation in cell culture. Adipocyte. 2016;5(4):351.

17. Lee Y-H, Chen S-Y, Wiesner RJ, Huang Y-F. Simple flow cytometric method used to assess lipid accumulation in fat cells. J Lipid Res. 2004;45(6):1162–7.

18. Vichai V, Kirtikara K. Sulforhodamine B colorimetric assay for cytotoxicity screening. Nat Protoc. 2006;1(3):1112–6.

19. van Tonder A, Joubert AM, Cromarty A. Limitations of the 3-(4,5-dimethylthiazol-2-yl)-2,5-diphenyl-2H-tetrazolium bromide (MTT) assay when compared to three commonly used cell enumeration assays. BMC Res Notes. 2015;8(1):47.

20. Bruggisser R, Daeniken K von, Jundt G, Schaffner W, Tullberg-Reinert H. Interference of plant extracts, phytoestrogens and antioxidants with the MTT tetrazolium assay. Planta Med. 2002;68(5):445–8.

21. Vybrant ® MTT cell proliferation assay kit (V-13154). Eugene, Oregon: Molecular Probes; 2002.

22. Falzone N, Huyser C, Franken DR. Comparison between propidium iodide and 7-amino-actinomycin-D for viability assessment during flow cytometric analyses of the human sperm acrosome. Andrologia. 2010;42(1):20–6.

23. Drehmer DL, de Aguiar AM, Brandt AP, Petiz L, Cadena SMSC, Rebelatto CK, et al. Metabolic switches during the first steps of adipogenic stem cells differentiation. Stem Cell Res. 2016;17(2):413–21.

24. Phelan MC. Basic techniques in mammalian cell tissue culture. Curr Protoc cell Biol. 2007;36(1):1.1.1-1.1.18.

25. Bourin P, Bunnell BA, Casteilla L, Dominici M, Katz AJ, March KL, et al. Stromal cells from the adipose tissue-derived stromal vascular fraction and culture expanded adipose tissue-derived stromal/ stem cells: a joint statement of the International Federation for Adipose Therapeutics (IFATS) and Science and the International S. Cytotherapy. 2013;15(6):641–8.

26. Safwani WKZW, Makpol S, Sathapan S, Chua K. Impact of adipogenic differentiation on stemness and osteogenic gene expression in extensive culture of human adipose-derived stem cells. Arch Med Sci. 2014;10(3):597–606.

27. Park Y-K, Lee J, Hong VS, Choi J-S, Lee T-Y, Jang B-C. Identification of KMU-3, a Novel Derivative of Gallic Acid, as an Inhibitor of Adipogenesis. Taneja R, editor. PLoS One. 2014;9(10):e109344.

28. Liu G-S, Chan EC, Higuchi M, Dusting GJ, Jiang F, Hospital Q. Redox mechanisms in regulation of adipocyte differentiation: beyond a general stress response. Cells. 2012;1(4):976–93.

29. Castro JPJP, Grune T, Speckmann B, Access O. The two faces of reactive oxygen species (ROS) in adipocyte function and dysfunction. Biol Chem. 2016;397(8):709–24.

30. Hamad I, Arda NN, Pekmez M, Karaer S, Temizkan G. Intracellular scavenging

activity of Trolox (6hydroxy2,5,7,8tetramethylchromane2carboxylic acid) in the fission yeast, Schizosaccharomyces pombe. J Nat Sci Biol Med. 2016;1(1):16–21.

31. Sugahara S, Chiyo A, Fukuoka K, Ueda Y, Tokunaga Y, Nishida Y, et al. Unique antioxidant effects of herbal leaf tea and stem tea from Moringa oleifera L. especially on superoxide anion radical generation systems. Biosci Biotechnol Biochem. 2018;1–12.

32. Alves H, Mentink A, Le B, van Blitterswijk CA, de Boer J. Effect of antioxidant supplementation on the total yield, oxidative stress levels, and multipotency of bone marrow-derived human mesenchymal stromal cells. Tissue Eng Part A. 2013;19(7–8):928–37.

33. Huang D, Boxin OU, Prior RL. The chemistry behind antioxidant capacity assays. J Agric Food Chem. 2005;53(6):1841–56.

34. Choi S-I, Lee JS, Lee S, Lee J-H, Yang H-S, Yeo J, et al. Radical scavenging-linked anti-adipogenic activity of Alnus firma extracts. Int J Mol Med. 2018;41(1):119–28.

35. Heumuller S, Wind S, Barbosa-Sicard E, Schmidt HH, Busse R, Schroder K, et al. Apocynin is not an inhibitor of vascular NADPH oxidases but an antioxidant. Hypertension. 2008;51(2):211–7.

36. Vejražka M, Míček R, Štípek S. Apocynin inhibits NADPH oxidase in phagocytes but stimulates ROS production in non-phagocytic cells. Biochim Biophys Acta - Gen Subj. 2005;1722(2):143–7.

37. Lee YS, Choi EM. Apocynin stimulates osteoblast differentiation and inhibits bone-resorbing mediators in MC3T3-E1 cells. Cell Immunol. 2011;270(2):224–9.

38. Nakagawa-Yagi Y, Sato Y, Matsumoto E, Nakatsuka S, Sakaki T, Muramatsu Y, et al. Pharmacological modulation of histone demethylase activity by a small molecule isolated from subcritical water extracts of Sasa senanensis leaves prolongs the lifespan of Drosophila melanogaster. BMC Complement Altern Med. 2012;12(1):1225.

39. Kojima T, Norose T, Tsuchiya K, Sakamoto K. Mouse 3T3-L1 cells acquire

resistance against oxidative stress as the adipocytes differentiate via the transcription factor FoxO. Apoptosis. 2010;15(1):83–93.

40. Higuchi M, Dusting GJ, Peshavariya H, Jiang F, Hsiao ST-F, Chan EC, et al. Differentiation of human adipose-derived stem cells into fat involves reactive oxygen species and forkhead box O1 mediated upregulation of antioxidant enzymes. Stem Cells Dev. 2013;22(6):878–88.

Chapter 5: Effects of ROS scavengers on intracellular and extracellular ROS production during adipogenesis

5.1 Introduction

Reactive oxygen species (ROS) are unstable oxygen containing molecules and free radicals, that can be derived exogenously or through endogenous generation in cells to meet various cellular physiological processes[1,2]. In adipocytes, the main ROS producers are NADPH oxidase 4 (NOX4) and the mitochondria generating hydrogen peroxide (H_2O_2) and superoxide ($O_2^{\bullet-}$) respectively[3–6]. ROS have been suggested to play a role in the conversion of stem cells to adipocytes. Several studies have demonstrated that endogenous ROS production in stem cells increases in parallel with adipogenic differentiation[5–7]. In addition, adipogenesis has also been reported to be associated with extracellular ROS release. This was demonstrated in experiments by Mouche and colleagues (2007), where spontaneous extracellular H_2O_2 release was observed in 3T3-L1 preadipocytes and adipocytes *in vitro*[8]. Increase in ROS production during adipogenic differentiation is accompanied by activation of antioxidant defence systems e.g. superoxide dismutase (SOD), catalase, glutathione peroxidase to counter the damaging effects of excess ROS production[6,9]. Suggesting that antioxidant treatment can inhibit ROS production and several researchers have reported that antioxidant addition to differentiating stem cells can abrogate ROS production[5,6,10].

Various methods have been developed to measure ROS levels in cells *in vitro*. These include direct radical measurements using the electron spin resonance technique, chemiluminescent assays using luminol or lucigenin probes, mitochondria-specific fluorescent probes e.g. MitoSOX™ Red and MitoTracker Red CM-H_2XRos, as well as the cytochrome c reduction, nitro blue tetrazolium, Amplex Red and Dichlorodihydrofluorescein diacetate (DCFH-DA) assays[11,12]. The most commonly used and straight forward assays utilise fluorescent and chemiluminescent probes[11]. In cellular ROS measurements, the widely-used technique is the 2'-7'-Dichlorodihydrofluorescein diacetate (DCFH-DA) which detects general ROS production. Upon cellular uptake DCFH-DA is cleaved by intracellular esterases and subsequently oxidized by a variety of

ROS into 2'-7'-dichlorofluorescin (DCF) which is cell impermeable and highly fluorescent[11,12]. A major disadvantage with this method is the possible DCF-free radical formation that can lead to $O_2^{\bullet-}$ generation[13]. In this study, we used CellROX® Deep Red reagent which detects ROS signals localised in the cytoplasm[14]. CellROX® reagents are fluorogenic probes for general ROS detection in cells. They are cell permeable reagents, non-fluorescent in the reduced state but fluorescent upon oxidation. The assays are easy to run, sensitive, some can be fixed by formalin allowing combination with other reagents e.g. antibodies, hence the choice for use in this study.

To investigate whether mitochondrial ROS are involved in adipogenesis as well as to determine if ROS scavengers can influence mitochondrial derived ROS. The MitoSOX™ Red mitochondrial superoxide indicator was used. MitoSOX™ Red is a widely used live-cell permeant indicator for the selective detection of superoxide in the mitochondria of live cells. It is a cationic derivative of dihydroethidum. Oxidation of MitoSOX™ Red by superoxide in the mitochondria exhibits a red fluorescence that can be measured by flow cytometry[11,12].

For extracellular ROS release measurements, the OxyBURST® H_2HFF Green BSA reagent was utilised. This reagent consists of dihydro-2',4,5,6,7,7'-hexafluorofluorescein (H_2HFF) coupled to bovine serum albumin. This assay is more sensitive to spectrophotometer based methods like the cytochrome c reduction for extracellular ROS detection, thus aided its choice of use in this study[14,15].

The aim of this study is to investigate the effects of ROS and ROS scavengers on adipogenesis. Therefore, the purpose of this chapter is to investigate the influence of Trolox and apocynin addition on intracellular ROS levels during adipogenesis as well as to describe their possible cellular sources.

5.2 Materials and Methods

5.2.1 Treatment and adipogenic differentiation of ASCs

Isolation of ASCs from fat tissue, expansion and characterisation was performed as described in Chapter 2, section 2.1 to 2.3. Following the selection of the appropriate concentration of ROS scavenger, experiments to quantify ASC adipogenic differentiation under different treatments were set up were set up as described in Chapter 2 section 2.4.

5.2.2 Flow cytometric intracellular ROS measurements

Intracellular ROS measurements were performed as described in Chapter 2, section 2.5.

5.2.3 Flow cytometer set up and data analysis

Instrument start-up, protocol set up and gating strategies employed are as described in Chapter 2, section 2.3.1 and 2.5.1.

5.2.4 Extracellular ROS measurements

To detect extracellular ROS release during adipogenesis the OxyBURST™ Green H_2HFF BSA reagent (Molecular Probes by Life Technologies, USA) was used. OxyBURST™ Green reagent is excited at 488 nm and emits at 530 nm. Cell isolation, expansion and characterisation of ASCs were performed as described in Chapter 2, section 2.1 to 2.3. Seeding of ASCs in 6-well plates, treatment and adipogenic differentiation were performed as described in Chapter 2, section 2.4. However, for the extracellular ROS assay, medium in wells was only replaced once every 7 days with the appropriately supplemented medium for each of the respective conditions. On days 0, 7, 14 and 21 post induction, prior to replacement of medium, 1 ml of supernatant was aspirated from each well and transferred to labelled flow cytometry tubes. The supernatant was then centrifuged at 500 x g for 10 minutes, to remove any floating debris present. After centrifuging, 198 µl of supernatant was transferred to a well labelled 96-well plate and OxyBURST™ Green reagent was added to a final concentration of 10 µg/ml. Fluorescence was measured immediately using a FLUOstar® Omega multi-mode microplate reader (BMG LABTECH, Germany). Results were expressed as relative fluorescence units and fluorescence increase was calculated as follows:

Equation 5.1

Fluorescence increase = Mean test sample relative fluorescence value – Mean background fluorescence value.

Media for background fluorescence (cell free) measurements was added to separate cell free culture plates and incubated under the same conditions as test samples. Background fluorescence was also measured at day 0, 7, 14 and 21.

5.2.5 Statistical analysis

Flow cytometry data analysed using the Kaluza software was exported to Microsoft excel spread sheets. Statistical analysis was then performed using GraphPad Prism version 6 (GraphPad Software Inc., San Diego, USA). The non-parametric Kruskal-Wallis test was used to test for differences among the means. Follow up Dunn's multiple comparisons test was applied to determine where differences occurred between the groups. The non-parametric Mann-Whitney test was also used in testing for significant difference between two data sets. Data was generated from four donor ASC cultures and expressed as the mean ± standard deviation (SD) of all replicates. Differences were considered statistically significant at $p \leq 0.05$.

5.3 Results

5.3.1 Effects of ROS scavengers on total intracellular ROS levels in ASCs during adipogenesis

The CellROX® Deep Red reagent measures ROS signals that are localized in the cell cytoplasm. Thus, the CellROX® Deep Red assay gives a measure of the total intracellular ROS levels. Total intracellular ROS levels were expressed as relative mean fluorescence intensity (MFI).

The addition of adipogenic induction medium to ASCs increased total intracellular ROS levels from 2.86 ± 1.51 in non-induced ASCs to 4.6 ± 2.23 in induced ASCs on day 14, while on day 21 total intracellular ROS levels increased from 2.80 ± 1.19 in non-induced

ASCs to 4.04 ± 2.25 in induced ASCs (Figure 5.1). This reflected a 1.6- and 1.4-fold increase in total intracellular ROS levels on day 14 and day 21 respectively from non-induced to induced ASCs. The increase in total intracellular ROS levels in induced ASCs was however not statistically significant on day 14 (p=0.2000) and day 21 (p=0.4857) (Figure 5.1).

Having observed the increase in total intracellular ROS levels with adipogenic induction, the effects of ROS scavenger addition on total intracellular ROS levels in adipogenic induced ASCs was then investigated. Trolox addition to adipogenic induced ASCs decreased total intracellular ROS levels by 1.2-fold (from 4.6 ± 2.23 in ASCs only to 3.86 ± 2.26) on day 14 and while there was no appreciable change (from 4.04 ± 2.25 in ASCs only to 3.95 ± 2.58) in total intracellular ROS levels on day 21 (Figure 5.1). The decrease in total intracellular ROS levels observed with the addition Trolox was not statistically significant on day 14 (p=0.8286).

The addition of apocynin to adipogenic induced ASCs also decreased total intracellular ROS levels by 1.1-fold (from 4.60 ± 2.23 in ASCs only to 4.30 ± 1.24) on day 14 while there was also no appreciable change (from 4.04 ± 2.25 in ASCs only to 3.88 ± 3.55) on day 21 (Figure 5.1). The decreased levels of total intracellular ROS levels observed in induced ASCs following treatment with apocynin was not statistically significant on day 14 (p=0.8286).

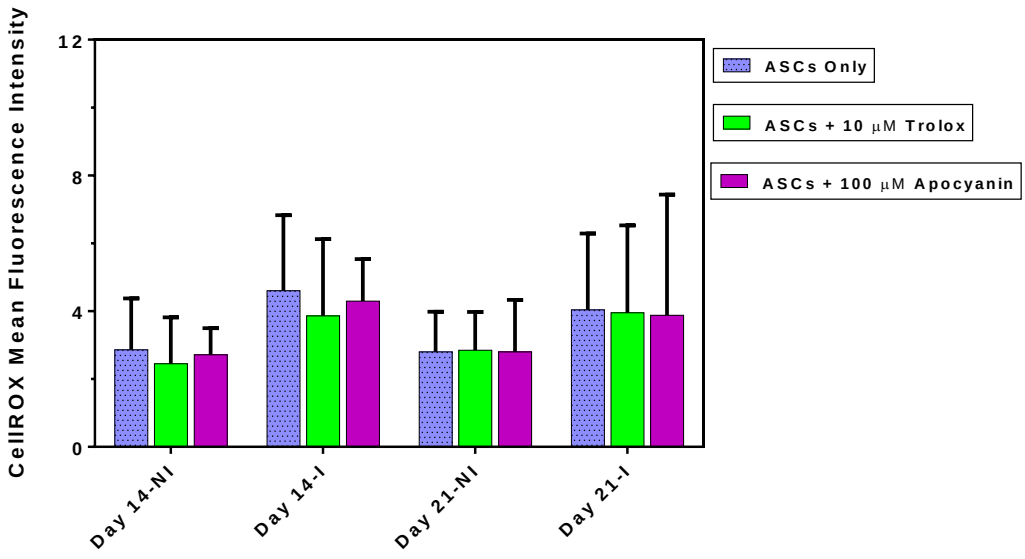

Figure 5.1 Effects of ROS scavenger addition on total intracellular ROS levels in ASCs during adipogenesis
Total intracellular ROS levels were determined by the CellROX® Deep Red reagent. Adipogenic induction had no effect on total intracellular ROS levels in induced ASCs on day 14 and day 21 when compared to non-induced ASCs. Trolox and apocynin addition to differentiating ASCs also resulted in no effect in total intracellular ROS levels on day 14 and day 21 when compared to ASCs only. ASCs incubated with complete DMEM only served as the non-induced controls. n = 4. NI: Non-induced; I: Induced.

5.3.2 Effects of extracellular H_2O_2 addition on total intracellular ROS levels during adipogenesis

The influence of extracellular H_2O_2 treatment on total intracellular ROS levels was also investigated in this study. ASCs were either pre-treated with 20 µM H_2O_2 for 24 hours followed by adipogenic differentiation or were prolong treated with 20 µM H_2O_2 throughout the differentiation period.

Total intracellular ROS levels in pre-treated ASCs increased marginally by 1.1-fold (from 4.6 ± 2.23 in ASCs only to 5.25 ± 2.86) on day 14 while there was no appreciable change (from 4.04 ± 2.25 in ASCs only to 3.89 ± 2.83) on day 21 (Figure 5.2). Changes in total intracellular ROS levels observed in pre-treated ASCs were not statistically significant on day 14 ($p>0.9999$).

Prolonged treatment of ASCs with 20 µM H_2O_2 followed by adipogenic differentiation did not have any appreciable effect on the total intracellular ROS measurements (from 4.6 ± 2.23 in ASCs only to 4.76 ± 1.87) on day 14 while on day 21 there was a 1.4-fold increase (from 4.04 ± 2.25 in ASCs only to 5.49 ± 3.99) in total intracellular ROS levels (Figure 5.2). There was no statistically significant difference in total intracellular ROS levels when comparing induced H_2O_2 prolong treated ASCs and ACSs only on day 21 (p=0.6571) (Figure 5.2).

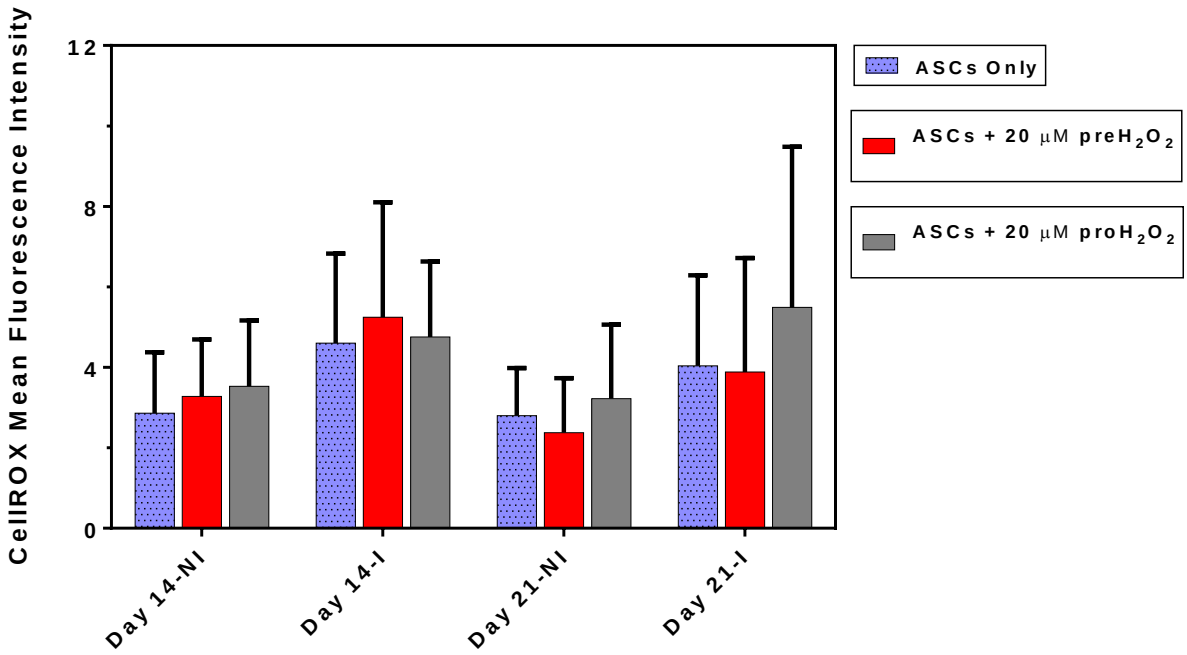

Figure 5.2 Effects of extracellular H_2O_2 addition on total intracellular ROS levels in ASCs during adipogenesis.
Total intracellular ROS levels were determined using the CellROX® Deep Red reagent. Adipogenic induction had no effect on total intracellular ROS levels on day 14 and day 21 when compared to non-induced ASCs. Pre-treatment as well as prolonged treatment of ASCs with extracellular H_2O_2 also resulted in no effect on total intracellular ROS levels on day 14 and day 21 when compared to ASCs only. ASCs incubated with complete DMEM only served as the non-induced controls. n = 4. NI: Non-induced; I: Induced.

5.3.3 Effect of ROS scavengers on total intracellular ROS levels in H_2O_2 treated ASCs during adipogenesis

Having shown the effects of extracellular H_2O_2 treatment on total intracellular ROS levels in differentiating ASCs, the influence of ROS scavenger addition to both H_2O_2 pre-treated and prolong treated ASCs was investigated. A control condition consisted of ASCs treated in the same way as the experiment but without the addition of scavengers.

5.3.3.1 Effects of ROS scavengers on total intracellular ROS levels in H_2O_2 pre-treated ASCs during adipogenesis

The addition of Trolox to H_2O_2 pre-treated ASCs followed by adipogenic differentiation increased total intracellular ROS levels by 1.2-fold (from 5.25 ± 2.86 in the ASC control to 6.55 ± 3.00) on day 14 and 1.1-fold (from 3.89 ± 2.83 in the ASC control to 4.19 ± 3.27) on day 21 (Figure 5.3). There was however, no statistically significant difference in total intracellular ROS levels when comparing Trolox addition to H_2O_2 pre-treated ASCs and the ASC control on day 14 ($p=0.3429$) and on day 21 ($p=0.8286$).

On the other hand, the addition of apocynin to H_2O_2 pre-treated ASCs induced to differentiate, decreased the total intracellular ROS levels (from 5.25 ± 2.86 in the ASC control to 4.61 ± 2.25) on day 14. Whereas, on day 21 apocynin addition marginally increased total intracellular ROS levels (from 3.89 ± 2.83 in the ASC control to 4.32 ± 2.88). This reflected a 1.1-fold decrease and a 1.1- fold increase in total intracellular ROS levels on day 14 and day 21 respectively. There was however, no statistically significant difference in total intracellular ROS levels on day 14 ($p=0.8286$) and on day 21 ($p=0.6571$) when comparing apocynin addition to H_2O_2 pre-treated ASCs and the ASC control (Figure 5.3).

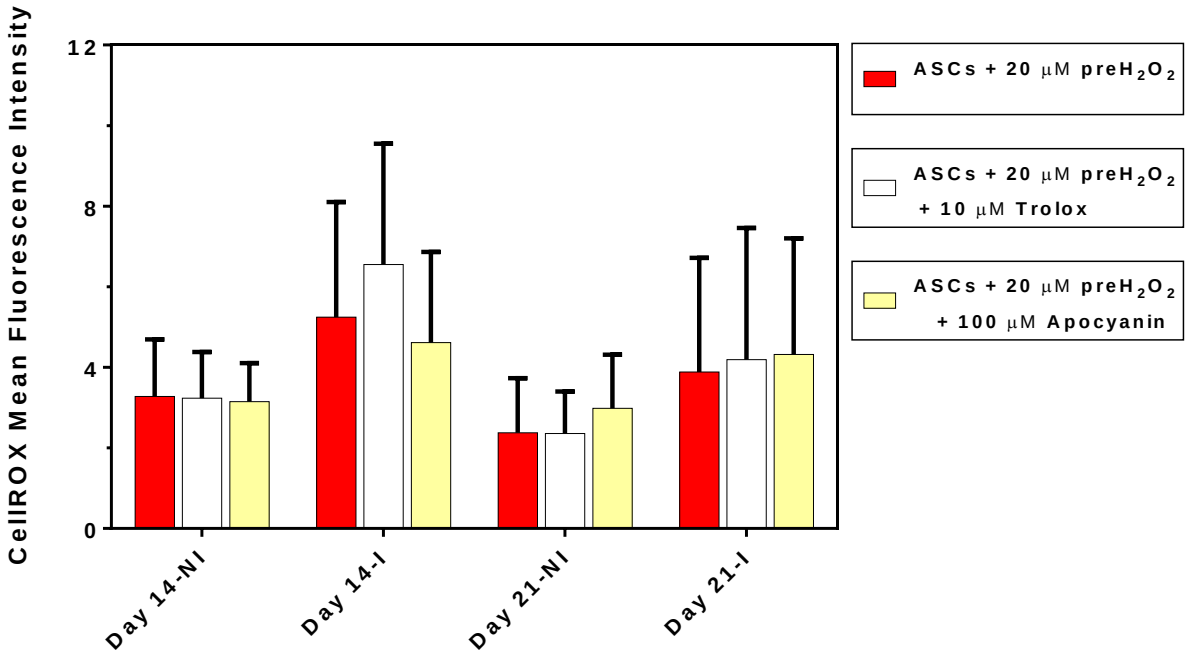

Figure 5.3 Effects of ROS scavengers on total intracellular ROS levels in H_2O_2 pre-treated ASCs during adipogenesis.
Total intracellular ROS levels were measured by the CellROX® Deep Red reagent. Trolox and apocynin addition to induced H_2O_2 pre-treated ASCs had no effect on total intracellular ROS levels on day 14 and day 21 when compared to H_2O_2 pre-treated ASCs only. ASCs incubated with complete DMEM only served as the non-induced controls. n = 4. NI: Non-induced; I: Induced.

5.3.3.2 Effects of ROS scavengers on total intracellular ROS levels in H_2O_2 prolong treated ASCs during adipogenesis

Trolox addition to H_2O_2 prolong treated ASCs followed by adipogenic differentiation caused a negligible decrease in total intracellular ROS levels (from 4.76 ± 1.87 in the ASC control to 4.69 ± 1.98) on day 14. Whereas on day 21 Trolox addition decreased total intracellular ROS by 1.3-fold (from 5.49 ± 3.99 in the ASC control to 4.27 ± 2.57), which was however not statistically significant (p=0.9131) (Figure 5.4).

On the contrary, apocynin addition to H_2O_2 prolong treated ASCs undergoing adipogenic differentiation resulted in no appreciable change in total intracellular ROS levels on day

14 (from 4.76 ± 1.87 in the ASC control to 5.00 ± 2.21) and day 21 (from 5.49 ± 3.99 in the ASC control to 5.53 ± 4.58) (Figure 5.4).

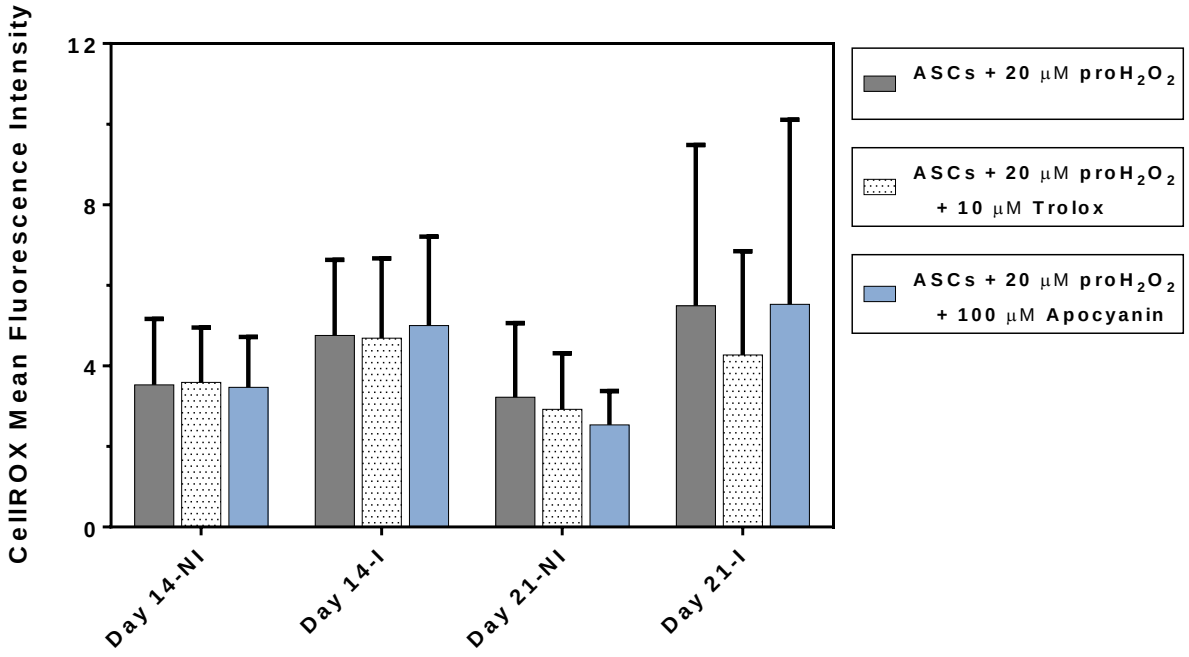

Figure 5.4 Effects of ROS scavengers on total intracellular ROS levels in H_2O_2 prolonged treated ASCs during adipogenesis.
Total intracellular ROS levels were determined by the CellROX® Deep Red reagent. Trolox and apocynin addition to ASCs treated with prolonged exposure to H_2O_2 followed by adipogenic induction had no effect on total intracellular ROS levels on day 14 and day 21 when compared to H_2O_2 prolonged treated ASCs only. ASCs incubated with complete DMEM only served as the non-induced controls. n = 4. NI: Non-induced; I: Induced.

5.3.4 Effects of ROS scavengers on mitochondrial ROS levels in ASCs during adipogenesis

Mitochondria are a major ROS source in adipocytes and as such the effects of ROS scavengers on mitochondrial ROS levels during adipogenesis was also investigated. Mitochondrial ROS levels were expressed as relative mean fluorescence intensity (MFI).

Adipogenic induction of ASCs increased mitochondrial ROS levels by 1.5-fold (from 2.34 ± 0.59 in non-induced to 3.43 ± 1.83 in induced ASCs) on day 14. Whereas on day 21 mitochondrial ROS levels increased by 1.1-fold (from 2.64 ± 0.72 to 2.96 ± 1.07) when comparing non-induced and induced ASCs (Figure 5.5). There was no statistically significant difference in the increase in mitochondrial ROS levels on day 14 ($p=0.5143$) and on day 21 ($p=0.6571$) when comparing non-induced and induced ASCs (Figure 5.5).

Having observed an increase in mitochondrial ROS levels with adipogenic induction, the effects of ROS scavenger addition on the mitochondrial ROS levels in adipogenic induced ASCs was then investigated. Trolox addition to adipogenic induced ASCs decreased by 1.1-fold the mitochondrial ROS levels from 3.43 ± 1.83 in ASCs only to 3.04 ± 1.14 on day 14. Whereas on day 21 mitochondrial ROS levels increased by 1.4-fold (from 2.96 ± 1.07 in ASCs only to 4.04 ± 1.68) (Figure 5.5). There was no statistically significant difference in mitochondrial ROS levels on day 14 ($p>0.9999$) and day 21 ($p=0.3429$) when comparing Trolox addition to adipogenic induced ASCs and ASCs only (Figure 5.5).

The addition of apocynin to adipogenic induced ASCs decreased mitochondrial ROS levels by 1.2-fold (from 3.43 ± 1.83 in ASCs only to 2.95 ± 0.93) on day 14. Whereas the mitochondrial ROS levels increased by 1.2-fold (from 2.96 ± 1.07 in ASCs only to 3.43 ± 1.43) on day 21 (Figure 5.5). These changes in the mitochondrial ROS levels with apocynin addition were not statistically significant when comparing the induced ASCs on day 14 ($p=0.8286$) and day 21 ($p=0.4000$) to ASCs only.

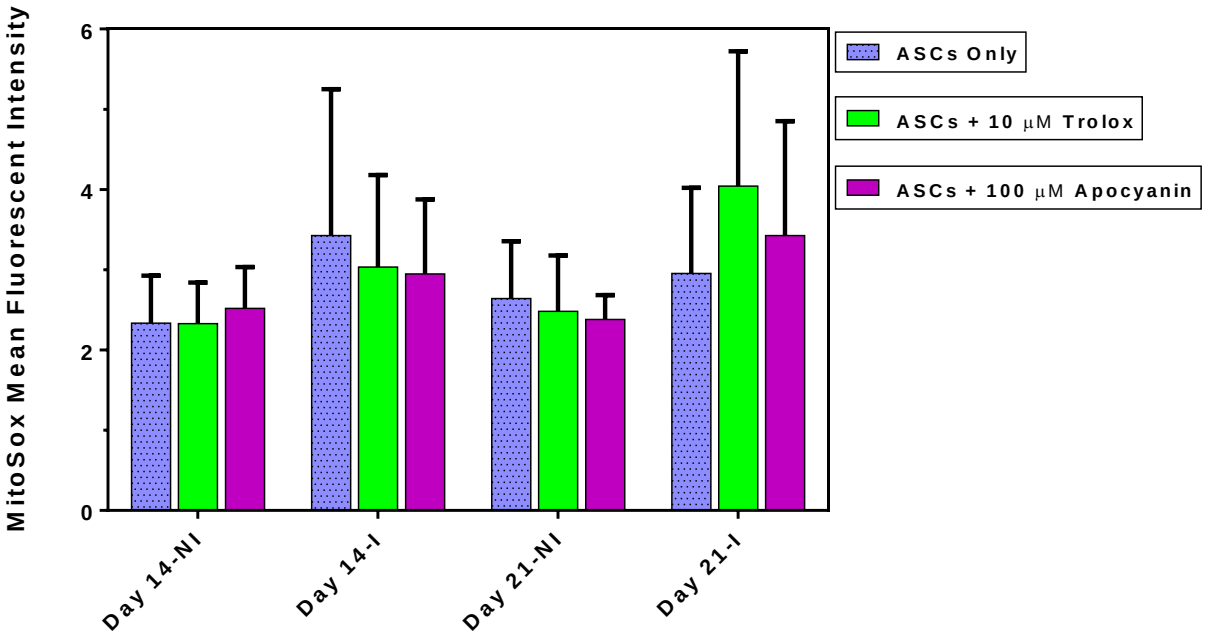

Figure 5.5 Effects of ROS scavenger addition on mitochondrial ROS levels in ASCs during adipogenesis.
Mitochondrial ROS levels were determined using the MitoSOX™ Red mitochondrial superoxide indicator reagent. Trolox and apocynin addition to ASCs followed by adipogenic differentiation, resulted in no change in mitochondrial ROS levels on day 14 and on day 21 when compared to ASCs only. ASCs incubated with complete DMEM only served as the non-induced controls. n = 4. NI: Non-induced; I: Induced.

5.3.5 Effects of extracellular H_2O_2 treatment on mitochondrial ROS levels in ASCs during adipogenesis

This study also investigated the influence of extracellular H_2O_2 treatment on mitochondrial ROS levels. ASCs were either pre-treated with 20 µM H_2O_2 for 24 hours followed by adipogenic differentiation or were prolong treated with 20 µM H_2O_2 throughout the differentiation period.

Pre-treatment of ASCs with H_2O_2 followed by adipogenic differentiation decreased mitochondrial ROS levels by 1.2-fold (from 3.43 ± 1.83 in ASCs only to 2.87 ± 0.74) on day 14, whereas an increase of 1.2-fold in mitochondrial ROS levels (from 2.96 ± 1.07 in ASCs only to 3.50 ± 1.36) was measured on day 21 (Figure 5.6). There was however no statistically significant difference in mitochondrial ROS levels on day 14 (p=0.6286) and

on day 21 (p=0.3429) when comparing induced H_2O_2 pre-treated ASCs and ACSs only (Figure 5.6).

Prolonged treatment of ASCs with 20 µM H_2O_2 throughout the differentiation period decreased mitochondrial ROS levels by 1.2-fold (from 3.43 ± 1.83 in ASCs only to 2.88 ± 1.03) on day 14. Whereas the mitochondrial ROS levels increased by 1.1-fold (from 2.96 ± 1.07 in ASCs only to 3.33 ± 1.37) on day 21 (Figure 5.6). There was again no statistically significant difference in mitochondrial ROS levels when comparing induced H_2O_2 prolong treated ASCs and ACSs only on day 14 (p=0.8286) and on day 21 (p=0.3429) (Figure 5.6).

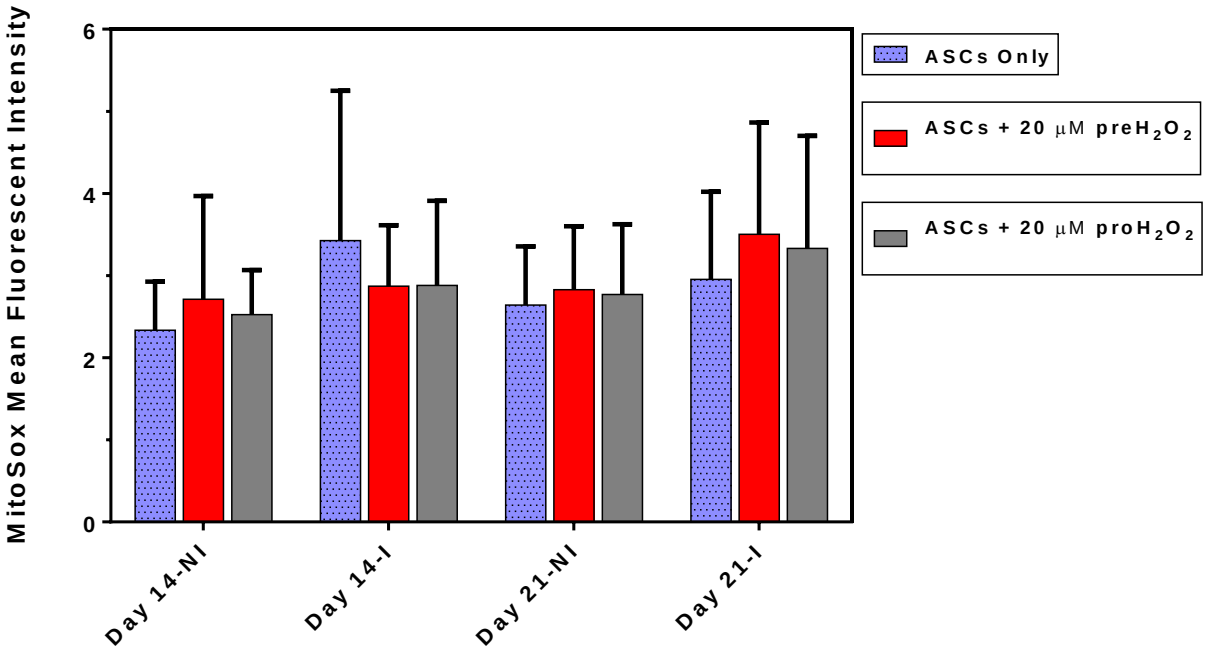

Figure 5.6 Effects of extracellular H_2O_2 treatment on mitochondrial ROS levels in ASCs during adipogenesis.
Mitochondrial ROS levels were determined using the MitoSOX™ Red mitochondrial superoxide indicator reagent. Pre- and prolonged treatment of ASCs with extracellular H_2O_2 followed by adipogenic differentiation resulted in no change in mitochondrial ROS levels on day 14 and day 21 when compared to ASCs only. ASCs incubated with complete DMEM only served as the non-induced controls. n = 4. NI: Non-induced; I: Induced.

5.3.6 Effect of ROS scavengers on mitochondrial ROS levels in H_2O_2 treated ASCs during adipogenesis

This study further investigated the influence of ROS scavenger addition to both H_2O_2 pre-treated and prolong treated ASCs. A control condition consisted of ASCs treated in the same way as the experiment but without the addition of scavengers.

5.3.6.1 Effects of ROS scavengers on mitochondrial ROS levels in H_2O_2 pre-treated ASCs during adipogenesis

Trolox addition to H_2O_2 pre-treated ASCs followed by adipogenic induction for 14 days increased mitochondrial ROS levels by 1.1-fold (from 2.87 ± 0.74 in ASCs only to 3.24 ± 0.78) on day 14 while there was no appreciable change (from 3.50 ± 1.36 in the ASC control to 3.67 ± 1.62) in the mitochondrial ROS levels on day 21 (Figure 5.7). The observed increase in mitochondrial ROS levels in H_2O_2 pre-treated ASCs following the addition of Trolox was however not statistically significant on day 14 ($p=0.4571$).

On the other hand, apocynin addition followed by adipogenic differentiation resulted in no change in mitochondrial ROS levels on day 14 (mitochondrial ROS levels remained 2.87). Whereas, on day 21 there was an increase in mitochondrial ROS levels by 1.1-fold (from 3.50 ± 1.36 in the ASC control to 3.79 ± 1.82). There was however, no statistically significant difference in mitochondrial ROS levels on day 21 ($p>0.9999$) when comparing apocynin addition to H_2O_2 pre-treated ASCs and the ASC control (Figure 5.7).

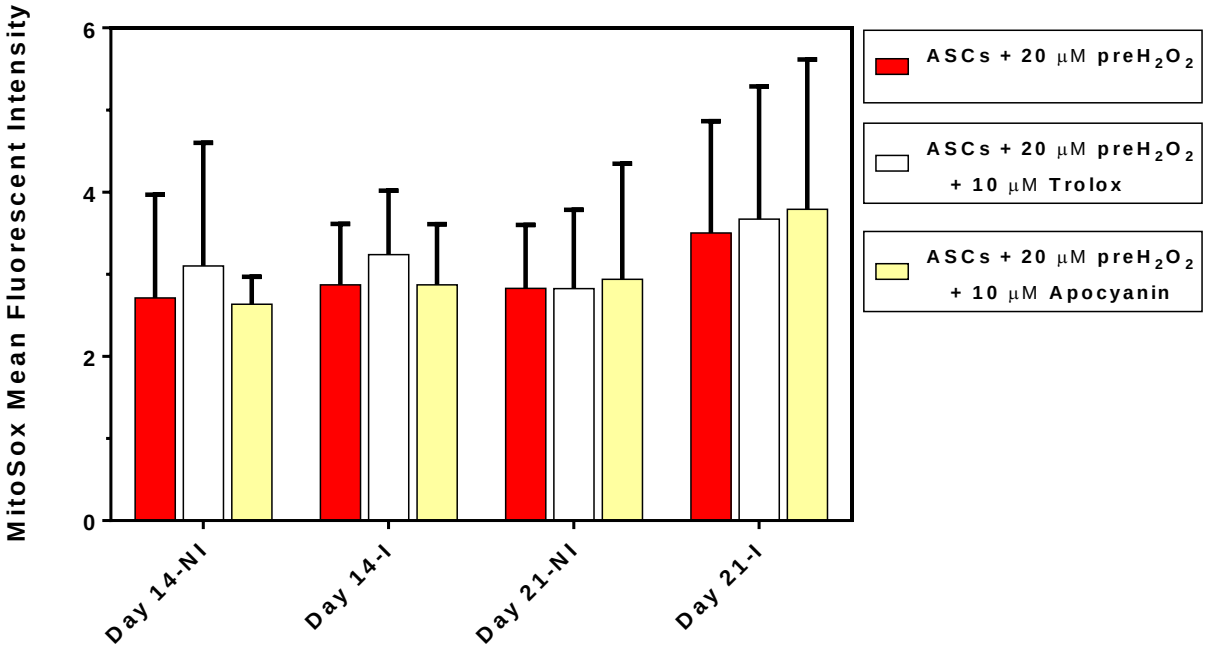

Figure 5.7 Effects of ROS scavengers on mitochondrial ROS levels in H_2O_2 pre-treated ASCs during adipogenesis.
Mitochondrial ROS levels were determined using the MitoSOX™ Red mitochondrial superoxide indicator reagent. The addition of Trolox and apocynin to H_2O_2 pre-treated ASCs resulted in no change in mitochondrial ROS levels on day 14 and day 21 when compared to H_2O_2 pre-treated ASCs only. ASCs incubated with complete DMEM only served as the non-induced controls. n = 4. NI: Non-induced; I: Induced.

5.3.6.2 Effects of ROS scavengers on mitochondrial ROS levels in H_2O_2 prolong treated ASCs during adipogenesis

Trolox addition to H_2O_2 prolong treated ASCs followed by adipogenic differentiation increased mitochondrial ROS levels by 1.2-fold (from 2.88 ± 1.03 in the ASC control to 3.41 ± 0.93) on day 14, whereas on day 21 there was no appreciable change in the mitochondrial ROS levels (from 3.33 ± 1.37 in the ASC control to 3.47 ± 1.26) (Figure 5.8). There was no statistically significant difference in mitochondrial ROS levels on day 14 ($p=0.4857$) when comparing Trolox addition to induced H_2O_2 prolong treated ASCs and the ASC control (Figure 5.8).

On the other hand, apocynin addition to ASCs treated with prolonged exposure to H_2O_2 followed by adipogenic differentiation similarly increased mitochondrial ROS levels by

1.3-fold (from 2.88 ± 1.03 in the ASC control to 3.33 ± 1.37) on day 14 but showed no appreciable change (from 3.33 ± 1.37 in the ASC control to 3.44 ± 1.15) in the mitochondrial ROS levels on day 21. There was however, no statistically significant difference in mitochondrial ROS levels on day 14 ($p=0.3429$) when comparing apocynin addition to H_2O_2 prolong treated ASCs and the ASC control (Figure 5.8).

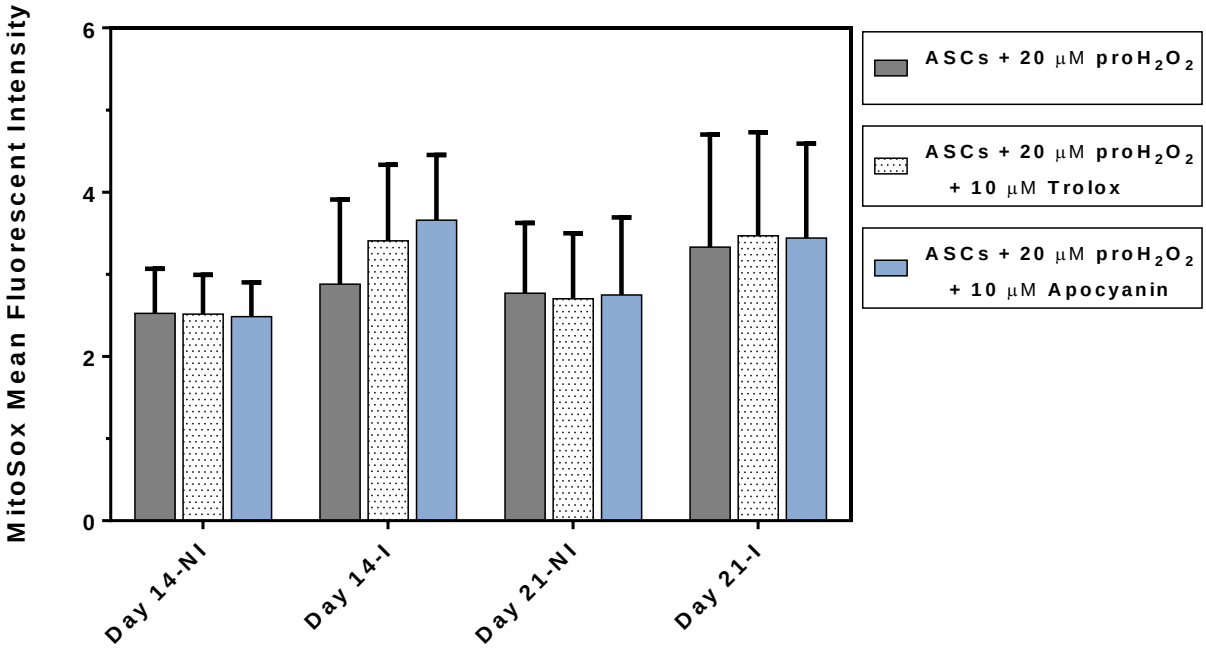

Figure 5.8 Effects of ROS scavengers on mitochondrial ROS levels in H_2O_2 prolong treated ASCs during adipogenesis.
Mitochondrial ROS levels were determined using the MitoSOX™ Red mitochondrial superoxide indicator reagent. Trolox and apocynin addition to adipogenic differentiating H_2O_2 prolonged treated ASCs had no effect on mitochondrial ROS levels on day 14 and day 21 when compared to H_2O_2 prolonged treated ASCs only. ASCs incubated with complete DMEM only served as the non-induced controls. n = 4. NI: Non-induced; I: Induced.

5.3.7 Effects of ROS scavenger addition to ASCs on extracellular ROS release during adipogenesis

The effect of ROS scavengers on the extracellular release of ROS by ASCs during adipogenic differentiation on day 0, 7 14 and 21 was also measured using the

OxyBURST™ Green H_2HFF BSA assay. Negative fluorescence values were recorded in all treatment conditions, suggesting that there was no extracellular ROS release detected during adipogenic differentiation or that adipogenic differentiation made use of the surrounding extracellular ROS. In ASCs only (without ROS scavenger treatment) the average fluorescence value for all time points throughout the differentiation period was -6709 ± 4381. Following the addition of Trolox to ASCs the average fluorescence value for all time points throughout the differentiation period was -4556 ± 3936. This indicated a 1.5-fold increase in the fluorescence value with Trolox addition when compared to ASCs only. Whereas with apocynin addition to ASCs the average fluorescence value was -20705 ± 7447. This reflected a 3.1-fold decrease in the average fluorescence values when compared to ASCs only (Figure 5.9). There was however no statistically significant difference (p=0.0867) in fluorescence values between the groups when compared to day 0 (Figure 5.9).

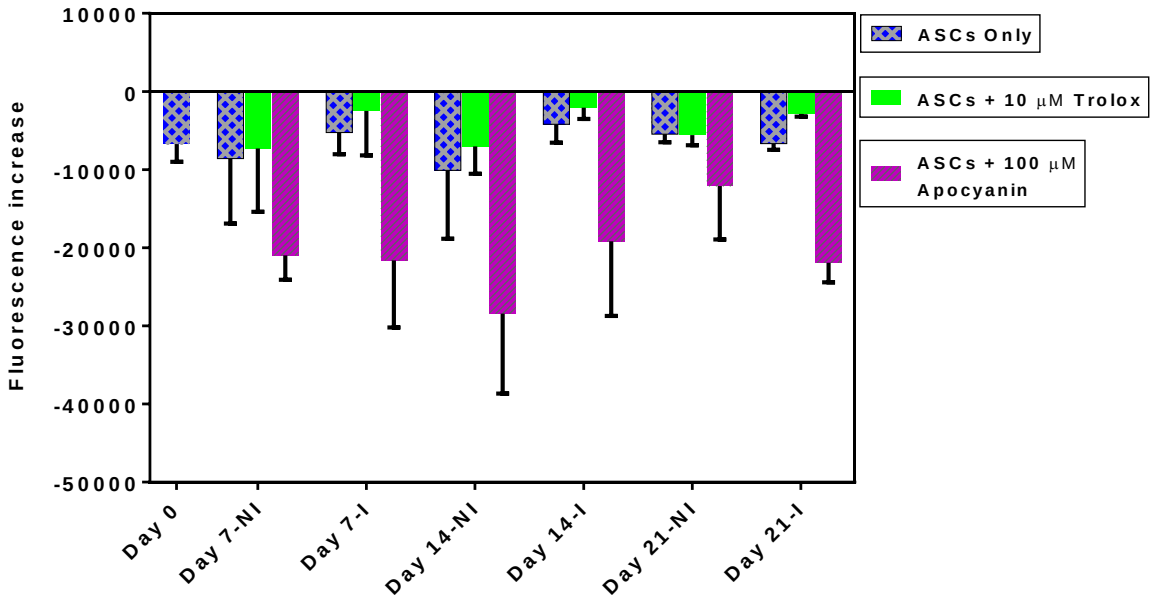

Figure 5.9 Effects of ROS scavenger addition to ASCs on extracellular ROS release during adipogenesis.
There were negative fluorescence values throughout the differentiation period for all the treatment conditions. Fluorescence values were more negative with the addition of apocynin to ASCs as compared with Trolox addition throughout the differentiation period. ASCs incubated with complete DMEM only served as the non-induced controls. n = 4. NI: Non-induced; I: Induced.

5.3.8 Effects of ROS scavenger addition to H_2O_2 pre-treated ASCs on extracellular ROS release during adipogenesis

Following the addition of Trolox to H_2O_2 pre-treated ASCs, the average fluorescence value for all time points throughout the differentiation period was -6910 ± 3191. This reflected a 1.1-fold increase in fluorescence values when compared to H_2O_2 pre-treated ASCs (-7610 ± 3845). However, with apocynin addition to H_2O_2 pre-treated ASCs, there was an observed further decrease in the average fluorescence value to -20492 ± 10253. This represented a 3.1-fold decrease in fluorescence value when compared to H_2O_2 pre-treated ASCs (-7610 ± 3845). There was however, no statistically significant difference (p=0.2125) in fluorescence values between the groups when compared to day 0 (Figure 5.10).

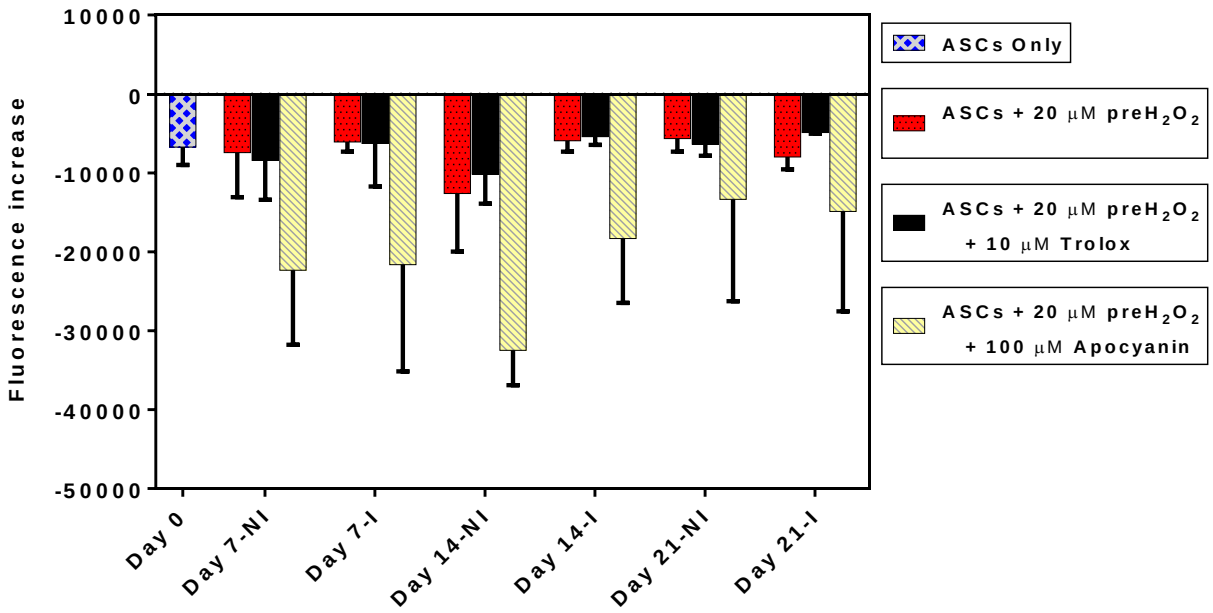

Figure 5.10 Effects of ROS scavenger addition to H_2O_2 pre-treated ASCs on extracellular ROS release during adipogenesis.
There were negative fluorescence values throughout the adipogenic differentiation period for all the treatment conditions. Addition of apocynin to pre-treated ASCs resulted in more negative fluorescence values throughout the differentiation period when compared to day 0. ASCs incubated with complete DMEM only served as the non-induced controls. n = 4. NI: Non-induced; I: Induced

5.3.9 Effects of ROS scavenger addition to H_2O_2 prolonged treated ASCs on extracellular ROS release during adipogenesis

The addition of Trolox to H_2O_2 prolonged treated ASCs resulted in an average fluorescence value for all time points throughout the differentiation period of -9214 ± 5105. This reflected no fold change in fluorescence values when compared to H_2O_2 prolonged treated ASCs (-9001 ± 5948). Interestingly, with apocynin addition to H_2O_2 prolonged treated ASCs, there was a further decrease in fluorescence value. The average extracellular ROS fluorescence value was -19494 ± 11811 indicating a 2.1-fold decrease when compared to H_2O_2 prolonged treated ASCs (-9001 ± 5948). There was however, no statistically significant difference (p=0.5559) in fluorescence values between the groups when compared to day 0 (Figure 5.11).

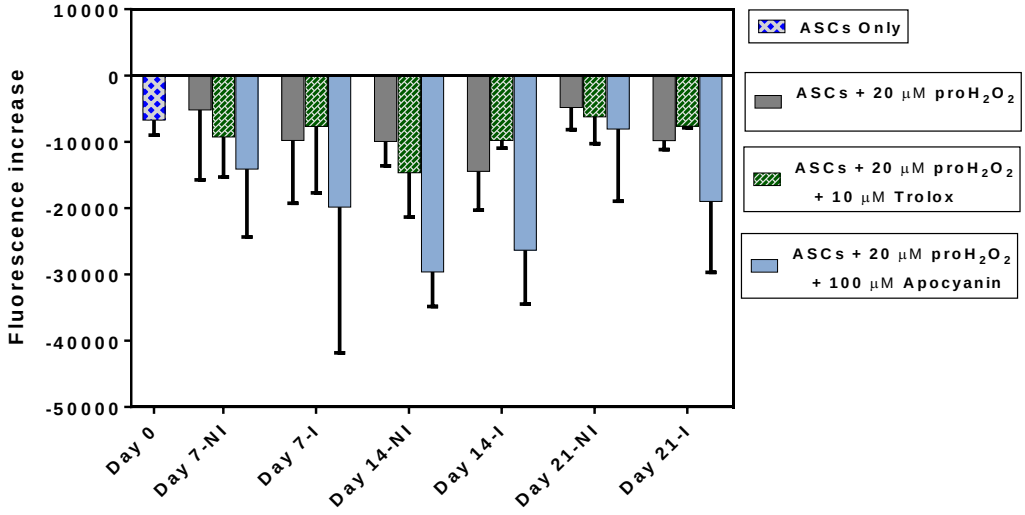

Figure 5.11 Effects of ROS scavenger addition to H_2O_2 prolonged treated ASCs on extracellular ROS release during adipogenesis.
There were negative fluorescence values throughout the adipogenic differentiation period for all the treatment conditions. Addition of apocynin to prolonged treated ASCs resulted in more negative fluorescence values throughout the differentiation period when compared to day 0. ASCs incubated with complete DMEM only served as the non-induced controls. n = 4. NI: Non-induced; I: Induced.

5.4 Discussion

In this study, we investigated the effects of ROS and ROS scavenger addition on the adipogenic differentiation of human ASCs. Various studies have reported that ROS are involved in adipogenesis and endogenous ROS production increases in parallel with adipogenic differentiation[5–7]. As such this study went on further to investigate the corresponding changes in intracellular and extracellular ROS levels upon the addition of H_2O_2 and ROS scavengers to differentiating ASCs. ASCs were induced to adipogenic differentiation in the presence or absence of the ROS scavengers Trolox and apocynin. Thereafter total intracellular ROS levels were measured using CellROX® Deep Red and mitochondrial ROS production was also measured using MitoSOX™ Red.

Adipogenic differentiation of ASCs resulted in no change in total intracellular ROS levels when comparing non-induced and induced ASCs (Figure 5.1). This suggesting that intracellular ROS levels are not involved in adipogenic differentiation. This observation did not support previous research, where adipogenic differentiation of ASCs was reported to be associated with increase in ROS production[5–7,16]. The addition of Trolox which is a ROS scavenger to differentiating ASCs, resulted in no effect on total intracellular ROS levels on day 14 and day 21 when compared to ASCs only. This suggesting that Trolox does not scavenge intracellular ROS in differentiating human ASCs. Trolox is a water soluble analogue of vitamin E, that has been reported to possesses intracellular scavenging activity against H_2O_2, superoxide, hydroxyl and peroxyl radicals[17,18]. However, contradictory to this study, Alves and colleagues (2013) reported that Trolox addition to bone marrow-derived human mesenchymal stromal cells inhibited intracellular ROS levels[19]. Differences in stem cell sources (ASCs versus MSCs) may have possibly contributed to this contrasting finding. In support to this speculation, experiments by Mohamed-Ahmed and colleagues (2018) demonstrated that ASCs had a higher adipogenic differentiation capacity as compared to BM-MSCs[20].

Apocynin addition to adipogenic differentiating ASCs also resulted in no effect on the levels of total intracellular ROS levels on day 14 and day 21 when compared to ASCs only (Figure 5.1). Apocynin is a natural plant derived methoxy-substituted catechol that is

used to inhibit NADPH oxidase in cells thereby blocking superoxide production and is also a ROS scavenger[21–23]. The observed lack of an effect by apocynin on total intracellular ROS levels suggests that in ASCs, apocynin does not scavenge intracellular ROS and that NOX derived ROS are not involved in adipogenic regulation. On the contrary experiments by Drehmer and colleagues (2016) reported that treatment of human ASCs with 100 µM apocynin inhibited intracellular ROS levels during the first three days of adipogenic differentiation adipogenic differentiation[24]. This observation suggests that apocynin may probably have an intracellular ROS scavenging effect only during the very early phases of differentiation. Additional studies using apocynin during the early phases of differentiation would be useful to determine apocynin's mode of action in human ASCs.

Mitochondrial ROS levels were determined using the MitoSOX™ Red, mitochondrial ROS levels did not change with increase in adipogenic differentiation of ASCs suggesting that mitochondrial ROS were not involved in differentiation (Figure 5.5). This finding was in contrast to previous reports were mitochondrial ROS levels were observed to increase with adipogenic differentiation[25,26]. Trolox and apocynin addition to differentiating ASCs resulted in no change in mitochondrial ROS levels on day 14 and day 21 when compared to ASCs only. Suggesting that Trolox and apocynin are not inhibitors of mitochondrial derived ROS in differentiating ASCs. This finding also suggests that mitochondrial derived ROS are not a possible ROS source in differentiating ASCs. The influence of Trolox and apocynin on mitochondrial ROS levels in differentiating ASCs has not been extensively described in literature. However, previous studies from other investigators have reported contrasting results to this current study. Monticone and colleagues (2014) showed that the treatment of glioblastoma and tumorigenic initiating cells with Trolox, suppressed mitochondrial ROS levels[27]. Other researchers have reported on a prooxidant effect by Trolox and apocynin[22,28,29]. Further work is however required to define the mechanisms of action by Trolox and apocynin on mitochondrial ROS levels in differentiating ASCs. The mechanisms of action behind the prooxidative effects of Trolox and apocynin during adipogenesis are not entirely clear and require further investigation.

Pre-treatment of ASCs with H_2O_2 followed by adipogenic differentiation did not affect total intracellular ROS levels on day 14 and day 21 when compared to H_2O_2 pre-treated ASCs (Figure 5.2). This suggests that pre-treatment of ASCs with extracellular H_2O_2 does not promote further intracellular ROS generation in ASCs during adipogenic differentiation. This finding is in contrast to earlier findings by Li and colleagues (2001), who reported that treatment of vascular smooth muscle cells and fibroblasts with exogenous H_2O_2 amplified intracellular ROS production[30]. On the other hand, H_2O_2 pre- and prolonged treatment of ASCs induced to differentiate resulted in no effect on mitochondrial ROS levels on day 14 and day 21 when compared to ASCs only (Figure 5.6). This finding suggests that extracellular treatment of ASCs with H_2O_2 does not stimulate increased mitochondrial ROS production in differentiating ASCs. The presence of ROS in excess has been described to be associated with mitochondrial damage and loss of function[31,32]. It is possible that the presence of extracellular H_2O_2 may have altered the function of mitochondria thus resulting in no effect in mitochondrial ROS levels. However, additional studies are required to confirm this.

The addition of Trolox and apocynin to H_2O_2 pre-treated ASCs followed by adipogenic differentiation resulted in no effect in total intracellular ROS levels on day 14 and day 21 when compared to H_2O_2 pre-treated ASCs only (Figure 5.3). Suggesting that in H_2O_2 pre-treated ASCs Trolox and apocynin do not inhibit intracellular ROS generation in differentiating ASCs. The observed lack of an inhibition effect by apocynin suggests that in H_2O_2 pre-treated ASCs NOX is not a possible ROS source during adipogenic differentiation in ASCs. There was no change in mitochondrial ROS levels with Trolox and apocynin addition to H_2O_2 pre-treated ASCs on day 14 and day 21 when compared to H_2O_2 pre-treated ASCs only (Figure 5.7). These findings suggest that in H_2O_2 pre-treated ASCs mitochondrial derived ROS are not a possible ROS source during adipogenic differentiation. The results also suggest that Trolox and apocynin are not inhibitors of mitochondrial derived ROS in H_2O_2 pre-treated ASCs.

The addition of Trolox to adipogenic induced H_2O_2 prolong treated ASCs did not show any appreciable change in total intracellular ROS levels on day 14 and on day 21 when

compared to H_2O_2 prolong treated ASCs only (Figure 5.4). Suggesting that in ASCs with H_2O_2 present throughout the differentiation period Trolox does not inhibit intracellular ROS generation in differentiating ASCs. The simultaneous addition of Trolox and H_2O_2 may have neutralised Trolox thereby resulting in little to no Trolox left to scavenge intracellular ROS. This speculation has been supported in a previous study where Trolox was reported to scavenge ROS present in solution[18].

On the other hand, apocynin addition to induced H_2O_2 prolonged treated ASCs resulted in no appreciable change in total intracellular ROS levels on day 14 and day 21 (Figure 5.4). These findings show that apocynin does not inhibit total intracellular ROS levels in the presence of extracellular H_2O_2, thus suggesting that NOX enzymes are not involved in ROS production in ASCs subjected to constant presence of H_2O_2. Apocynin's lack of a ROS inhibition effect is supported in previous reports by Heumuller and colleagues (2008) as well as Vejrazka and colleagues (2005). They observed that apocynin inhibited intracellular ROS in non-phagocytic cells only in the presence of H_2O_2 and myeloperoxidase[21,22]. Since myeloperoxidase is mainly found in myeloid cells it is likely that the absence of myeloperoxidase in differentiating ASCs contributed to apocynin's lack of a ROS inhibition effect despite the presence of H_2O_2[33]. The differences in the effects of Trolox and apocynin on total intracellular ROS levels suggest that both scavengers have different mechanisms of action in the presence of extracellular H_2O_2 in differentiating ASCs.

Trolox and apocynin addition to differentiating ASCs treated with prolonged exposure to H_2O_2 resulted in no effect in mitochondrial ROS levels on day 14 and day 21 when compared to H_2O_2 prolong treated ASCs only (Figure 5.8). This finding may suggest that ASCs under the continuous presence of H_2O_2, mitochondrial derived ROS are not involved during the differentiation process. The results also indicate that in the presence of H_2O_2 Trolox and apocynin are not inhibitors of mitochondrial derived ROS.

Extracellular ROS release was measured in ASCs subjected to different treatments using the OxyBURST® H_2HFF Green BSA reagent. In all the treatment conditions throughout

the differentiation period, there were negative fluorescence values observed. As such, we concluded that there was no extracellular ROS release detected during adipogenic differentiation of ASCs. We speculate that most probably the concentration of H_2O_2 released by the cells was below the detection limit of the ROS detection probe used (OxyBURST® H_2HFF Green BSA reagent). Since ROS are unstable it is possible that the released H_2O_2 may have reacted with media components resulting in loss of signal detection[34]. Contrary to findings from this study Mouche and colleagues (2007) detected extracellular ROS release by 3T3-L1 preadipocytes and adipocytes[8]. However, ROS release was measured using the Amplex Red Hydrogen Peroxide/Peroxidase assay method in the presence of live cells. In future studies, the measurement of extracellular ROS release in the presence of live cells is recommended. Negative fluorescence values meant that background fluorescence values were higher than test sample values. The exact reasons behind this are not clear but we speculate that cells may have secreted factors or taken up some components in test sample media resulting in lower fluorescence values. Since the only difference between background media and test sample media was the presence of cells. Interestingly, apocynin addition resulted in more negative fluorescence values (Figures 5.9, 5.10 and 5.11). We assume that this is most likely because cells took up apocynin more or secreted factors that had a more pronounced effect on apocynin.

5.5 Conclusion

This study is among the few that have investigated the effects of Trolox and apocynin on total intracellular and mitochondrial ROS levels during adipogenic differentiation of primary human ASCs in the presence and absence of short term and prolonged exposure to extracellular H_2O_2. The results of this study suggest that Trolox and apocynin have no effect on total intracellular and mitochondrial ROS levels in differentiating ASCs. The findings from this study further suggest that in adipogenic differentiating ASCs, there is no extracellular ROS release since no H_2O_2 was detected in the culture media of the cells. Further studies are however required gain a deeper understanding on extracellular ROS release in differentiating ASCs.

The interpretation to this study is however limited by the fact that, the concentration of apocynin used was not validated for safety on ASC viability over the 21-day differentiation period. Another limitation in this study was that mitochondrial specific antioxidants were not used in this study and we could not with confidence implicate mitochondria as a ROS source during adipogenesis. The concentrations of ROS scavengers used in this study may not have been potent enough to produce a significant ROS inhibition effect *in vitro*. Thus, in future studies, it is recommended to select for the appropriate concentrations of ROS scavengers that have the maximum ROS inhibition effect without affecting cell viability. Altogether, this study suggests that Trolox and apocynin do not inhibit intracellular ROS generation in adipogenic differentiating human ASCs. However, it is recommended that additional studies be conducted to determine Trolox and apocynin's exact mechanisms of action in human ASCs.

References

1. Prasad S, Gupta SC, Tyagi AK. Reactive oxygen species (ROS) and cancer: role of antioxidative nutraceuticals. Cancer Lett. 2017;387:95–105.

2. Galadari S, Rahman A, Pallichankandy S, Thayyullathil F. Reactive oxygen species and cancer paradox: to promote or to suppress? Free Radic Biol Med. 2017;104:144–64.

3. Liu Y, Fiskum G, Schubert D. Generation of reactive oxygen species by the mitochondrial electron transport chain. J ofNeurochemistry. 2002;80:780–7.

4. Dikalov S. Cross talk between mitochondria and NADPH oxidases. Free Radic Biol Med. 2011;51(7):1289–301.

5. Furukawa S, Fujita T, Shimabukuro M, Iwaki M, Yamada Y, Nakajima Y, et al. Increased oxidative stress in obesity and its impact on metabolic syndrome. J Clin Invest. 2004;114(12):1752–61.

6. Higuchi M, Dusting GJ, Peshavariya H, Jiang F, Hsiao ST-F, Chan EC, et al. Differentiation of human adipose-derived stem cells into fat involves reactive oxygen species and forkhead box O1 mediated upregulation of antioxidant enzymes. Stem Cells Dev. 2013;22(6):878–88.

7. Kanda Y, Hinata T, Won S, Watanabe Y. Reactive oxygen species mediate adipocyte differentiation in mesenchymal stem cells. Life Sci. 2011;89(7–8):250–8.

8. Mouche S, Mkaddem S Ben, Wang W, Katic M, Tseng Y-HH, Carnesecchi S, et al. Reduced expression of the NADPH oxidase NOX4 is a hallmark of adipocyte differentiation. Biochim Biophys Acta - Mol Cell Res. 2007;1773(7):1015–27.

9. Kojima T, Norose T, Tsuchiya K, Sakamoto K. Mouse 3T3-L1 cells acquire resistance against oxidative stress as the adipocytes differentiate via the transcription factor FoxO. Apoptosis. 2010;15(1):83–93.

10. Lee H, Lee YJ, Choi H, Ko EH, Kim J. Reactive oxygen species facilitate adipocyte differentiation by accelerating mitotic clonal expansion. J Biol Chem.

2009;284(16):10601–9.

11. Eruslanov E, Kusmartsev S. Identification of ROS using oxidized DCFDA and flow-cytometry. Methods Mol Biol. 2010;594:57–72.

12. Probes M. The molecular probes handbook. 11th ed. 2010.

13. Dikalov S, Griendling KK, Harrison DG. Measurement of reactive oxygen species in cardiovascular studies. Hypertension. 2007;49(4):717–27.

14. CellROX ® oxidative stress reagents. Eugene, Oregon: Life Technologies Corporation; 2012.

15. Fc OxyBURST ® assay reagents. Eugene, Oregon: Molecular Probes; 2001.

16. O. Lee, Y. Kwon, H. Hong, C. Park, B. Lee YK, Lee OH, Kwon YI, Hong HD, Park CS, Lee BY, et al. Production of reactive oxygen species and changes in antioxidant enzyme activities during differentiation of 3T3-L1 adipocyte. J Korean Soc Appl Biol Chem. 2009;52(1):70–5.

17. Hamad I, Arda NN, Pekmez M, Karaer S, Temizkan G. Intracellular scavenging activity of Trolox (6hydroxy2,5,7,8tetramethylchromane2carboxylic acid) in the fission yeast, Schizosaccharomyces pombe. J Nat Sci Biol Med. 2016;1(1):16–21.

18. Sugahara S, Chiyo A, Fukuoka K, Ueda Y, Tokunaga Y, Nishida Y, et al. Unique antioxidant effects of herbal leaf tea and stem tea from Moringa oleifera L. especially on superoxide anion radical generation systems. Biosci Biotechnol Biochem. 2018;1–12.

19. Alves H, Mentink A, Le B, van Blitterswijk CA, de Boer J. Effect of antioxidant supplementation on the total yield, oxidative stress levels, and multipotency of bone marrow-derived human mesenchymal stromal cells. Tissue Eng Part A. 2013;19(7–8):928–37.

20. Mohamed-Ahmed S, Fristad I, Lie SA, Suliman S, Mustafa K, Vindenes H, et al. Adipose-derived and bone marrow mesenchymal stem cells: a donor-matched comparison. Stem Cell Res Ther. 2018;9(1):168.

21. Heumuller S, Wind S, Barbosa-Sicard E, Schmidt HH, Busse R, Schroder K, et al. Apocynin is not an inhibitor of vascular NADPH oxidases but an antioxidant. Hypertension. 2008;51(2):211–7.

22. Vejražka M, Míček R, Štípek S. Apocynin inhibits NADPH oxidase in phagocytes but stimulates ROS production in non-phagocytic cells. Biochim Biophys Acta - Gen Subj. 2005;1722(2):143–7.

23. Lee YS, Choi EM. Apocynin stimulates osteoblast differentiation and inhibits bone-resorbing mediators in MC3T3-E1 cells. Cell Immunol. 2011;270(2):224–9.

24. Drehmer DL, de Aguiar AM, Brandt AP, Petiz L, Cadena SMSC, Rebelatto CK, et al. Metabolic switches during the first steps of adipogenic stem cells differentiation. Stem Cell Res. 2016;17(2):413–21.

25. Wang W, Zhang Y, Lu W, Liu K. Mitochondrial reactive oxygen species regulate adipocyte differentiation of mesenchymal stem cells in hematopoietic stress induced by arabinosylcytosine. Saretzki G, editor. PLoS One. 2015;10(3):120629.

26. Tormos K V., Anso E, Hamanaka RB, Eisenbart J, Joseph J, Kalyanaraman B, et al. Mitochondrial complex III ROS regulate adipocyte differentiation. cell metab. 2011;14(4):537–44.

27. Monticone M, Taherian R, Stigliani S, Carra E, Monteghirfo S, Longo L, et al. NAC , Tiron and Trolox impair survival of cell cultures containing glioblastoma tumorigenic initiating cells by inhibition of cell cycle progression. Harrison JK, editor. PLoS One. 2014;9(2):e90085.

28. Wattamwar PP, Hardas SS, Butterfield DA, Anderson KW, Dziubla TD. Tuning of the pro-oxidant and antioxidant activity of trolox through the controlled release from biodegradable poly(trolox ester) polymers. J Biomed Mater Res - Part A. 2011;99 A(2):184–91.

29. Albertini R, Abuja PM. Prooxidant and antioxidant properties of Trolox C, analogue of vitamin E, in oxidation of low-density lipoprotein. Free Radic Res. 1999;30(3):181–8.

30. Li WG, Miller FJ, Zhang HJ, Spitz DR, Oberley LW, Weintraub NL. H(2)O(2)-induced O(2) production by a non-phagocytic NAD(P)H oxidase causes oxidant injury. J Biol Chem. 2001;276(31):29251–6.

31. Guo C, Sun L, Chen X, Zhang D. Oxidative stress, mitochondrial damage and neurodegenerative diseases. Neural Regen Res. 2013;8(21):2003–14.

32. Franchina DG, Dostert C, Brenner D. Reactive oxygen species: involvement in T Cell signaling and metabolism. Trends Immunol. 2018;39(6):489–502.

33. Hachiya M, Osawa Y, Akashi M. Role of TNFα in regulation of myeloperoxidase expression in irradiated HL60 promyelocytic cells. Biochim Biophys Acta - Mol Cell Res. 2000;1495(3):237–49.

34. Uy B, McGlashan SR, Shaikh SB. Measurement of reactive oxygen species in the culture media using Acridan lumigen PS-3 assay. J Biomol Tech. 2011;22(3):95–107.

Chapter 6: General discussion and conclusion

6.1 General discussion

Reactive oxygen species (ROS) have been reported to be involved in the regulation of adipogenesis[1]. The process of adipogenesis has in turn been described to be associated with an increase in intracellular ROS levels[2,3]. Excessive adipogenesis ultimately leads to obesity and its related complications. The global incidence and prevalence of obesity have reached alarming proportions, yet effective prevention and therapeutic strategies remain to be developed[4]. In addition, the process of adipogenesis and the role played by ROS in the process is poorly understood[1,5]. This study therefore set out to investigate the effects of ROS and ROS scavengers on adipogenesis in human ASCs particularly to gain knowledge on how ROS is regulated in adipogenesis as well as to evaluate the ROS scavengers Trolox and apocynin as possible anti-adipogenic agents.

The addition of adipogenic induction medium to ASCs resulted in an increase in adipogenesis on day 14 and day 21 (Chapter 4 Figure 4.2). This was however accompanied by no change in total intracellular (Chapter 5 Figure 5.1) as well as mitochondrial ROS levels (Chapter 5 Figure 5.5). This suggesting that adipogenic differentiation of human ASCs is not associated with an increase in intracellularly generated ROS as well as mitochondrial derived ROS.

Trolox and apocynin addition to adipogenic induced ASCs had no effect on adipogenesis on day 14 and day 21 (Chapter 4 Figure 4.2). There was also no corresponding change in total intracellular (Chapter 5 Figure 5.1) as well as mitochondrial (Chapter 5 Figure 5.5) ROS levels in the differentiating ASCs. This suggesting that in this study Trolox and apocynin had no influence on adipogenesis and are not scavengers of total intracellular and mitochondrial ROS. These findings also suggest that intracellularly derived ROS including mitochondrial ROS are not involved in adipogenic differentiation.

Treatment of ASCs with H_2O_2 accelerated their adipogenic differentiation capacity with a greater adipogenic enhancement effect observed in ASCs differentiating in the constant presence of H_2O_2 (prolong treated ASCs) on day 14 (Chapter 4 Figure 4.3). Both pre- and prolonged H_2O_2 treated ASCs and the untreated control ASCs achieved similar levels of adipogenesis (no change in adipogenesis between all three conditions) on day 21, indicating that the influence of extracellular H_2O_2 treatment on adipogenesis predominant only in the early phases of differentiation. However, the observed adipogenic enhancement with extracellular ROS treatment was not associated with a corresponding increase in total intracellular (Chapter 5 Figure 5.2) and mitochondrial ROS levels (Chapter 5 Figure 5.6). This suggests that extracellular ROS enhance adipogenesis in human ASCs through mechanisms that do not involve changes intracellular ROS levels including mitochondrial derived ROS.

The addition of the ROS scavenger, Trolox to adipogenic induced H_2O_2 pre-treated ASCs had no effect on adipogenesis on day 14 and day 21 (Chapter 4 Figure 4.4). This was accompanied with no corresponding change in both the total intracellular (Chapter 5 Figure 5.3) and mitochondrial (Chapter 5 Figure 5.7) ROS levels. This suggests that in H_2O_2 pre-treated ASCs intracellular ROS are not involved in adipogenesis. On the contrary, the addition of apocynin to differentiating H_2O_2 pre-treated ASCs suppressed adipogenesis on day 14 (Chapter 4 Figure 4.4), which was accompanied with no corresponding change in total intracellular ROS levels (Chapter 5 Figure 5.3) and mitochondrial ROS levels (Chapter 5 Figure 5.7). This suggests that apocynin suppressed ASCs adipogenesis during the early phase only after the cells had been exposed to extracellular H_2O_2, suggesting that it could be an effective anti-adipogenic agent in the presence of an oxidative stress condition.

In differentiating H_2O_2 prolong treated ASCs, the addition of Trolox had no effect on adipogenesis on day 14 and day 21 (Chapter 4 Figure 4.5). There was also no change in the total intracellular (Chapter 5 Figure 5.4); as well as in mitochondrial ROS levels (Chapter 5 Figure 5.8). The absence of an effect by Trolox on ASCs adipogenesis suggests that the continuous presence of H_2O_2 abated the effect of Trolox on

differentiating ASCs. The addition of apocynin to H_2O_2 prolonged treated ASCs resulted in no effect on adipogenesis on day 14 and day 21, although a slight non-significant decreasing trend in adipogenesis was observed (Chapter 4 Figure 4.5). There was no corresponding change in the total intracellular (Chapter 5 Figure 5.4) and mitochondrial ROS levels (Chapter 5 Figure 5.8). This suggests that in the continuous presence of extracellular H_2O_2 apocynin has no effect on ASC adipogenesis.

6.2 Concluding remarks

Trolox and apocynin are well known ROS scavengers, however their effect as adipogenic inhibitors in differentiating human ASCs has not been extensively described in literature[6,7]. This study is one of the few that has investigated the influence of Trolox and apocynin in differentiating ASCs (in the presence or absence of H_2O_2 treatment) as well as attempt to decipher their possible mechanisms of action.

This study showed that apocynin supresses adipogenesis in human ASCs particularly in the presence of extracellular H_2O_2 pre-treatment during the early phases of differentiation. This suggesting that NOX derived ROS may possibly be involved in regulating adipogenesis in the presence of extracellular H_2O_2 pre-treatment. The study also showed that the ROS scavengers Trolox and apocynin did not scavenge intracellularly derived ROS including mitochondrial ROS. It was also shown that Trolox had no effect on adipogenic differentiation of ASCs in the presence and absence of H_2O_2. Apocynin also had no effect on adipogenesis in the absence of extracellular H_2O_2. However, the results of this study suggested that extracellular ROS release was not involved during adipogenesis.

Limitations of study and recommendations for future work

Additional studies need to be conducted to further define the precise molecular mechanisms of action by the ROS scavengers during adipogenesis. Gene expression studies of adipocyte specific and antioxidative enzyme genes as well as studies to identify intracellular ROS sources will be pivotal in deciphering the possible mechanisms of action by Trolox and apocynin during adipogenesis. This study was limited by the lack of

adequate information on donor characteristics that are possible contributors for heterogeneity. This heterogeneity coupled with the relatively small number of biological replicates (n=4) could possibly have influenced the lack of statistical significance observed between the different treatment conditions in this study. It is therefore recommended for future studies to keep such donor factors constant to minimise heterogeneity and further increase the number of biological replicates used in the study. This study only investigated adipogenesis during the later stages of differentiation. It is recommended that in future studies, the effects of ROS scavengers be also investigated during the very early phases of differentiation. Above all, having shown that apocynin could be a possible anti-adipogenic/anti-obesity agent, further studies involving animal models will help provide clearer insights into its role as a suppressor of adipogenesis. The findings from this will enhance current knowledge in the field that will in turn assist in developing new and improved therapeutic interventions in the treatment of obesity and its comorbidities.

References

1. de Villiers D, Potgieter M, Ambele MA, Adam L, Durandt C, Pepper MS. The role of reactive oxygen species in adipogenic differentiation. In: Advances in Experimental Medicine and Biology. Springer, Boston, MA; 2017. p. 125–44.

2. Higuchi M, Dusting GJ, Peshavariya H, Jiang F, Hsiao ST-F, Chan EC, et al. Differentiation of human adipose-derived stem cells into fat involves reactive oxygen species and forkhead box O1 mediated upregulation of antioxidant enzymes. Stem Cells Dev. 2013;22(6):878–88.

3. Kanda Y, Hinata T, Won S, Watanabe Y. Reactive oxygen species mediate adipocyte differentiation in mesenchymal stem cells. Life Sci. 2011;89(7–8):250–8.

4. Kusminski CM, Bickel PE, Scherer PE. Targeting adipose tissue in the treatment of obesity-associated diabetes. Nat Publ Gr. 2016;15(9):639–60.

5. Atashi F, Modarressi A, Pepper MS. The role of reactive oxygen species in mesenchymal stem cell adipogenic and osteogenic differentiation: a review. Stem Cells Dev. 2015;24(10):1150–63.

6. Heumuller S, Wind S, Barbosa-Sicard E, Schmidt HH, Busse R, Schroder K, et al. Apocynin is not an inhibitor of vascular NADPH oxidases but an antioxidant. Hypertension. 2008;51(2):211–7.

7. Hamad I, Arda NN, Pekmez M, Karaer S, Temizkan G. Intracellular scavenging activity of Trolox (6hydroxy2,5,7,8tetramethylchromane2carboxylic acid) in the fission yeast, Schizosaccharomyces pombe. J Nat Sci Biol Med. 2016;1(1):16–21.

Appendix A: Absolute cell count calculation

Absolute cell counts were obtained by taking the number of events in the region of interest (nucleated intact cells: N) and dividing that number by the number of events in the Flow Count™ region (G). The result of which was multiplied by the calibration factor (C) of the Flow Count™ beads. The lot-number specific calibration factor (concentration of beads/µl) is supplied with each Flow Count vial. This gave the cell count per microliter (see formula below).

Absolute cell count/µl = (N/G) x C

Appendix B: MSc committee and ethics approval letters

UNIVERSITEIT VAN PRETORIA
UNIVERSITY OF PRETORIA
YUNIBESITHI YA PRETORIA

MSc Committee
School of Medicine
Faculty of Health Sciences

MSc Committee
15 May 2017

Dr M Ambele
Department of Immunology
Faculty of Health Sciences

Dear Dr,

Mr LT Adam, Student no 14456550

Please receive the following comments with reference to the MSc Committee submission of the abovementioned student:

Student name	Mr LT Adam	**Student number**	14456550
Name of study leader	Dr Melvin Ambele		
Department	Immunology		
Title of MSc	Effects of reactive oxygen species scavengers on adipogenesis		
Date of first submission	March 2017		
March 2017	• Thank you for submitting the revised protocol.		
May 2017	• Thank you for submitting the ethics approval certificate.		
Decision	This protocol has been approved. Ethical approval has been obtained. The internal and external examiners can be nominated and submitted to the MSc Committee six months prior to submission of the dissertation. Please ensure that the CV of the examiners includes: supervision, examination and publication records.		

Yours sincerely

Dr Marleen Kock
Chair: MSc Committee

MSc Committee, School of Medicine
Faculty of Health Sciences
University of Pretoria,
Private Bag X323
Pretoria 0001, South Africa
Tel +27 (0)12 319 2325
Fax +27 (0)12 323 0732

Fakulteit Gesondheidswetenskappe
Lefapha la Disaense tša Maphelo

The Research Ethics Committee, Faculty Health Sciences, University of Pretoria complies with ICH-GCP guidelines and has US Federal wide Assurance.
- FWA 00002567, Approved dd 22 May 2002 and Expires 03/20/2022.
- IRB 0000 2235 IORG0001762 Approved dd 22/04/2014 and Expires 03/14/2020.

UNIVERSITEIT VAN PRETORIA
UNIVERSITY OF PRETORIA
YUNIBESITHI YA PRETORIA

Faculty of Health Sciences Research Ethics Committee

28/04/2017

Approval Certificate
New Application

Ethics Reference No.: 134/2017

Title: Effects of reactive oxygen species scavengers on adipogenesis.

Dear Mr Ladislaus Adam

The **New Application** as supported by documents specified in your cover letter dated 18/04/2017 for your research received on the 19/04/2017, was approved by the Faculty of Health Sciences Research Ethics Committee on its quorate meeting of 26/04/2017.

Please note the following about your ethics approval:
- Ethics Approval is valid for 3 years
- Please remember to use your protocol number (**134/2017**) on any documents or correspondence with the Research Ethics Committee regarding your research.
- Please note that the Research Ethics Committee may ask further questions, seek additional information, require further modification, or monitor the conduct of your research.

Ethics approval is subject to the following:
- The ethics approval is conditional on the receipt of **6 monthly written Progress Reports**, and
- The ethics approval is conditional on the research being conducted as stipulated by the details of all documents submitted to the Committee. In the event that a further need arises to change who the investigators are, the methods or any other aspect, such changes must be submitted as an Amendment for approval by the Committee.

We wish you the best with your research.

Yours sincerely

Dr R Sommers, MBChB; MMed (Int); MPharMed,PhD
Deputy Chairperson of the Faculty of Health Sciences Research Ethics Committee, University of Pretoria

The Faculty of Health Sciences Research Ethics Committee complies with the SA National Act 61 of 2003 as it pertains to health research and the United States Code of Federal Regulations Title 45 and 46. This committee abides by the ethical norms and principles for research, established by the Declaration of Helsinki, the South African Medical Research Council Guidelines as well as the Guidelines for Ethical Research: Principles Structures and Processes, Second Edition 2015 (Department of Health).

☎ 012 356 3084 deepeka.behari@up.ac.za / fhsethics@up.ac.za http://www.up.ac.za/healthethics
✉ Private Bag X323, Arcadia, 0007 - Tswelopele Building, Level 4, Room 60, Gezina, Pretoria

Appendix C: Informed consent form

PATIENT INFORMATION LEAFLET AND INFORMED CONSENT FORM
(Each patient must receive, read and understand this document before the start of the study)

STUDY TITLE
The isolation, characterisation and differentiation of mesenchymal stem cells from adipose tissue.

The mesenchymal stem/stromal cells isolated from the voluntary donated adipose (fat) tissue will be used in various studies. The current studies are listed below. The isolated cells may also be used in future studies. Permission to use the cells in future experiments/studies will be obtained from the Ethics Committee at the Faculty of Health Sciences, University of Pretoria before the cells are used.

1. Do adipose-derived stromal cells possess endocytic function?
2. The role of Pref-1 in *in vitro* adipogenic differentiation of mesenchymal stromal/stem cells (MSCs)
3. Characterization of adipose-derived stromal cell heterogeneity
4. Comparison of the effect of human platelet lysate and foetal bovine serum on adipose-derived stem cell characteristics in culture
5. Is HIV-1 able to infect mesenchymal stromal/ stem cells (MSC)?
6. Effects of reactive oxygen species on adipogenesis.
7. An assessment of the efficacy of human alternatives to fetal bovine serum for the expansion of human adipose-derived stem cells

Dear Patient/Participant: _____

INTRODUCTION

You are invited to participate in a research study that is being carried out by the Department of Immunology at the University of Pretoria. This information leaflet is to help you to decide if you would like to participate. Before you agree to take part in this study you should fully understand what is involved. If you have any questions, which are not fully explained in this leaflet, do not hesitate to ask the investigator. You should not agree to take part unless you are completely happy about all the procedures involved. Your personal health will not be compromised at all by the procedures. These procedures have already been discussed with your doctor beforehand.

THE PURPOSE OF THE STUDY

Researchers at the University of Pretoria would like to investigate the healing properties of adult stem cells for possible future application in regenerative medicine. Regenerative medicine refers to experimental (current status) medicine where researchers try to replace, improve or restore the function of cells that do not function optimally in the body. Adult stem cells are present in various tissues in the body, including fat (adipose) tissue. These adult stem cells could potentially be used to cure patients with various kinds of injuries or diseases. In order to use these cells to cure humans in the future, researchers must first study their characteristics, behaviour, growth and interactions with other cells and/or organisms in the body. This is done by isolating these cells from the fat (adipose) tissue and perform experiments in the laboratory (tissue culture) and/or using experimental animal models.
These adult stem cells can also be used to investigate the process of fat formation. Scientists are able to mimic the formation of fat cells using adult stem cells isolated from fat (adipose) tissue. Obesity is becoming an increasing problem worldwide and in order to find solutions to combat obesity it is important to understand the biological processes involved in the formation of fat. It is also important to understand the interactions of infectious organisms, like HIV and *Mycobacterium tuberculosis* (organism that cause tuberculosis in humans), with stem cells in order to provide safe treatment options in the future. It is therefore important that researchers also investigate the interactions between these infectious organisms and stem cells by performing experiments in the laboratory as well as using experimental animal models. Investigations will be performed on cellular (intact cells) and molecular (investigating the effect on various treatments/exposures to the genetic footprint of cells) levels. For molecular studies we will need to isolate genetic material (DNA and RNA) from your cells.

Many of the experiments that researchers perform require the isolation of genetic material, also known as DNA and RNA, from cells. Genetic material contains information about the cell that only can be revealed if researchers perform specialized tests on the genetic material. These tests are often needed in order to completely understand the characteristics of cells. Genetic information also allows researchers to look into what effect infectious agents, such as *Mycobacterium tuberculosis* (cause tuberculosis in humans) and HIV, might have on these cells. In addition, molecular biology tests (tests that make use of DNA or RNA) are often the

most sensitive tests available to detect if cells are infected with bacteria (such as *Mycobacterium tuberculosis)* and/or viruses (such as HIV).

No unethical procedures will be used when collecting the samples and performing the experiments.

ADIPOSE TISSUE COLLECTION

During various normal plastic surgery operations, adipose tissue (fat) will be excised (cut out) or aspirated (sucked out), and discarded. This adipose tissue, does not serve a purpose to the patient's body anymore, but could serve as a valuable source of stem cells for researchers in the field of regenerative medicine. No additional fat will be collected for the study. Only the fat that the doctor planned to aspirate/cut away during the procedures discussed with you during the consultation visits will be collected.

There will be no added risks or discomfort with the collection of the adipose tissue other than normally associated with the specific procedure the patient will experience during normal operative procedures.

CONFIDENTIALITY

Each participant's sample will be assigned a specific code and this code will be used from there on in all research studies. Certain information, including race, ethnicity, gender and medical history, may be important for scientific reasons. This information will be linked to the sample code and not to your identity. Research reports and articles in scientific journals will not include any information that may identify you.

In some isolated cases it might however be important for the doctors or researchers involved in the study to convey medical information to medical personnel or appropriate Research Ethics committees. In such a case, you by signing this document, give permission to the investigator to release your medical records to regulatory health authorities or an appropriate Research Ethics committee. If necessary, these medical professionals will discuss the results with your doctor and everyone will act in your best interest.

ETHICAL APPROVAL

The protocol involved for this study was submitted to the Research Ethics Committee. This study has received written approval from the Research Ethics Committee of the Faculty of Health Sciences at the University of Pretoria. The study is structured in accordance with the Declaration of Helsinki, which deals with the recommendations of guiding doctors in biomedical research involving humans.
You are also welcome to contact the Faculty of Health Sciences Ethics Committee at the University of Pretoria if you have any concerns or questions. Their contact details are:

The Research Ethics Office:
Tel: 012 - 354 1330 or 012 - 354 1677
Fax: 012 - 354 1367

RIGHTS OF THE PARTICIPANT

Your participation in this study is entirely voluntary and you can refuse to participate or withdraw consent at any time without stating any reason. Your withdrawal will not affect your access to medical care or the quality of medical care that you will receive. Your participation or withdrawal from the study would not affect you in any way.

FINANCIAL GAIN OR LOSS

There will be no financial gain or loss to you, should you participate or withdraw from the study. This research could potentially lead to future profitable treatments. However, you will not have access to these profits. There will be no additional financial costs for you to participate in the study.

The participant has no legal remedy and will not share in any financial gain that may be derived from the study

INFORMATION AND CONTACT PERSON

If at any time you would like to find out more information or have any questions regarding the study, please do not hesitate to contact the researchers.
Dr. C. Durandt: 012 -319 2101
Prof. M.S. Pepper: 012 420 3845 or 012 420 5317

PERSONAL/MEDICAL INFORMATION

The information below may be important for scientific reasons. This information will be linked to the sample code and not to your identity.

Gender: _____

Ethnicity: _____

Date of Birth: _____

Weight: _____

Height: _____

Waste Circumference: _____

Do you smoke? YES NO

Are you suffering from:

Diabetes YES NO

Cardiovascular disease YES NO

Hypertension YES NO

INFORMED CONSENT

WHAT IS EXPECTED?

I confirm that the person asking my consent to take part in this study has told me about the nature, process, risks, discomforts and benefits of the study. I have also received, read and understood the above written information regarding the study. I am aware that the results of the study, including personal details, will be anonymously processed into research reports. I am participating willingly. I have had time to ask questions and have no objection to participate in the study. I understand that there is no penalty should I wish to discontinue with the study and my withdrawal will not affect my access to medical care or the quality of medical care I will receive.

I also understand that certain laboratory tests may require the isolation of genetic material, also known as DNA and RNA and give herewith permission that the researchers may extract RNA/DNA from cells isolated from the adipose tissue.

YES	NO

I hereby give the researchers permission to perform routine HIV, hepatitis B and hepatitis C tests on the adipose tissue donated. Testing for these infectious agents is important for our work as we only like to work with tissue that is negative for these infections. If the researchers detect HIV or hepatitis B or C in the sample, the codified sample details will be sent to _____, who will notify you. If you do not wish us to test your tissue for HIV or hepatitis B or hepatitis C, or if you do not wish to know the results of these tests, we will not be able to include you in the study. In the case on an HIV positive result, you will be counselled and treated by qualified medical personnel.

YES	NO

I have received a copy of this informed consent agreement.

Participant full names (print):_____

Participant signature: _____Date: _____

Investigator full names (print):_____

Investigator signature:_____Date:_____

Witness full names (print):_____

Witness signature:_____Date:_____

Witness full names (print):_____

Witness signature:_____Date:_____

Appendix D: Springer Nature License

SPRINGER NATURE LICENSE
TERMS AND CONDITIONS

Feb 10, 2019

This Agreement between Ladislaus Adam ("You") and Springer Nature ("Springer Nature") consists of your license details and the terms and conditions provided by Springer Nature and Copyright Clearance Center.

License Number	4525311310601
License date	Feb 10, 2019
Licensed Content Publisher	Springer Nature
Licensed Content Publication	Springer eBook
Licensed Content Title	The Role of Reactive Oxygen Species in Adipogenic Differentiation
Licensed Content Author	Danielle de Villiers, Marnie Potgieter, Melvin A. Ambele et al
Licensed Content Date	Jan 1, 2017
Type of Use	Thesis/Dissertation
Requestor type	academic/university or research institute
Format	print and electronic
Portion	figures/tables/illustrations
Number of figures/tables/illustrations	2
Will you be translating?	no
Circulation/distribution	<501
Author of this Springer Nature content	yes
Title	Mr
Institution name	University of Pretoria
Expected presentation date	Feb 2019
Portions	Figure 2 on page 130 Figure 3 on page 131
Requestor Location	Ladislaus Adam 20444 Tati River villas Francistown, 00267 Botswana Attn: Ladislaus Adam
Billing Type	Invoice
Billing Address	Ladislaus Adam 20444 Tati River villas Francistown, Botswana 00267 Attn: Ladislaus Adam
Total	0.00 USD
Terms and Conditions	

Springer Nature Terms and Conditions for RightsLink Permissions

Springer Nature Customer Service Centre GmbH (the Licensor) hereby grants you a non-exclusive, world-wide licence to reproduce the material and for the purpose and requirements specified in the attached copy of your order form, and for no other use, subject to the conditions below:

1. The Licensor warrants that it has, to the best of its knowledge, the rights to license reuse of this material. However, you should ensure that the material you are requesting is original to the Licensor and does not carry the copyright of another entity (as credited in the published version).

   If the credit line on any part of the material you have requested indicates that it was reprinted or adapted with permission from another source, then you should also seek permission from that source to reuse the material.

2. Where **print only** permission has been granted for a fee, separate permission must be obtained for any additional electronic re-use.

3. Permission granted **free of charge** for material in print is also usually granted for any electronic version of that work, provided that the material is incidental to your work as a whole and that the electronic version is essentially equivalent to, or substitutes for, the print version.

4. A licence for 'post on a website' is valid for 12 months from the licence date. This licence does not cover use of full text articles on websites.

5. Where **'reuse in a dissertation/thesis'** has been selected the following terms apply: Print rights of the final author's accepted manuscript (for clarity, NOT the published version) for up to 100 copies, electronic rights for use only on a personal website or institutional repository as defined by the Sherpa guideline (www.sherpa.ac.uk/romeo/).

6. Permission granted for books and journals is granted for the lifetime of the first edition and does not apply to second and subsequent editions (except where the first edition permission was granted free of charge or for signatories to the STM Permissions Guidelines http://www.stm-assoc.org/copyright-legal-affairs/permissions/permissions-guidelines/), and does not apply for editions in other languages unless additional translation rights have been granted separately in the licence.

7. Rights for additional components such as custom editions and derivatives require additional permission and may be subject to an additional fee. Please apply to Journalpermissions@springernature.com/bookpermissions@springernature.com for these rights.

8. The Licensor's permission must be acknowledged next to the licensed material in print. In electronic form, this acknowledgement must be visible at the same time as the figures/tables/illustrations or abstract, and must be hyperlinked to the journal/book's homepage. Our required acknowledgement format is in the Appendix below.

9. Use of the material for incidental promotional use, minor editing privileges (this does not include cropping, adapting, omitting material or any other changes that affect the meaning, intention or moral rights of the author) and copies for the disabled are permitted under this licence.

10. Minor adaptations of single figures (changes of format, colour and style) do not require the Licensor's approval. However, the adaptation should be credited as shown in Appendix below.

Appendix — Acknowledgements:

For Journal Content:

Reprinted by permission from [**the Licensor**]: [**Journal Publisher** (e.g.

Nature/Springer/Palgrave)] [**JOURNAL NAME**] [**REFERENCE CITATION** (Article name, Author(s) Name), [**COPYRIGHT**] (year of publication)

For **Advance Online Publication papers:**
Reprinted by permission from [**the Licensor**]: [**Journal Publisher** (e.g. Nature/Springer/Palgrave)] [**JOURNAL NAME**] [**REFERENCE CITATION** (Article name, Author(s) Name), [**COPYRIGHT**] (year of publication), advance online publication, day month year (doi: 10.1038/sj.[JOURNAL ACRONYM].)

For Adaptations/Translations:
Adapted/Translated by permission from [**the Licensor**]: [**Journal Publisher** (e.g. Nature/Springer/Palgrave)] [**JOURNAL NAME**] [**REFERENCE CITATION** (Article name, Author(s) Name), [**COPYRIGHT**] (year of publication)

Note: For any republication from the British Journal of Cancer, the following credit line style applies:

Reprinted/adapted/translated by permission from [**the Licensor**]: on behalf of Cancer Research UK: : [**Journal Publisher** (e.g. Nature/Springer/Palgrave)] [**JOURNAL NAME**] [**REFERENCE CITATION** (Article name, Author(s) Name), [**COPYRIGHT**] (year of publication)

For **Advance Online Publication** papers:
Reprinted by permission from The [**the Licensor**]: on behalf of Cancer Research UK: [**Journal Publisher** (e.g. Nature/Springer/Palgrave)] [**JOURNAL NAME**] [**REFERENCE CITATION** (Article name, Author(s) Name), [**COPYRIGHT**] (year of publication), advance online publication, day month year (doi: 10.1038/sj.[JOURNAL ACRONYM])

For Book content:
Reprinted/adapted by permission from [**the Licensor**]: [**Book Publisher** (e.g. Palgrave Macmillan, Springer etc) [**Book Title**] by [**Book author**(s)] [**COPYRIGHT**] (year of publication)

Other Conditions:

Version 1.1

Questions? customercare@copyright.com or +1-855-239-3415 (toll free in the US) or +1-978-646-2777.